AD 680298

AD

AMMRC CR 68-09(F)

AMMRC CR 68-09(F)

INFLUENCE OF ALLOYING ELEMENTS ON THE TOUGHNESS OF LOW ALLOY MARTENSITIC HIGH STRENGTH STEELS

Final Technical Report
July 1967 to September 1968

by

C. Vishnevsky
E. A. Steigerwald

November, 1968

TRW Inc.
Cleveland, Ohio

D D C
RECEIVED
DEC 30 1968
B

Contract DAAG 46-67-C-0171

This document has been approved for publication and sale; its distribution is unlimited.

ARMY MATERIALS AND MECHANICS RESEARCH CENTER
WATERTOWN, MASSACHUSETTS 02172

107

DISCLAIMER NOTICE

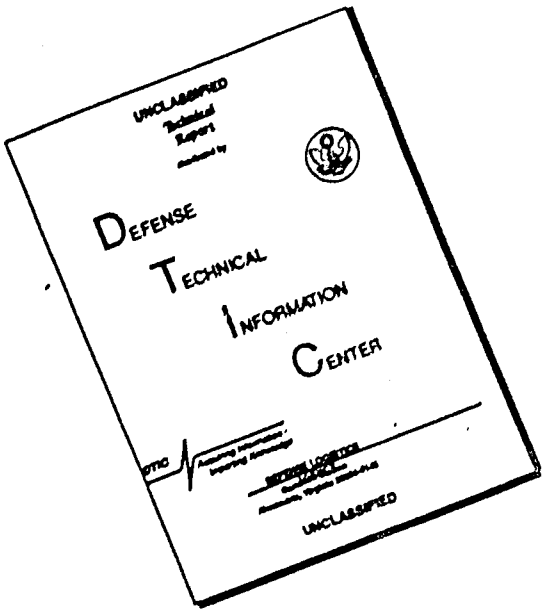

THIS DOCUMENT IS BEST QUALITY AVAILABLE. THE COPY FURNISHED TO DTIC CONTAINED A SIGNIFICANT NUMBER OF PAGES WHICH DO NOT REPRODUCE LEGIBLY.

INFLUENCE OF ALLOYING ELEMENTS ON THE TOUGHNESS OF LOW ALLOY MARTENSITIC HIGH STRENGTH STEELS

AMMRC CR 68-09(F)
Final Technical Report
July 1967 to September 1968

by

C. Vishnevsky
E. A. Steigerwald

November 1968
TRW Inc.
Cleveland, Ohio

Contract DAAG 46-67-C-0171
D/A Project 1C024401A349
AMCMS Code 5025.13.842
Materials Research for Specific Army Requirements

This document has been approved for publication and sale; its distribution is unlimited

Army Materials and Mechanics Research Center
Watertown, Massachusetts 02172

ABSTRACT

This study has examined the effects of various elements on the notch bend fracture toughness and Charpy impact behavior of a 0.35%C, 3%Ni, Cr-Mo-V martensitic steel having a room temperature yield strength of approximately 160-180 ksi. A classical approach was used in the design of alloys which permitted a direct evaluation of single element effects rather than interactions.

The elements C, Mn, Si, Cr, and Mo raised both the notch bend fracture mode transition temperature and the Charpy V-notch transition temperature (100% fibrosity criterion). In amounts above that required for deoxidation and grain refinement aluminum degraded the transition temperature and toughness slightly. A minimum toughness occurred at a vanadium content of 0.1%. Over the entire range of compositions examined (1.26 - 6.23%) nickel decreased the transition temperature and improved toughness at the lower test temperatures.

Charpy shelf energy, C_V (max), and fracture toughness, K_{max} (at 75°F), did not correlate well with work hardening exponent (n). Good agreement was obtained however when these parameters were plotted versus true fracture strain. At -321°F, toughness was essentially fracture strain independent suggesting that a critical strain criterion based on fracture strain is valid only when fracture is fibrous.

A comparison was made of measured K_{Ic} calculated from tensile data using the Hahn-Rosenfield model $K_{Ic} = (2/3EY\bar{\varepsilon}^{*}n^{2})^{1/2}$, where E = Young's modulus, Y = yield strength, $\bar{\varepsilon}^{*}$ = true fracture strain, n = work hardening exponent. The results indicated that the increased contribution on non-ductile fracture which accompanies increases in strength and/or decreases in test temperature in low alloy steels can lead to large errors in the predicted toughness.

FOREWORD

This report, TRW ER 7217-1, presents the final results of a program performed by the Materials Research Department of the TRW Equipment Laboratories for the Army Materials and Mechanics Research Center under contract DAAG 46-67-C-0171. The work was conducted by C. Vishnevsky and E. A. Steigerwald. F. R. Larson was program director for AMMRC.

An earlier phase of this program, "Literature Survey on the Influence of Alloy Elements on the Fracture Toughness of High Strength Steels," was published in February, 1968 as a separate report AMMRC CR 67-13(F).

Prepared by: C. Vishnevsky
C. Vishnevsky

E. A. Steigerwald
E. A. Steigerwald

TABLE OF CONTENTS

		Page
I.	INTRODUCTION	1
II.	MATERIALS AND PROCEDURE	4
III.	RESULTS AND DISCUSSION	16
	Effects of Alloy Additions	17
	Carbon	17
	Manganese	29
	Silicon	29
	Chromium	29
	Nickel	29
	Molybdenum	29
	Vanadium	30
	Aluminum	30
	Summary	30
	Relation of Toughness to Tensile Properties	30
	Work Hardening Exponent	33
	Quantitative Models	41
IV.	SUMMARY AND CONCLUSIONS	47
V.	LIST OF REFERENCES	48
VI.	APPENDIX	50

I INTRODUCTION

Although numerous high strength low alloy steels are currently utilized in applications requiring good toughness, relatively little systematic information exists on the effects of composition on toughness properties. The major factors contributing to this situation are the complexity of steel compositions, heat treatment and structure, the variety of toughness tests which complicate efforts at establishing meaningful cross correlations between parameters, and in many instances an insufficient appreciation for relationships between laboratory tests and service performance.

An important problem area involving low alloy steels is gun tubes for 175 mm cannon. At the present time no compositional requirements are specified for this application. Instead, certain yield strength, ductility, and Charpy impact test requirements are used with the chemical composition being the responsibility of the commercial steel producers (1,2). The normal yield strength of these steels is in the range of 160-180 ksi The application is particularly severe and cracks usually initiate at rifling marks after a few rounds The propagation of these cracks under cyclic stresses poses a serious problem in reducing useful tube life by promoting catastrophic failure. To date, effective methods of eliminating the early initiation of cracks have not been developed. The problem is therefore one of controlling the rate of crack growth and minimizing the probability of catastrophic brittle failure

The gun tube problem involves crack growth in thick sections (i.e., under plane strain conditions), and lends itself to analysis by linear elastic fracture mechanics. The understanding of fracture toughness is most advanced regarding crack propagation under plane strain conditions and test methods are available for measuring the plane strain fracture toughness, (K_{Ic}). In addition to defining critical crack size under tensile loading, experimental data exists for gun tube steels which show that the rate of fatigue crack propagation is inversely related to the K_{Ic} (3). Thus, a large value of K_{Ic} indicates that fatigue crack growth rate is decreased and a larger crack can be stable before the onset of rapid crack propagation.

The Charpy V-notch impact test, however, provides a less direct evaluation of toughness as required for this application. In particular, it measures both energy for crack initiation and propagation in a section which is appreciably thinner than the gun tube The presence of shear lips in broken Charpy specimens does not accurately reflect the flat, macroscopically shearless, crack propagation in thick sections. It is also important to note that the Charpy impact test, which has been

valuable in toughness studies of low strength steels, becomes increasingly insensitive as strength increases. It is thus reasonable to expect that an analysis of steel composition requirements for large gun barrels using recent fracture mechanics knowledge will provide more insight into material behavior than approaches depending on conventional toughness tests.

The present program was divided into two stages. The first consisted of a review of the literature on the effects of alloying elements on toughness of low alloy steels. The results of this survey have been presented in separate form (4). The conclusions of this work were as follows:

1. The low alloy martensitic steels should be used with the lowest possible carbon content consistent with hardenability and strength level requirements.

2. Oxygen, nitrogen, phosphorus, sulfur, and the tramp elements are all detrimental to toughness and should be maintained at minimum levels.

3. Nickel is an alloying element which improves fracture toughness.

4. Manganese is an alloying element which has a detrimental effect on the fracture toughness of the high-strength steels.

5. Although the data are not systematic, the carbide formers, chromium, molybdenum, and vanadium, produce no consistent effect on fracture toughness when added in the normal range of compositions used in the high-strength steels. Molybdenum, however,can be beneficial for minimizing the effects of reversible temper embrittlement.

6. Silicon effectively retards the tempering reactions which promote irreversible (500°F) embrittlement. When used with vacuum melting, silicon improves the fracture toughness of 4340 steel at the high-strength levels.

7. Fracture toughness is improved when the desired hardenability is obtained by a combination of alloying elements rather than a single alloying element, provided that nickel is one of the principal additions.

8. The superposition of a secondary hardening mechanism which involves precipitation of copper, aluminum, or complex carbides in a 0.30 - 0.40% carbon martensite does not improve the fracture toughness at the higher strength levels. At the lower strengths however (below approximately 215 ksi tensile) there may be some advantage in the use of a precipitation hardening mechanism involving copper or the use of secondary hardening with complex alloy carbides.

These conclusions suggest the validity of applying certain general principles to alloy steel development from a fracture toughness viewpoint. They cannot be applied rigorously to any specific alloy composition but rather serve as guidelines for more detailed work on particular steel types.

Based on the results of the above literature review, an experimental program was adopted which permitted the systematic study of compositional effects on toughness in a typical gun steel having a room temperature yield strength of 160 - 180 ksi. The base steel chosen for this portion of the investigation had a nominal composition of 0.35%C, 0.65%Mn, 0.35%Si, 0.85%Cr, 3.0%Ni, 0.30%Mo, 0.10%V. The effects of all these elements together with aluminum were examined by varying individual elements around the base composition. This classical approach permitted a direct evaluation of single element effects. The objectives of this portion of the program were to define the influence of the various alloying elements on fracture toughness as a function of test temperature and explore the possibility of relating standard tensile properties, as affected by composition, to fracture toughness. The program also sought to establish correlations between fracture toughness and the conventional Charpy V-notch impact test.

II MATERIALS AND PROCEDURE

A total of nineteen experimental heats of steel were evaluated. The list of compositions in Table I shows two base heats and seventeen other steels in which individual elements were varied deliberately from the base composition. Three compositional levels were obtained for C, Mn, Si, Cr, Mo, V, and Al while four levels were examined for Ni. These are listed below:

Element	Weight %			
C	0.28,	0.35*,	0.41	
Mn	0.21,	0.65*,	1.51	
Si	0.06,	0.36*,	1.38	
Cr	0.51,	0.82*,	1.61	
Ni	1.26,	2.83*,	4.45,	6.23
Mo	0.13,	0.30*,	1.04	
V	<.01,	0.10*,	0.28	
Al	0.033*,	0.13,	0.34	

* average of two base heats

The range of compositions examined was based primarily on hardenability requirements and anticipated response to heat treatment.

The steels were vacuum induction melted in an alumina lined furnace. Heats weighing approximately 40 pounds were cast into zircon ingot molds invested in steel shot to provide a rapidly solidified cast structure. The upper portion of the ingot molds was wrapped in a ceramic blanket and exothermic hot topping was applied after a solid skin had formed on the ingot surface. The specific melting practice used is given in Table II and a sketch of the ingot casting setup is shown in Figure 1. The ingots were hot worked by forging between flat dies using a 7 to 1 reduction. The forged product was approximately 2 1/2" wide x .6" thick.

The forging practice, outlined in Table III, involved appreciable redundant working to aid in breaking up the cast structure.

After forging all steels were cooled in air, normalized 1 hour at 1650°F, and spheroidized for 12 hours at 1300°F. Specimen blanks were cut from the forged plates, austenitized for 1/2-3/4 hours at 1550°F and quenched in agitated oil. The tempering treatment consisted of a double temper of 1+1 hours at 800°F for all but the 1.38%Si alloy which was double tempered for the same length of time at 1050°F in order to avoid the shift in the 500°F embrittlement range which occurs in high Si steels. The choice of these tempering conditions was based on pre-

TABLE I

CHEMICAL ANALYSES OF CAST AND FORGED HEATS*

Heat No.	C	Mn	Si	Cr	Ni	Mo	V	P	S	Al*
5, Base	.34	.75	.35	.87	2.70	.31	.10	.005	.004	.015
6, Base	.37	.55	.37	.76	2.97	.30	.11	.006	.004	.051
7	.33	.57	.36	.60	4.45	.29	.10	.006	.005	.043
8	.35	.56	.35	.84	1.26	.30	.10	.007	.006	.039
9	.34	.71	.33	.51	3.00	.35	.12	.007	.009	.048
12	.33	.69	.35	.82	2.82	.13	.10	.005	.003	.024
13	.36	.68	.32	.85	3.04	1.04	.09	.006	.006	.023
14	.34	.67	.06	.87	3.01	.33	.10	.007	.008	.037
16	.34	.68	1.38	.83	3.04	.34	.11	.010	.009	.022
17	.36	1.51	.33	.84	3.11	.37	.11	.006	.007	.013
18	.35	.75	.35	1.61	3.03	.34	.12	.008	.009	.013
19	.36	.73	.33	.85	3.12	.38	.12	.008	.009	.34
20	.37	.70	.34	.82	2.98	.37	.12	.008	.008	.13
21	.35	.74	.34	.84	2.95	.32	< .01	.008	.005	.030
22	.37	.70	.33	.85	2.99	.36	.28	.009	.008	.040
26	.33	.21	.35	.83	3.04	.35	.12	.006	.004	.038
27	.28	.70	.32	.86	3.00	.35	.11	.007	.004	.044
28	.41	.72	.34	.85	2.97	.34	.10	.007	.005	.042
29	.32	.70	.32	.80	6.23	.32	.11	.008	.006	.049

* Underlined values indicate deliberate variations from base composition.

** Acid soluble.

TABLE II

Steel Melting and Casting Procedure

Furnace - Vacuum Induction, 50# Capacity, Alumina Lined Crucible

1. Charge electrolytic iron (4" dia. bars previously cast from vacuum melted electrolytic Fe in flake form), Ni, Mo, Cr and .21%C as graphite rod.

2. Evacuate chamber; at first sign of melting fill chamber with argon to 1/2 atm. pressure.

3. After meltdown, cool bath until surface freezes then melt under low power to establish reference melting point temperature with optical pyrometer.

4. Initiate C boil by reducing pressure gradually. Initally maintain temperature at 50°F (optical) above melting point; near end of boil superheat is approximately 100°F (optical). After pressure of 50μ was achieved, an additional 12-15 min. were required to reduce pressure to the 10-15μ range.

5. After pressure of 10-15μ is reached, add Fe-Si.

6. Backfill chamber with argon to 1/2 atm. pressure.

7. Add remainder of C, permit to dissolve, raise temperature to 125-150°F (optical) above melting point.

8. Add Fe-Mn and Al (single addition of Fe-Mn wrapped in aluminum foil).

9. Pour at approximately 150°F (optical) superheat into zircon mold (see Figure 1). Entire mold setup was baked at 400-600°F and inserted hot into furnace chamber immediately before Step 1.

10. 1 minute after solid skin forms on ingot surface, furnace chamber is opened and exothermic hot topping added.

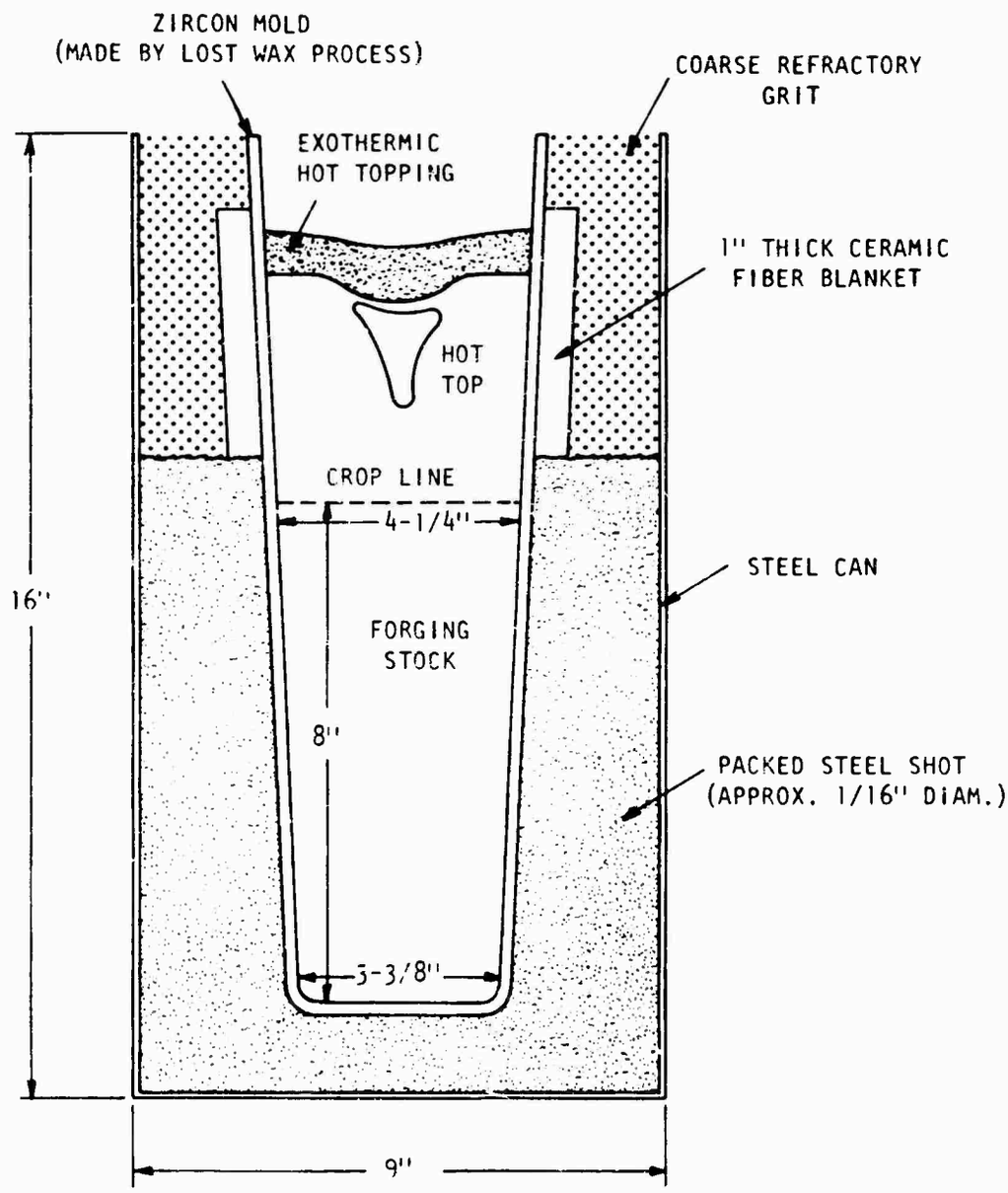

Figure 1. Setup used for casting steel ingots.

TABLE III

Forging Practice

Heat Ingot at 2100°F for 2 hours; Forge on 150 ton hydraulic press between preheated flat dies, no lubrication.

1. Forge ingot (approximately 4" round, Figure 1) to 3" square; reheat (2100°F).
2. Forge 3" square to 2 1/2" square; reheat (2100°F).
3. Forge 2 1/2" square to 2" square; reheat (2000°F).
4. Forge 2" square to 1 1/2" thick x 2 plus" wide; reheat (2000°F).
5. Forge 2 1/2"(plus) width to 2 1/2"; reheat (2000°F).
6. Forge 1 1/2"(plus) thickness to 1", reheat (2000°F).
7. Forge 1" thickness to .650"; reheat (2000°F).
8. Forge 2 1/2" (plus) width to 2 1/2"; reheat (2000°F).
9. Repeat steps 7 and 8.
10. Cool bar in still air.

liminary heat treatment studies which indicated that the 800°F tempering temperature (and 1050°F for 1.38% Si) produced desired strength levels, small variations in hardness between steels and a reasonable assurance of avoiding both the 500°F and temper brittleness ranges.

Three types of specimens were machined from heat treated bars. The dimensions of tensile and notch bend fracture toughness specimens are shown in Figure 2. Standard Charpy V-notch impact specimens were taken from the broken halves of notch bend bars. The orientations of test specimens and directions of crack extension relative to the dimensions of the forged bars are illustrated in Figure 3.

Tensile tests were conducted at temperatures of 75 to -321°F using a 60,000 pound capacity hydraulic testing machine at a crosshead speed of .01 inches per minute. An air environment was used for 75°F while the lower temperatures were achieved with ethyl alcohol and liquid nitrogen mixtures. In addition to the standard tensile properties such as tensile strength, .2% offset yield strength, reduction in area, and percent elongation the work hardening exponent, n, as used in the equation $\sigma = A\varepsilon^n$ (σ=stress, A=constant, ε=true plastic strain) was evaluated. A 1.0 inch gage length knife edge creep extensometer was adapted to provide chart records of load versus elongation during the entire tensile test. Only the portion of the stress-strain curve preceding maximum load (necking) was used to calculate n. The instantaneous stress was calculated using the instantaneous load and an area computed assuming a constant volume contribution from the plastic component of the elongation together with a slight correction because of an elastic Poisson contraction of the specimen diameter.

In most cases at least five values of stress and true plastic strain were obtained from the load-elongation curves. The work hardening coefficient or slope of a log σ-log ε plot was obtained from a linear regression analysis of the data. The standard deviation in n, and linear correlation coefficient of X-Y (σ-ε) were generally such as to indicate excellent straight line fits, thus supporting the use of a $\sigma = A\varepsilon^n$ strain hardening relationship to define n. All log σ-log ε data were also plotted manually as a precautionary qualitative visual check of the calculated results.

Complete tensile data were not obtained for all specimens tested because occasionally at low temperatures premature brittle failures initiated under the extensometer knife edges. These failures always occurred after maximum load was reached so that acceptable yield strength, tensile strength, and n values were obtained. However, under these conditions, ductility data were incorrect and additional specimens were tested without the extensometer in order to generate valid results. These extra tests yielded duplicate tensile strength data but not yield strength or n values.

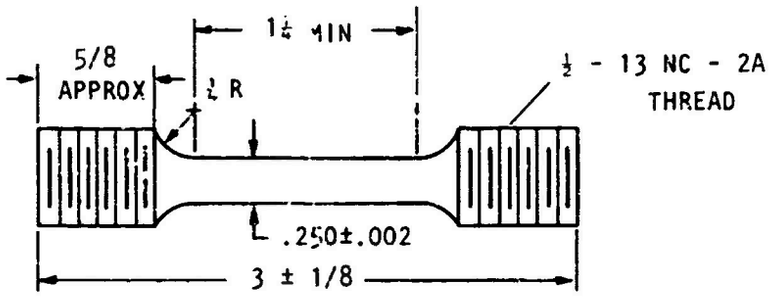

a) Tensile Specimen

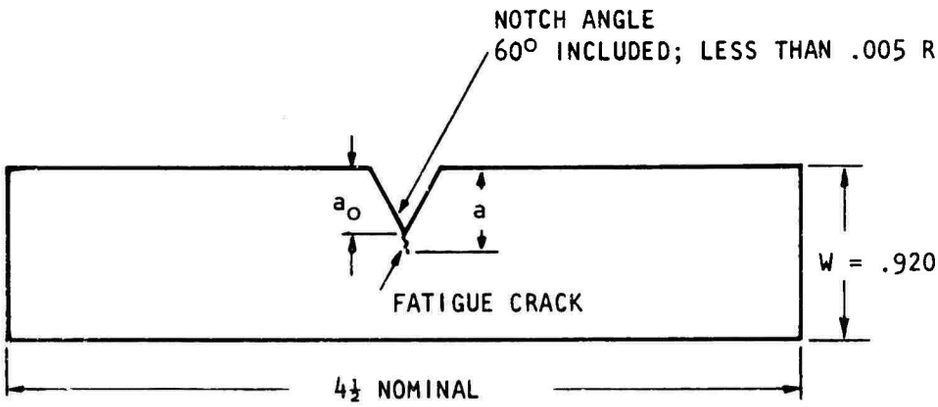

THICKNESS, B = .480
SPAN, 2L = 4W
a_o = .365-.385
$\frac{a}{w}$ = .45-.55

b) Slow bend fracture toughness specimen (three point loading).

Figure 2. Dimensions of tensile and fracture toughness specimens.

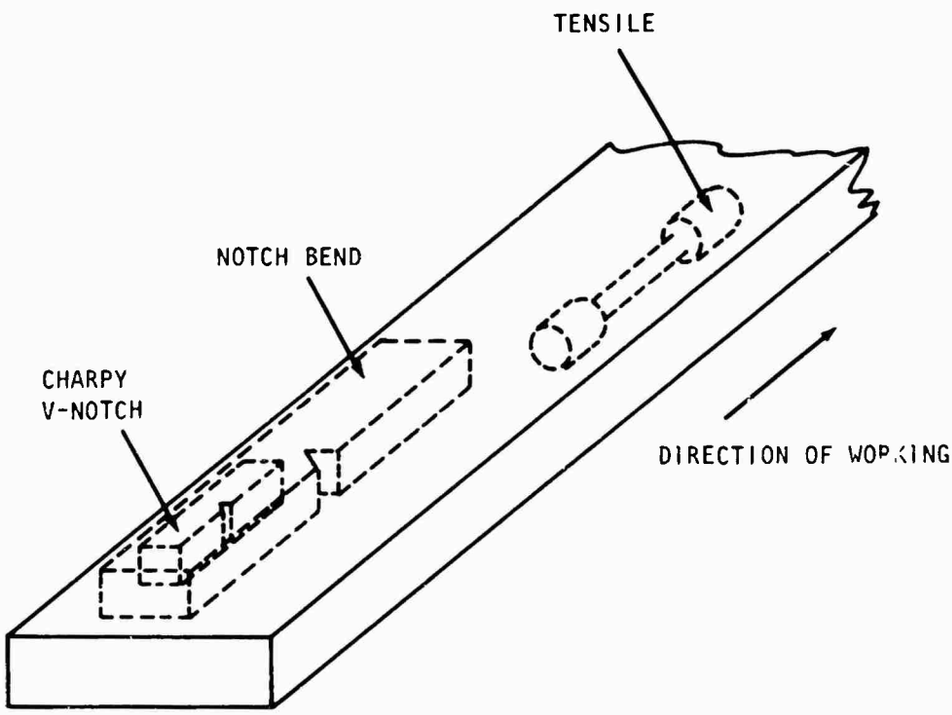

Figure 3. Locations of test specimens in relation to forged product.

Notch bend tests were performed using the specimen illustrated in Figure 2b. The range of test temperatures and coolants were identical with those used in tensile testing. The machined notch used for generating a fatigue crack was of a straight through rather than chevron design currently recommended by ASTM (5,6). However, this notch geometry did not introduce any difficulties in obtaining reasonably straight and uniform crack fronts. Current ASTM recommendations call for precracking at a rate sufficient to generate the last .050 inches of the fatigue crack in not less than 50,000 cycles (5). Evidence exists showing that at least in high strength steels, this requirement may be too stringent (7,8). In the present study the rate of precracking was such that the last .050 inches of crack depth were produced in approximately 20,000 cycles. The ratio of minimum to maximum load used in precracking was .25.

The fracture toughness tests were conducted in three point bending. A continuous load displacement record was generated using a clip gage attached to single edge razor blade knife edges spot welded to the specimen as shown in Figure 4. The shape of the load displacement curves could be classified into one of the three classes shown in Figure 5. For each test two load values were obtained from the load-displacement record. The maximum load, P_{max}, was used to compute a maximum value of stress intensity factor, K_{max}, using equation 1 in Figure 4. A load was also obtained for calculating the plain strain fracture toughness, K_{Ic}, corresponding to the stress intensity for measurable crack growth under plain strain conditions. The procedure, illustrated in Figure 5, consisted of drawing a secant line OP_5 with a slope 5% less than the straight line portion of the load-displacement record. The load P_Q, required to calculate K_{Ic}, was the maximum load on the record preceding or including P_5. Thus in the case of Class I curves $P_Q = P_5$ for Class II curves $P_Q > P_5$, and for Class III curves $P_Q = P_{max} = P_5$. For Class III curves the first measurable crack extension corresponded to unstable crack growth. In the other cases some slow crack growth beyond that corresponding to K_{Ic} preceded the onset of rapid fracture and the peak load in the record occurred at a position past OP_5. The load P_Q was then used to calculate a tentative K_{Ic} value, K_Q using equation 1.

The load-displacement records were examined further by drawing a horizontal line at .63 P_Q and measuring the deviation between OA and the load-displacement record at that point If this deviation exceeded 1/5 the value of the deviation of line OP_5 from OA, K_Q was rejected as a valid K_{Ic} number. Furthermore, in order for K_Q to be accepted as a valid K_{Ic}, the ASTM recommendation that the specimen thickness B must equal or exceed 2.5 $(K_Q/\sigma_{ys})^2$, where σ_{ys} is the yield strength, was used.

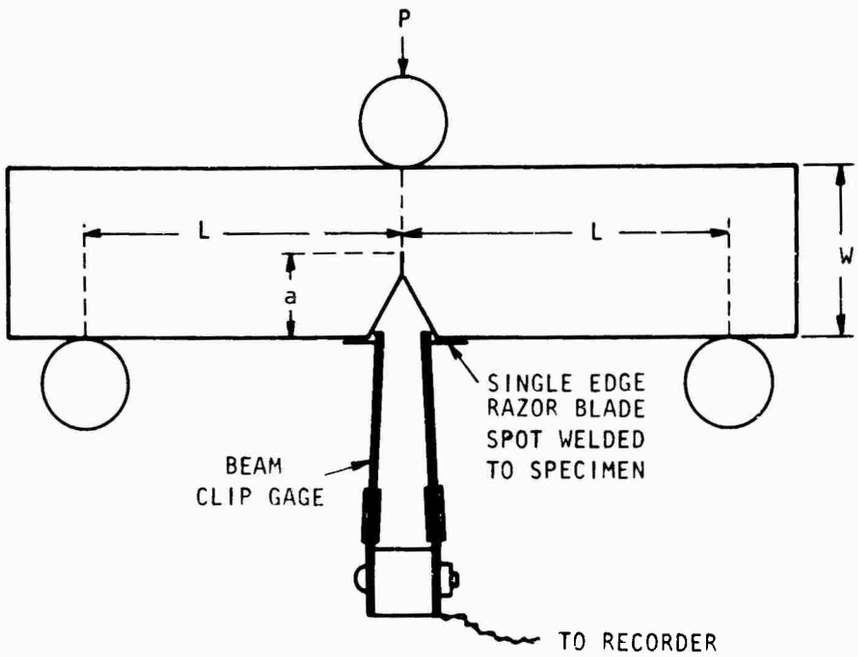

Equation 1): $$K = \frac{P\,La^{1/2}}{B\,W^2}\left[5.8 - 9.2\frac{a}{W} + 43.6\left(\frac{a}{W}\right)^2 - 75.3\left(\frac{a}{W}\right)^3 + 77.4\left(\frac{a}{W}\right)^4\right]$$

P = load in pounds
L = 1/2 total span length
a = crack depth (machined notch plus fatigue crack)
W = specimen width
B = specimen thickness

To obtain: K_{max} use P_{max};
" K_Q use P_Q;
" K_{Ic} evaluate K_Q and load-deflection curves to determine if criteria for valid K_{Ic} are satisfied (see text for details).

Figure 4. Schematic of test setup used in notch bend tests and equation used to calculate fracture toughness.

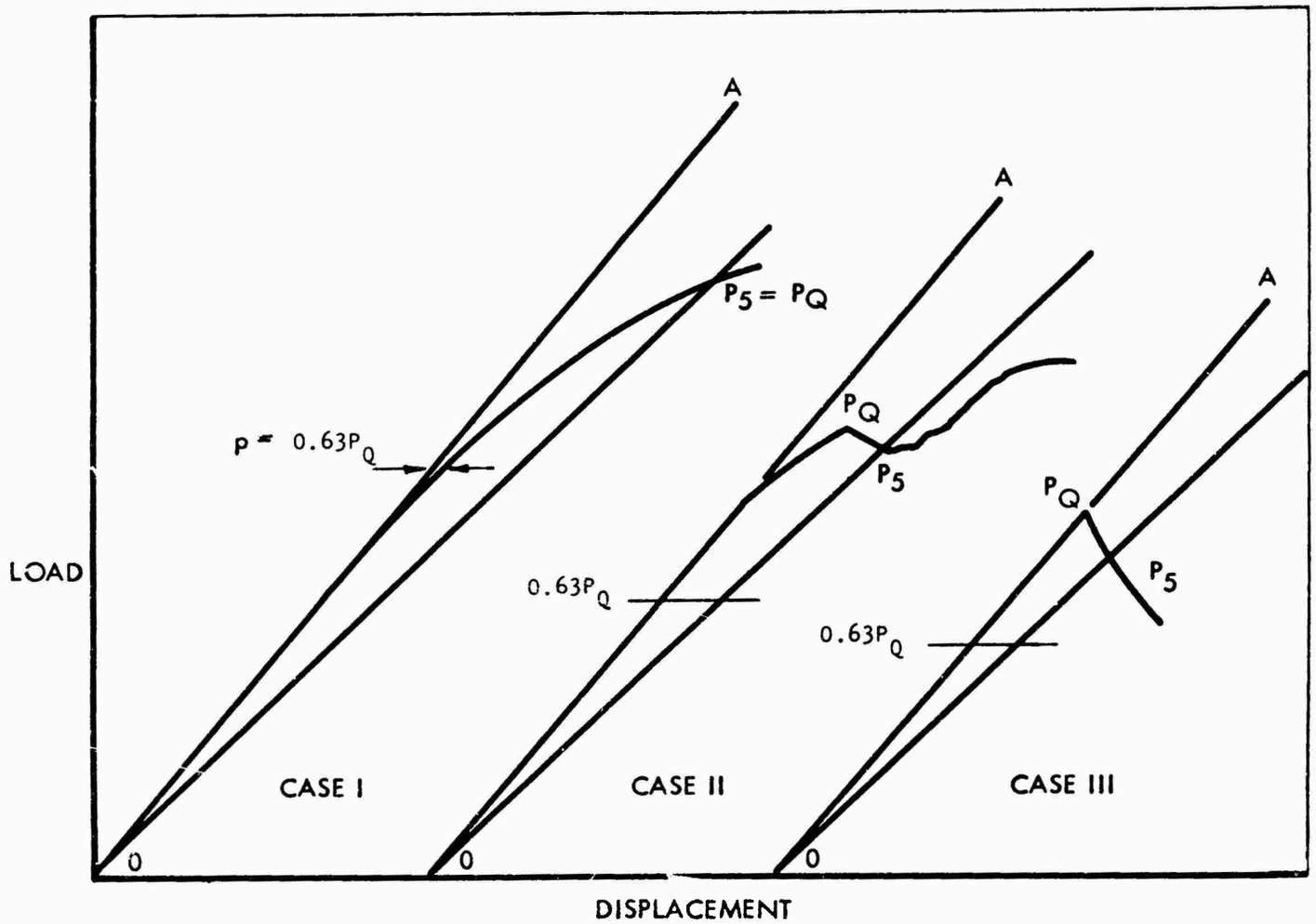

Figure 5. Representative load - displacement records
(Slopes OP_5 are exaggerated for clarity)

The crack length in cases where K_{Ic} was considered valid satisfied the criterion $a \geqslant 2.2(K_Q/\sigma_{ys})$. This is slightly less conservative than the recommended ASTM practive of $a \geqslant 2.5\ (K_Q/\sigma_{ys})$, however data for high strength steels have indicated that this variation produces a negligible systematic change in K_{Ic} (9).

Standard Charpy V-notch impact tests were performed using a 220 foot pound capacity impact machine having a striking velocity of 17 feet per second. Tests were conducted at temperatures ranging from -321 to 250°F. The 250°F temperature was achieved using a molten both of a low melting Bi base alloy. Baths for lower temperatures consisted of either water, dry ice and ethyl alcohol mixtures, or liquid nitrogen. An air environment was employed for the 75°F tests. Both impact energy and percent fibrous fracture were determined in these tests. The fibrosity readings were visual estimates made using master charts drawn to show various amounts of crystalline fracture, for a range of shear lip sizes, at hypothetical percentages of total fibrous fracture. Larson and Nunes (10) showed good agreement between visual estimates and more laborious planimetric measurements of percent fibrous fracture.

III RESULTS AND DISCUSSION

A detailed tabular and graphical presentation of test data for individual steels appears in the Appendix. The tensile test results, consisting of the tensile strength, .2% offset yield strength, reduction in area, elongation and work hardening exponent (n), are listed in Table AI(a) of the Appendix. Table AI(b) presents the results of limited tensile tests for base heat 5, tempered at 1000°F, comparing properties of longitudinal and transverse specimens. The high values of ductility in the transverse specimens are indicative of good steel cleanliness and forging practice. The results of the notch bend tests appear in Table AII. This latter table gives the pertinent information required to calculate the fracture toughness K_{max} and the plane strain fracture toughness K_{Ic}. The impact energy and fracture appearance data obtained in Charpy V-notch impact testing are presented in Table AIII.

The significant tensile and notch bend test data are summarized for each heat in Figures A 1 to A 18. These show the effect of test temperature on the tensile and yield strengths, reduction in area, work hardening exponent (n), and the stress intensity factors K_{max} and K_{Ic}. The stress intensity factors incorporate the influence of an intrinsic temperature effect on toughness together with its effect on the transition from plane strain to plane stress fracture as temperature increases. At -321°F the yield strength was large and K_{Ic} sufficiently small such that valid K_{Ic} data were obtained for all steels. With rising test temperature K_{Ic} increased and the yield strength decreased so that a temperature was reached at which the specimen was too thin for obtaining valid K_{Ic} data. The meaningful parameter above this temperature, which varied with composition, was the maximum stress intensity factor, K_{max}. At still higher temperatures the fracture toughness continued to increase reflecting an increase in K_{Ic}, a further drop in yield strength, and an increasing contribution of ductile shearing in the fracture surfaces as revealed by growing shear lips and a shrinking central flat region. For some specimens at intermediate test temperatures both K_{max} and a lower valid K_{Ic} value were obtained. The two data points for such specimens are connected by a vertical line in the graphs. The data for the two base composition steels (heats 5 and 6) are plotted together in Figure A1 with single lines through the points to indicate the properties of a steel whose composition is the average of the two.

The transition temperature in the notch bend tests was defined as the temperature at which $K_{max}/\sigma_{ys} = .4$. At this stress intensity level B, the nominal specimen thickness of .480 inches, was equal to $3\ (K_{max}/\sigma_{ys})^2$.

A comparison of this ratio with the requirement that for valid K_{Ic} $B \geqslant 2.5\ (K_Q/\sigma_{ys})^2$ shows that this definition of transition temperature is a reasonable measure of the fracture mode transition from K_{Ic} to K_c.

The results of Charpy impact tests are plotted separately for each steel in Figures A 19 to A 27. These figures show both the variation in impact energy and percent fibrous fracture with temperature. In high strength steels Charpy impact curves are generally flat and do not show the distinct transition in energy that is common for lower strength body-centered cubic metals. The transition temperature can be defined in various ways depending on what energy, dimensional, or fracture appearance criterion is used. In the present study the lowest temperature at which the fracture surface was completely fibrous was employed to define the transition. Above this point, commonly called the propagation transition temperature, the energy is essentially constant and is referred to as the Charpy shelf energy C_v(max). In the present study C_v(max) was taken as the lowest energy for 100% fibrous fracture.

Effects of Alloy Additions

A comparison of the influence of alloying elements on toughness is provided in Figures 6 to 16. The changes in notch bend fracture toughness with single element variations are shown in Figures 6 to 13. Similarly, Figures 14 to 16 contain Charpy impact energy curves for the individual alloy series. The transition temperatures for both the notch bend and Charpy tests are identified on these curves.

The toughness properties for each alloy series are discussed in the following paragraphs:

Carbon:

Carbon was detrimental both to notch bend (Figure 6) and Charpy impact toughness (Figure 14a). The qualitative agreement between the notch bend and Charpy curves was generally good. At very low temperatures the relative effects of carbon were not consistent between test methods, but but this may merely reflect scatter in the very limited amount of data in this region. The fracture mode transition and propagation transition temperatures increased with increasing carbon content. The peak K values and C_v(max) were reduced; the change was most pronounced in the range of 0.28 - 0.35% C.

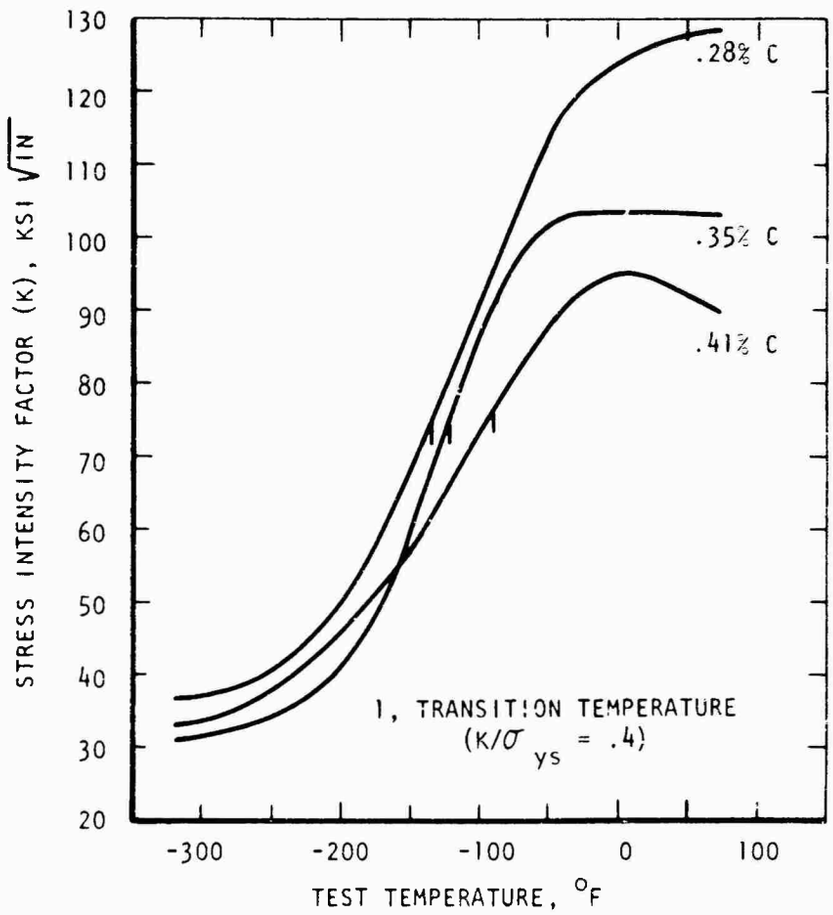

Figure 6. Effect of carbon on notch bend fracture toughness.

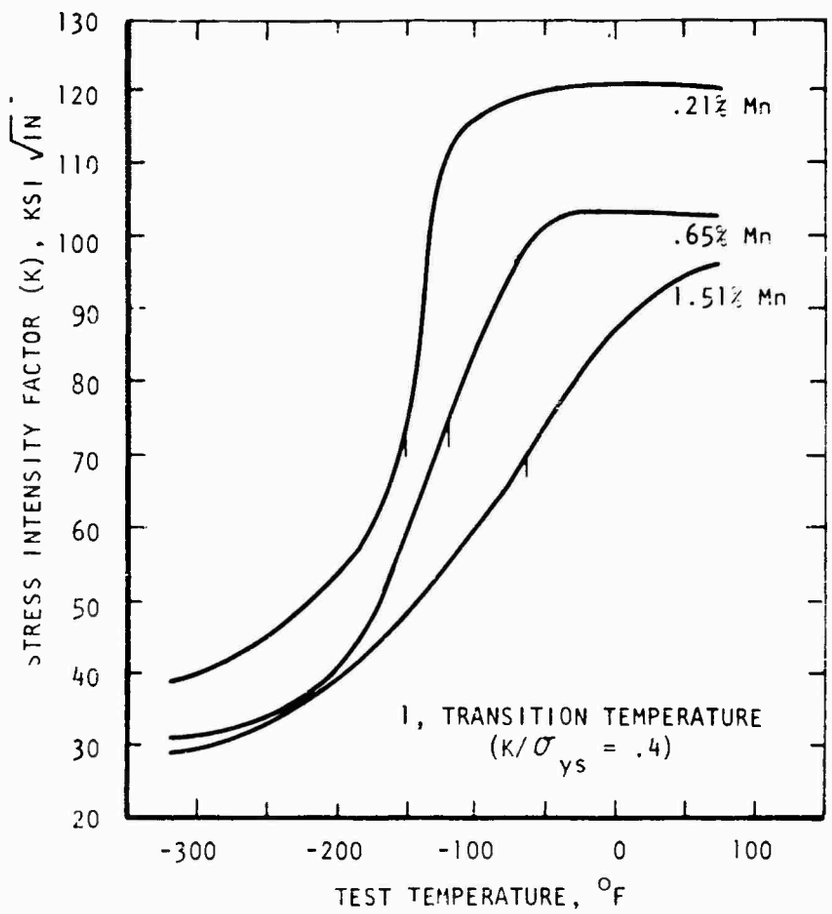

Figure 7. Effect of manganese on notch bend fracture toughness.

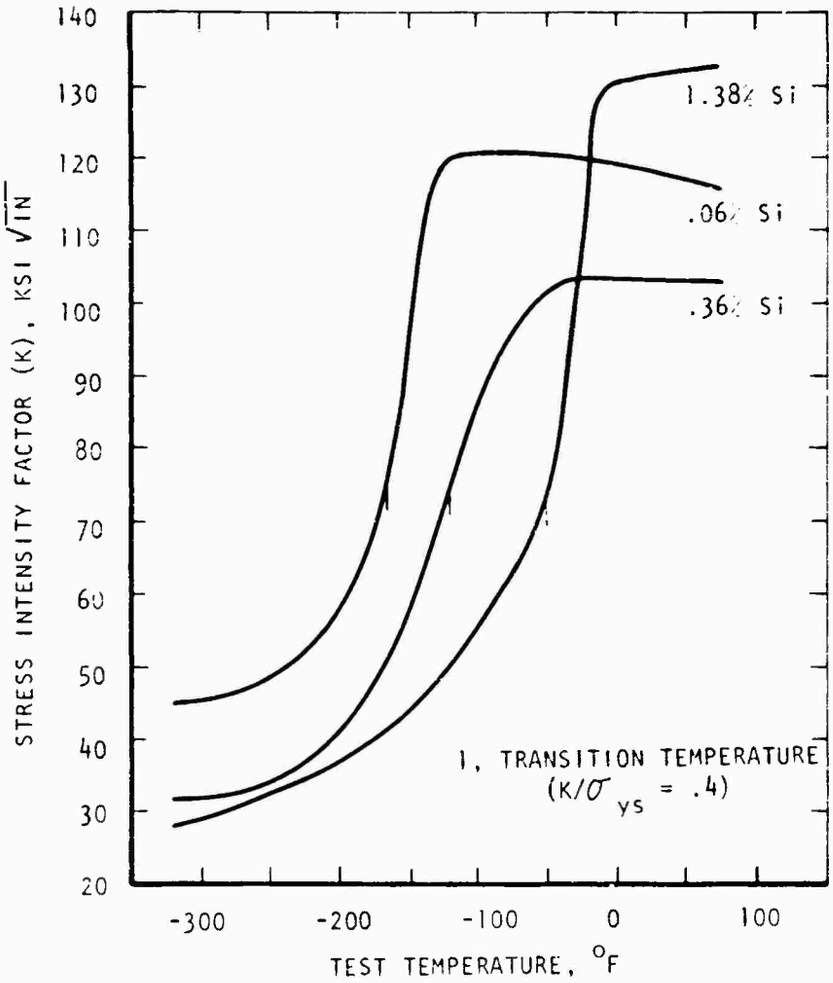

Figure 8. Effect of silicon on notch bend fracture toughness.

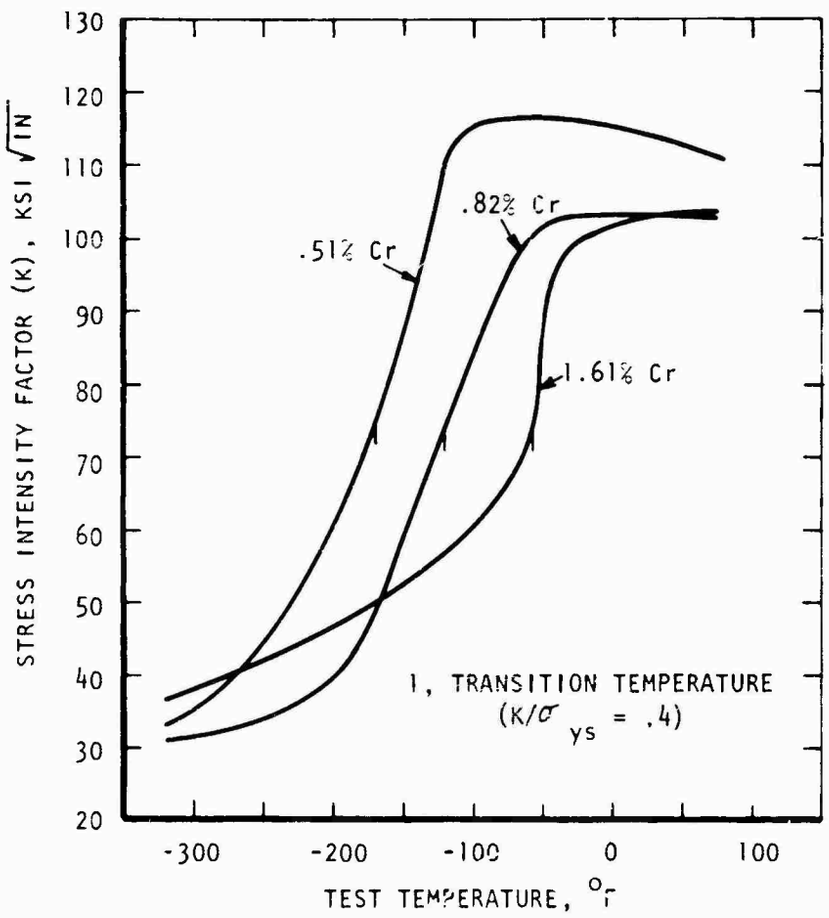

Figure 9. Effect of chromium on notch bend fracture toughness.

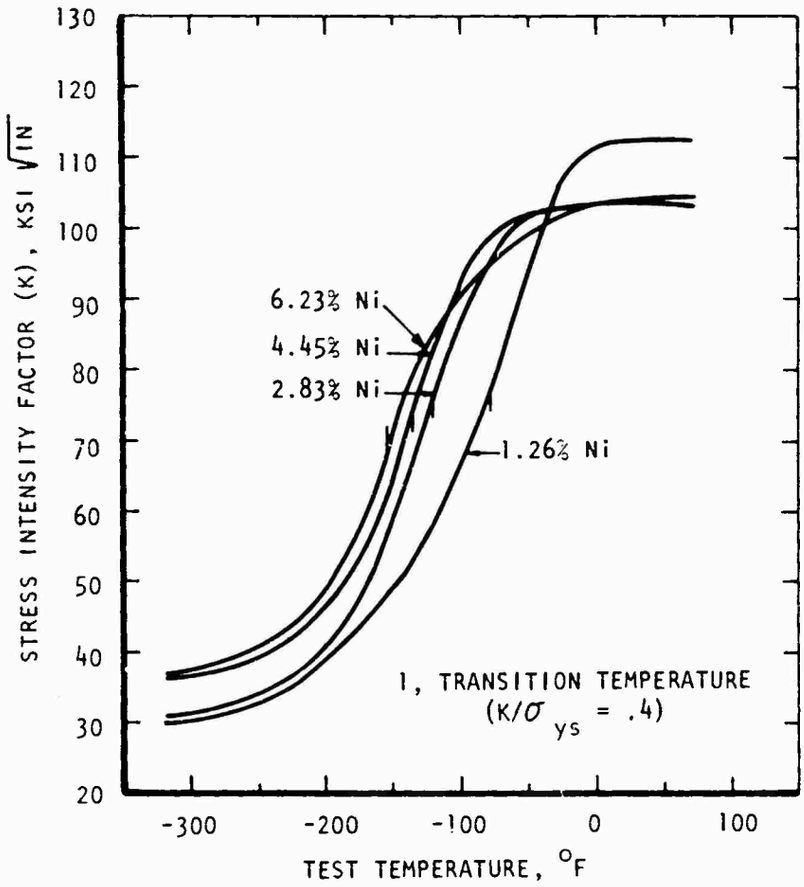

Figure 10. Effect of nickel on notch bend fracture toughness.

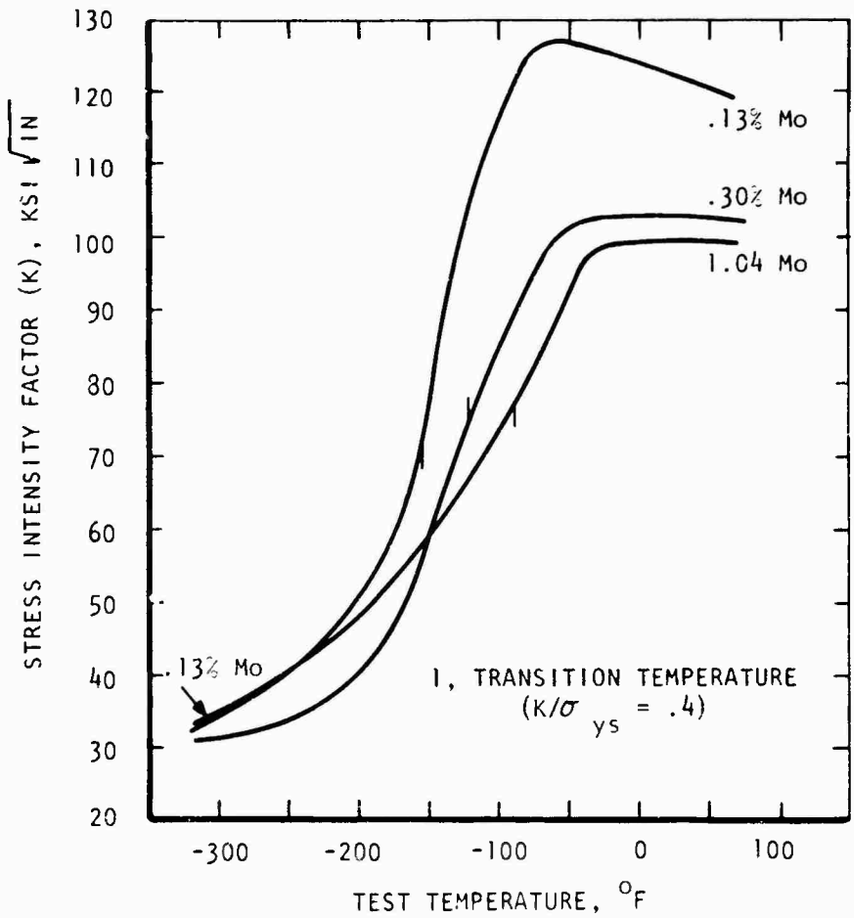

Figure 11. Effect of molybdenum on notch bend fracture toughness.

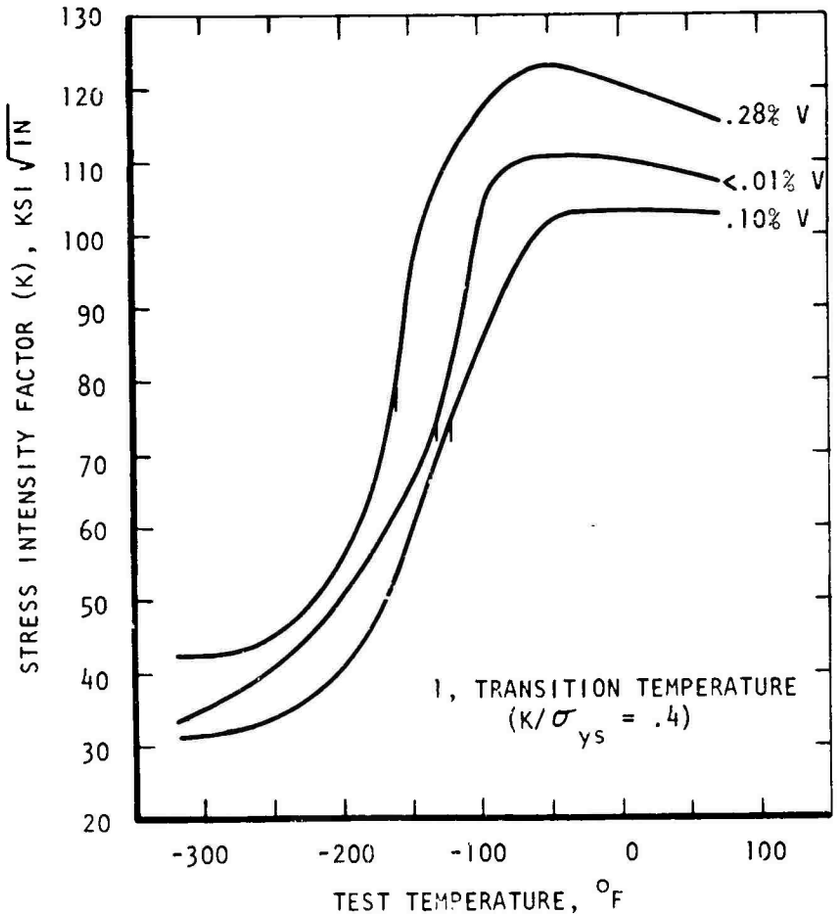

Figure 12. Effect of vanadium on notch bend fracture toughness.

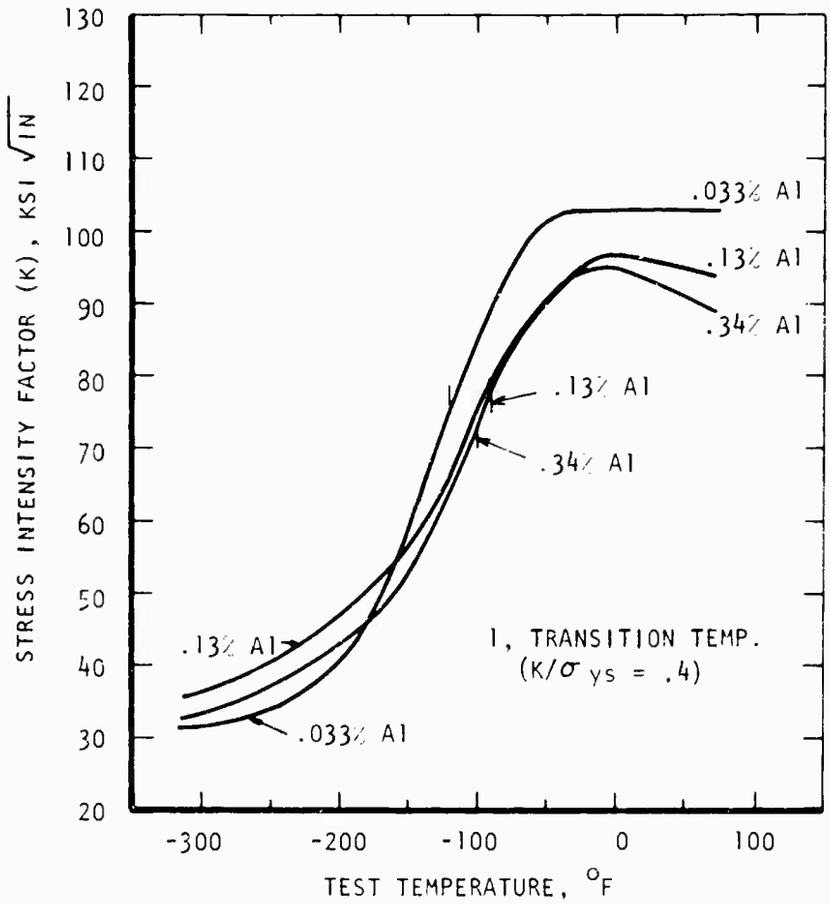

Figure 13. Effect of aluminum on notch bend fracture toughness.

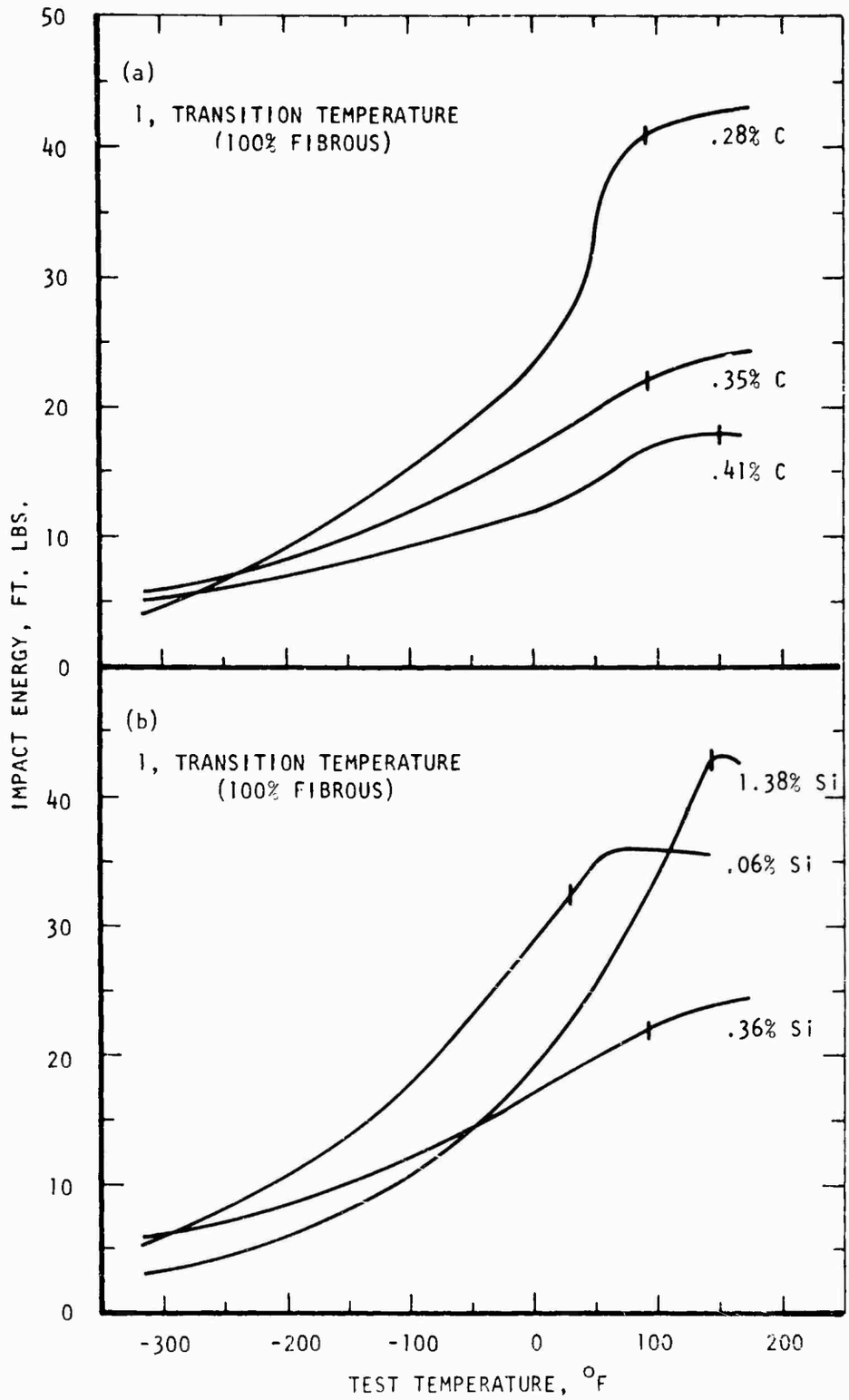

Figure 14. Variation of Charpy V-notch impact energy with carbon (a), silicon (b) content.

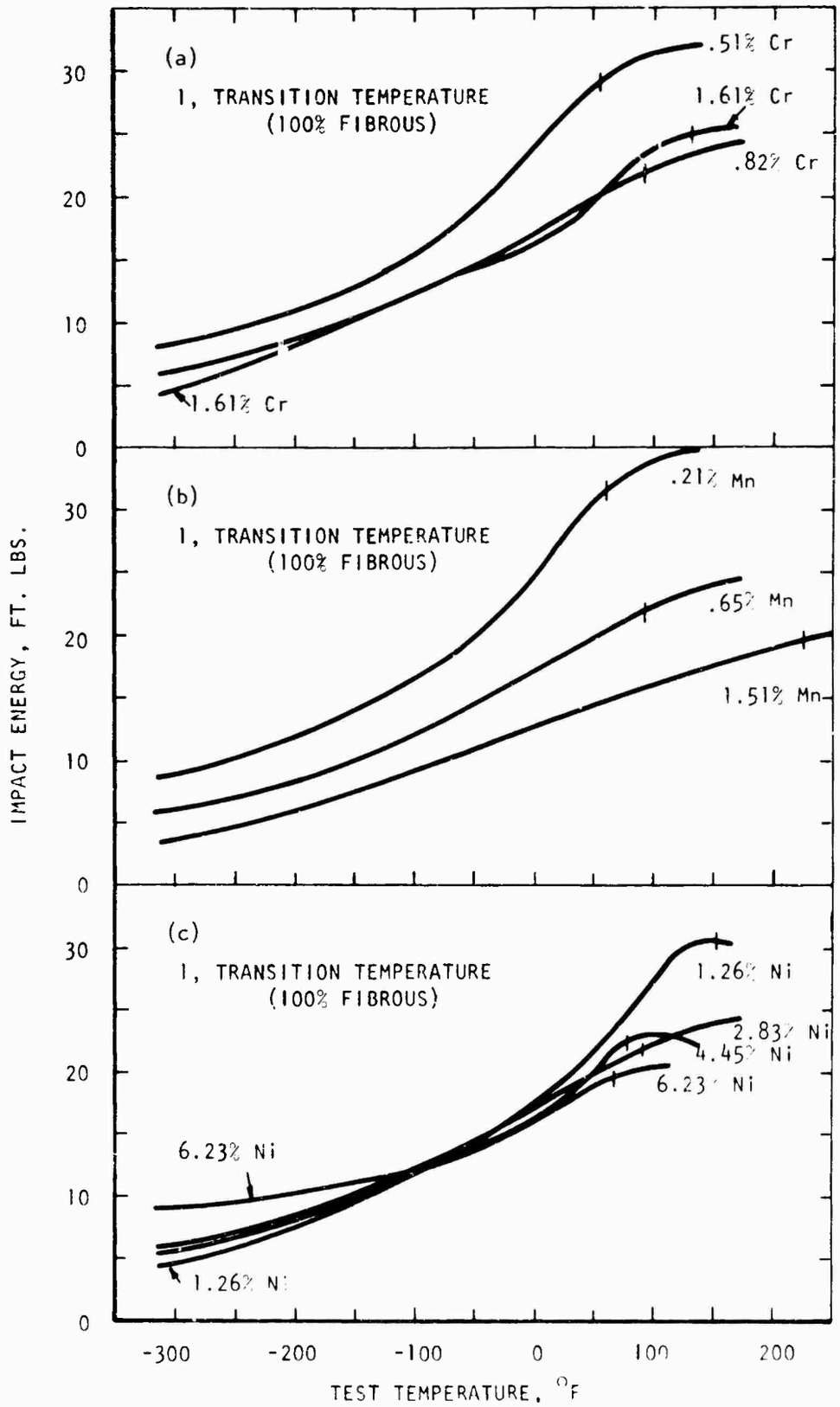

Figure 15. Variation of Charpy V-notch impact energy with chromium (a), manganese (b), and nickel (c) content.

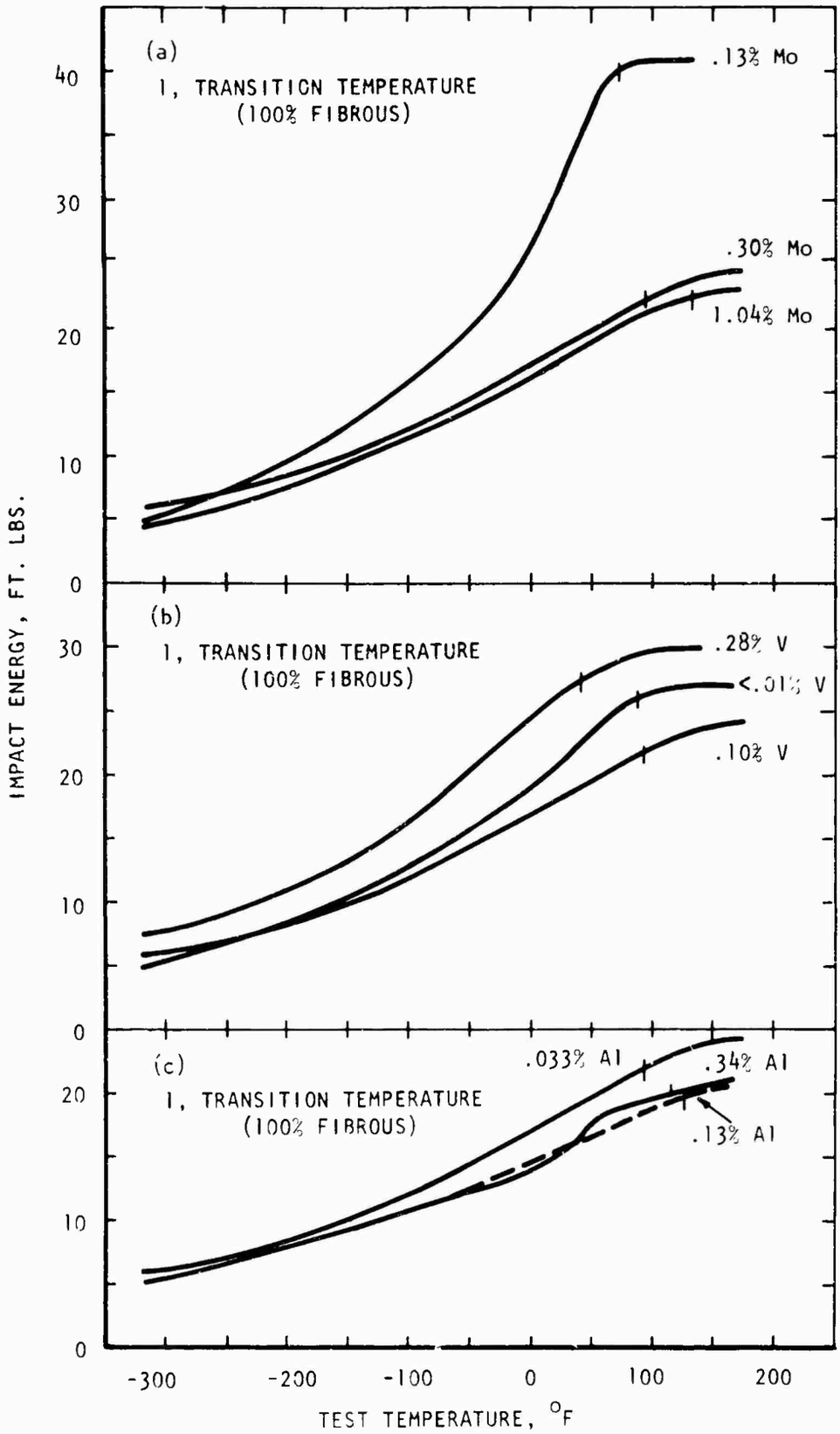

Figure 16. Variation of Charpy V-notch impact energy with molybdenum (a), vanadium (b), and aluminum (c) content.

Manganese:

Manganese reduced toughness at all temperatures in both tests as shown in Figures 7 and 15b. This behavior was also reflected in a pronounced rise in transition temperatures with increasing manganese content.

Silicon:

Silicon exhibited more complex behavior than carbon or manganese as shown in Figures 8 and 14b. The transition temperatures were raised consistently with increasing Si content. However, the maximum K values and C_v(max) were obtained at the highest Si level (1.38%Si) followed by the lowest (0.06%Si) rather than the intermediate (0.36%Si) level. Both in the notch bend and Charpy impact test a cross-over occurred between the 0.36% and 1.38% Si curves.

Chromium:

The notch bend and Charpy impact curves comparing the effects of various chromium contents appear in Figures 9 and 15a respectively. The best properties were obtained for the lowest level (0.51% Cr). With increasing chromium the transition temperatures were raised appreciably, but the effect on toughness was much smaller. In fact, both C_v(max) and peak fracture toughness were slightly higher for the 1.61% Cr alloy than the base .82% Cr level.

Nickel:

Figures 10 and 15c show the notch bend and Charpy impact curves for four nickel levels in the range 1.26 - 6.23% Ni. The largest effect of nickel occurred between 1.26 and 2.83%. The 1.26% nickel steel exhibited the highest room temperature fracture toughness and C_v(max). At the higher levels of 4.45% and 6.23% C (max) was reduced slightly below the value for 2.83% Ni. In both tests the transition temperature was reduced consistently with increasing nickel content, but the effect was most pronounced in the range of 1.26-2.83%. Low temperature toughness was also improved consistently with increasing nickel content.

Molybdenum

Highest Charpy and fracture toughness values were obtained with the lowest molybdenum level of 0.13% as shown in Figures 11 and 16a. Impact energy and fracture toughness were considerably lower at the intermediate (0.30%) level but a further increase in molybdenum content to 1.04% produced only a relatively small decrease in both toughness properties. Molybdenum raised the transition temperatures in both tests. The fact that toughness was not improved by increasing the molybdenum content above 0.13% suggests that the 800°F tempering temperature employed in this study did not introduce appreciable temper brittleness.

Vanadium

Changes in toughness and transition temperature were not consistent with changes in vanadium content as illustrated in Figures 12 and 16b. Lowest fracture toughness and Charpy impact energy values and highest transition temperatures were obtained for the 0.10% V steel. The toughness was improved and the transition temperatures lowered when vanadium was either virtually absent (<0.01%V) or increased to a level of 0.28%.

Aluminum

Aluminum was not beneficial to toughness above the average level of 0.033% utilized in the base composition as shown in Figures 13 and 16c. The notch bend toughness and Charpy impact energy were reduced slightly with increasing aluminum content, but the difference in toughness between 0.13% and 0.34% aluminum appears negligible. Similarly, the transition temperature was slightly lower for 0.033% aluminum and relatively constant in the range of 0.13% to 0.34%.

Summary:

A comparison of the influence of alloying elements on toughness as measured in the notch bend and Charpy impact tests indicates considerable qualitative agreement between these test methods. The agreement was particularly good between the notch bend fracture mode transition temperature at $K_{max}/\sigma_{ys} = .4$ and the Charpy impact test propagation transition temperature in the sense that relative changes due to alloying, for a given series, were essentially the same. A summary of the effects of alloying elements on both transition temperatures appears in Figure 17 and 18.

Relation of Toughness to Tensile Properties

A full interpretation of compositional effects on toughness requires an understanding of how structural and material parameters are affected by alloying and the relation of these properties to toughness. Currently the interplay of the various factors involved is not understood sufficiently well to permit this ideal coupling between composition, structure, and toughness properties in all but a few instances.

A more practical approach involves attempts to relate the tensile behavior of a material with toughness. This does not disregard the effects of alloying elements on structure but merely presumes that any structural changes will also affect common material parameters such as tensile properties which in turn can be correlated with toughness.

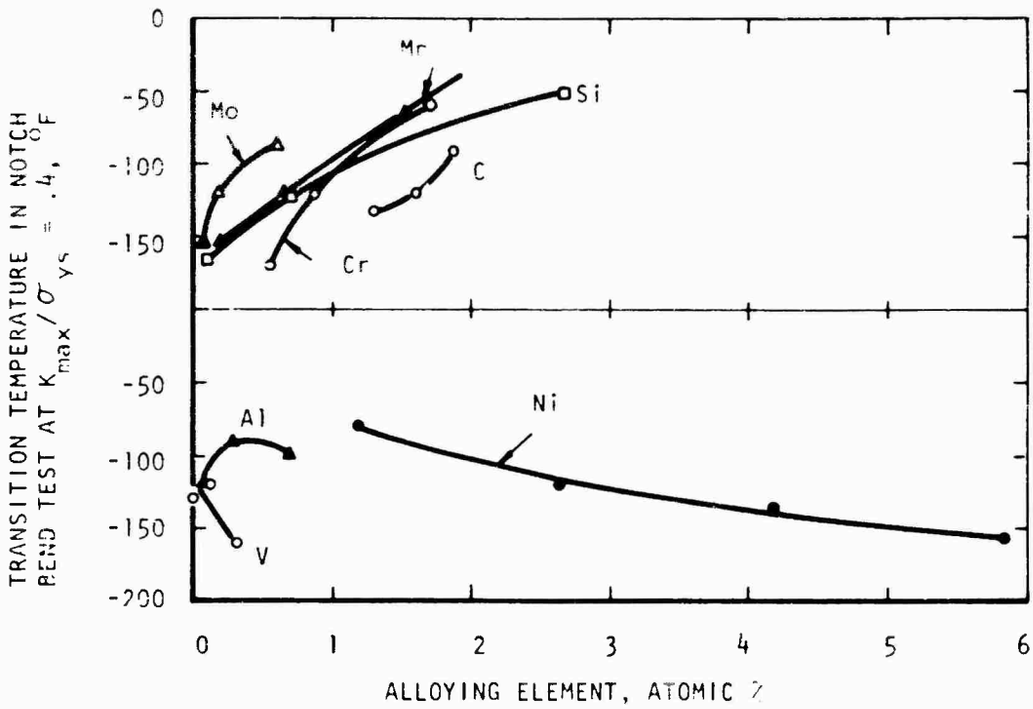

Figure 17. Effect of alloying elements on the notch bend test fracture mode transition temperature.

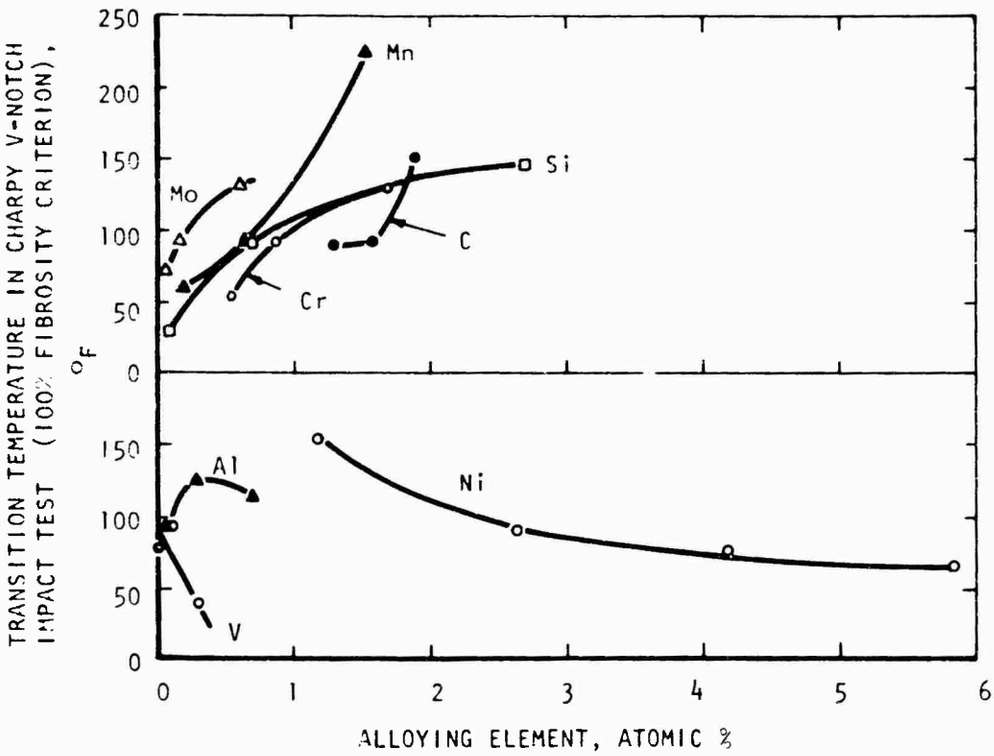

Figure 18. Effect of alloying elements on Charpy impact test propagation transition temperature.

Work Hardening Exponent:

An important factor affecting the stress-strain behavior of a metal and thus its energy absorbing characteristics at the tip of a crack is the work hardening exponent. Presumably any changes in flow characteristics which increase the ability of the plastic zone to absorb energy will result in improved toughness.

However the question of how toughness varies with n has been controversial. According to Gensamer (11) a large n is beneficial to toughness since it would increase the area under the stress-strain curve. The experimental work of Larson and Nunes (10) on 4340 steel heat treated to a wide range of strength levels supported this reasoning in that the Charpy V-notch impact toughness increased with the logarithm of n. The parameter correlated with n was the difference in impact energy between the lowest value required for 100% fibrous fracture, C_v(max), and that required for 0% fibrous fracture. However, other data are available which indicate that a low n can lead to improved fracture toughness in high strength steels (12,13). More recently, the question of whether a high or low value of strain hardening is beneficial to toughness has been related to the macroscopic fracture mode. Steigerwald and Hanna (14) analyzed the effect of n on toughness for various specimen thicknesses in high strength steels, aluminum, and titanium alloys. For thin specimens the fracture occurred entirely by plane stress mode and the surfaces were 100% slant. In this region a high work hardening exponent was beneficial to toughness. As thickness increased the fracture surfaces contained regions of both slant (shear lips) and flat fracture. In this region a low n improved toughness. A decrease in n also shifted the transition from slant to flat fracture to larger thicknesses. This behavior was placed on an analytical basis by plotting the normalized fracture toughness parameters $(K_c/\sigma_{ys})^2 1/2\text{-}B$ versus $(K_{Ic}/\sigma_{ys})^2 1/2\text{-}B$ on logarithmic coordinates. Figure 19 illustrates schematically this method of presentation and shows the effect of n on the curves.

In the present study the fracture mode transition was induced by varying temperature rather than thickness and changes in the normalized toughness parameters resulted from the effects of temperature on σ_{ys}, K_{Ic}, and K_c. The stress intensity factor versus temperature transition curves are analogous to the size induced transition curves described above and shown in Figure 19. The definition of a temperature induced fracture mode transition at $K_{max}/\sigma_{ys} = .4$ provides the required degree of normalization for valid comparisons between steels in terms of n.

The variation of n with alloying is shown in Figure 20. Increasing nickel and manganese content increased n appreciably. Carbon and molybdenum generally raised n, chromium increased n at all temperatures, while the effect of aluminum was negligible above approximately -100°F and

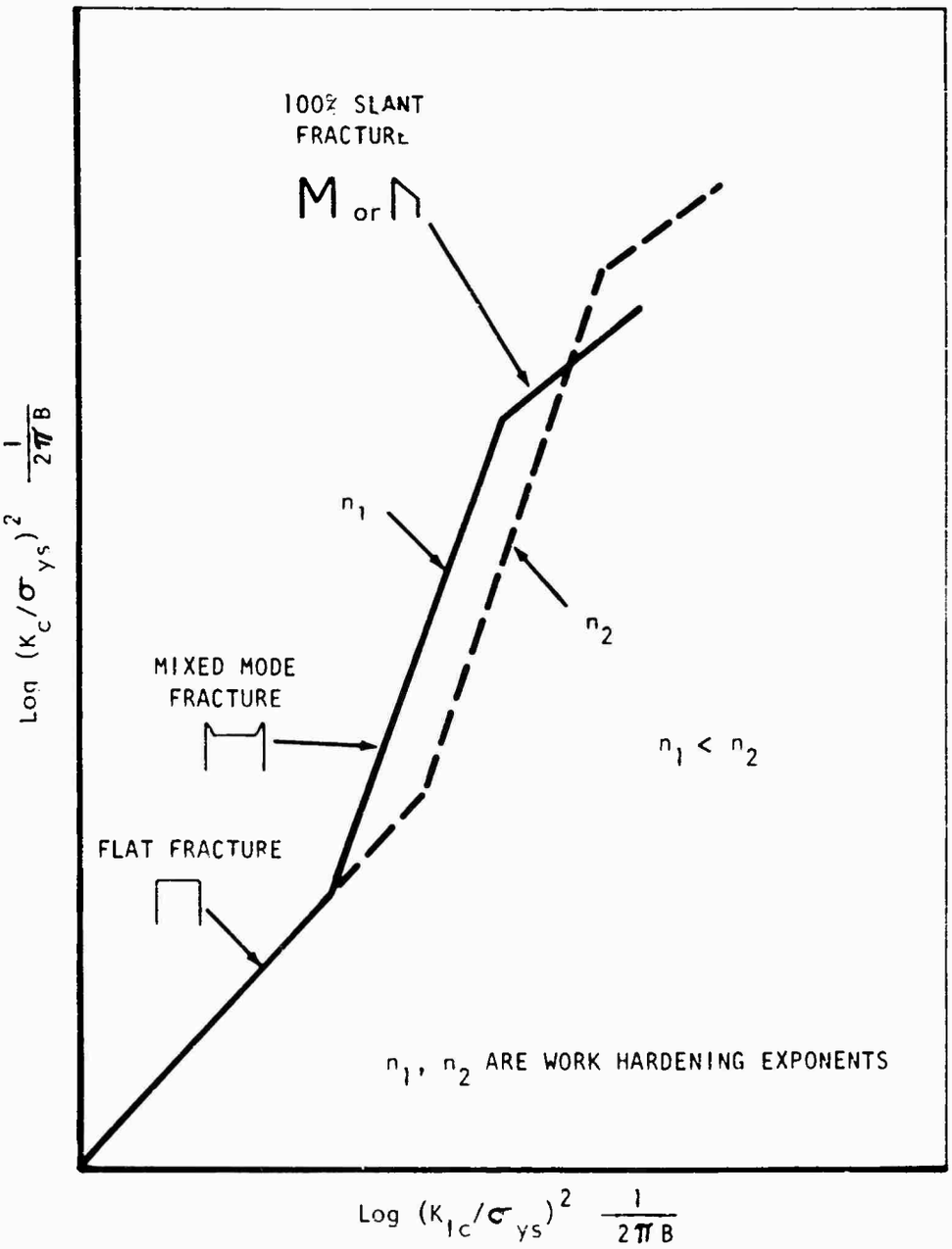

Figure 19. Schematic illustration of method for presenting .cture toughness parameters (ref. 14).

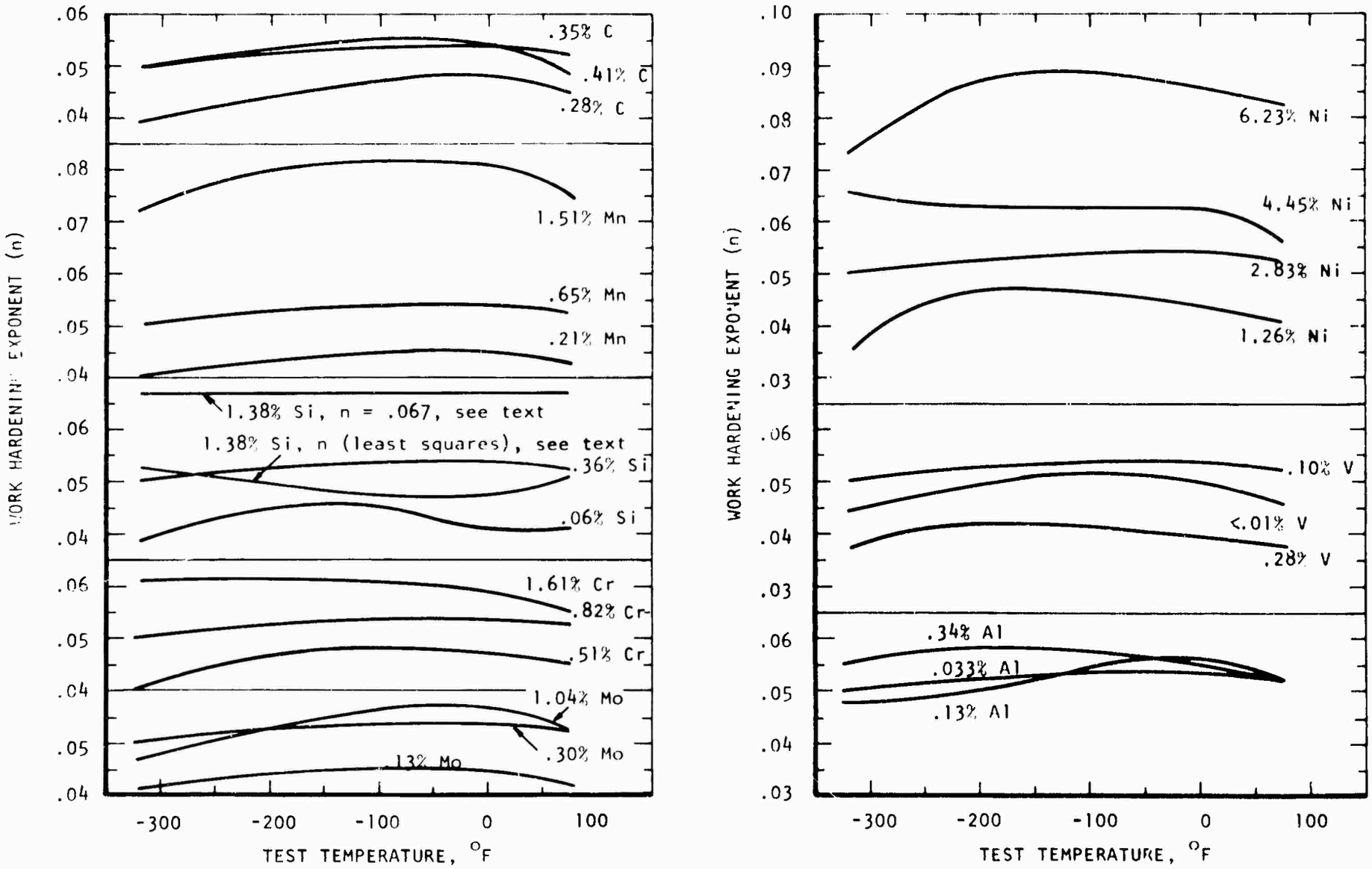

Figure 20. Variation of work hardening exponent with composition and temperature.

slight at lower temperatures. For the vanadium series n was highest for the 0.10% V alloy followed by <0.01% and 0.28% V steels. A constant n of .067 was used for the 1.38% Si alloy. This value corresponded to the slope of the $\log\sigma$ - $\log\varepsilon$ curve at higher strains near the necking point. The data for the silicon series also indicated a rise in n with alloy content providing the work hardening exponent was measured at approximately the necking strain. A manual plot of $\log\sigma$ - $\log\varepsilon$ for all steels showed that n was essentially strain independent for all but the highest silicon alloy, which exhibited a steadily increasing rate of work hardening with strain. The strain at maximum load for this alloy was higher at all temperatures than implied by the n obtained from the linear regression analysis. This suggests that although the relation $\sigma = A\varepsilon^n$ is not applicable for this composition the slope of the $\log\sigma$ -$\log\varepsilon$ curve in the vicinity of the necking strain is a more meaningful measure of n for comparison with other steels.

The temperature induced fracture mode transition defined by $K_{max}/\sigma_{ys} = .4$ is correlated with n in Figure 21 for the various alloy series. In general the transition temperature was reduced with decreasing n, consistent with the shift in fracture mode transition to larger thicknesses described earlier. The apparently inconsistent effect of vanadium on the notch bend transition curves Figure 12, acquires a rationale in terms of n in this representation. The effect of aluminum is not well defined and may be obscured by the small range of both n and transition temperature.

The effect of nickel was opposite to that of the other elements. Increasing nickel raised n markedly yet lowered the transition temperature. The different influence of nickel on the transition temperature is probably an indication that n is not a unique parameter which affects the temperature induced fracture mode transition. Instead the combined variation of alloying and test temperature may influence both microstructural and micro-fracture characteristics in a so-far undetermined manner which overshadows the effect of n.

The influence of n on C_v(max) and 75°F fracture toughness is illustrated in Figures 22 and 23 while Figure 24 shows a plot of the Charpy V-notch energy difference as described earlier versus the logarithm of n. The effect of n was not clear in any of these representations. The data lie in a broad band suggesting a drop rather than rise in toughness with work hardening exponent.

These results are in contrast with those of Larson and Nunes (10) on the effect of n in Charpy V-notch impact tests of 4340 steel. These authors varied n by changing the strength level through heat treatment whereas in the present study n was varied through composition changes

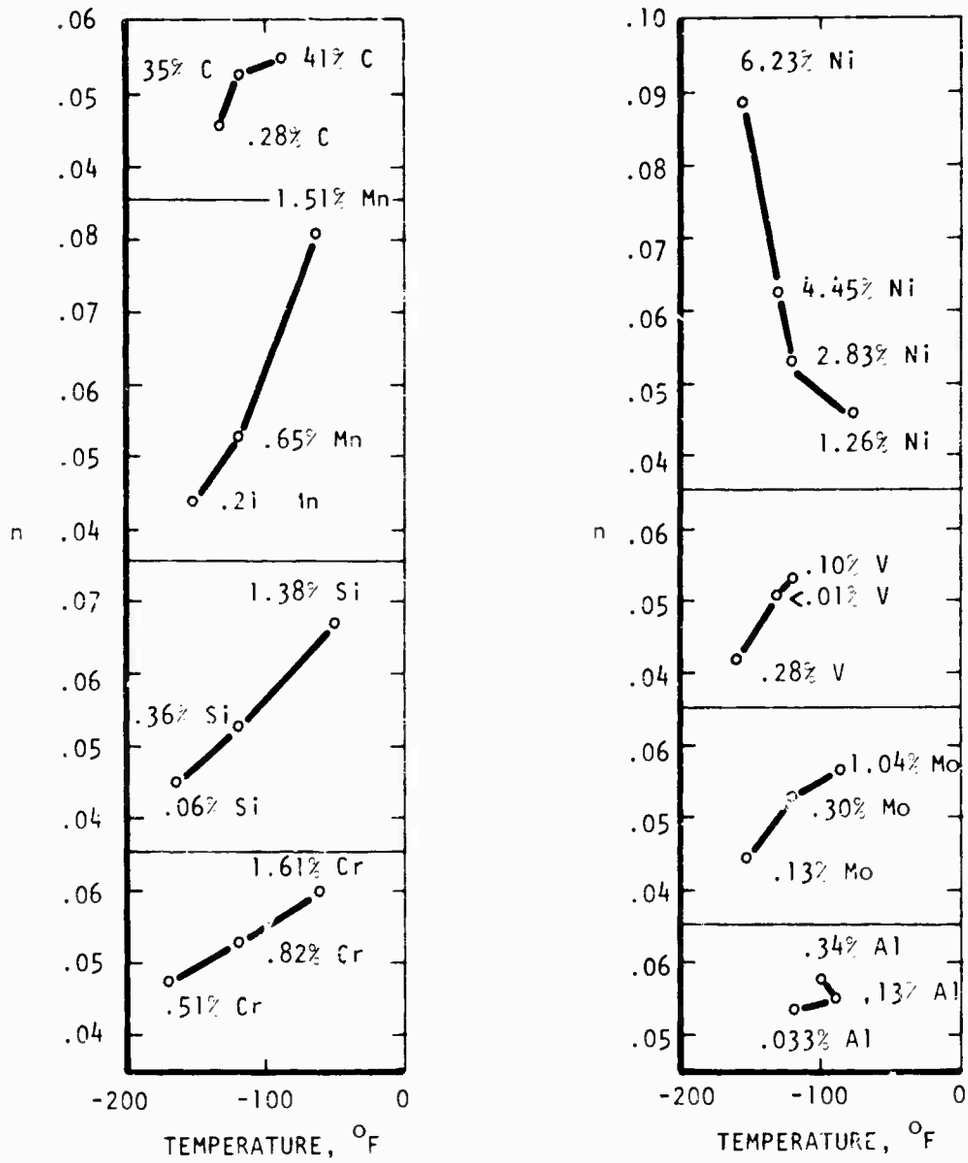

Figure 21. Variation of notch bend transition temperature (at K_{max}/σ_{ys}=.4) with work hardening exponent, n, at the transition temperature for various steels.

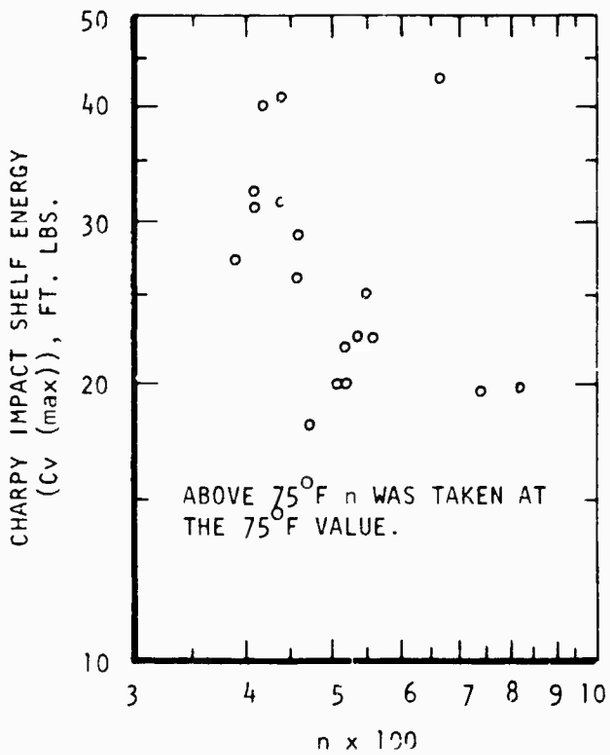

Figure 22. Effect of work hardening exponent on the Charpy shelf energy, C_v(max).

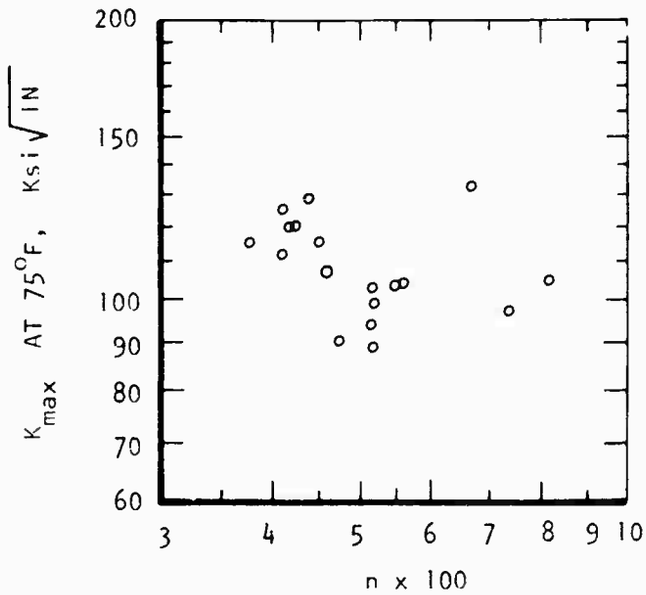

Figure 23. Effect of work hardening exponent on notch bend fracture toughness at 75°F.

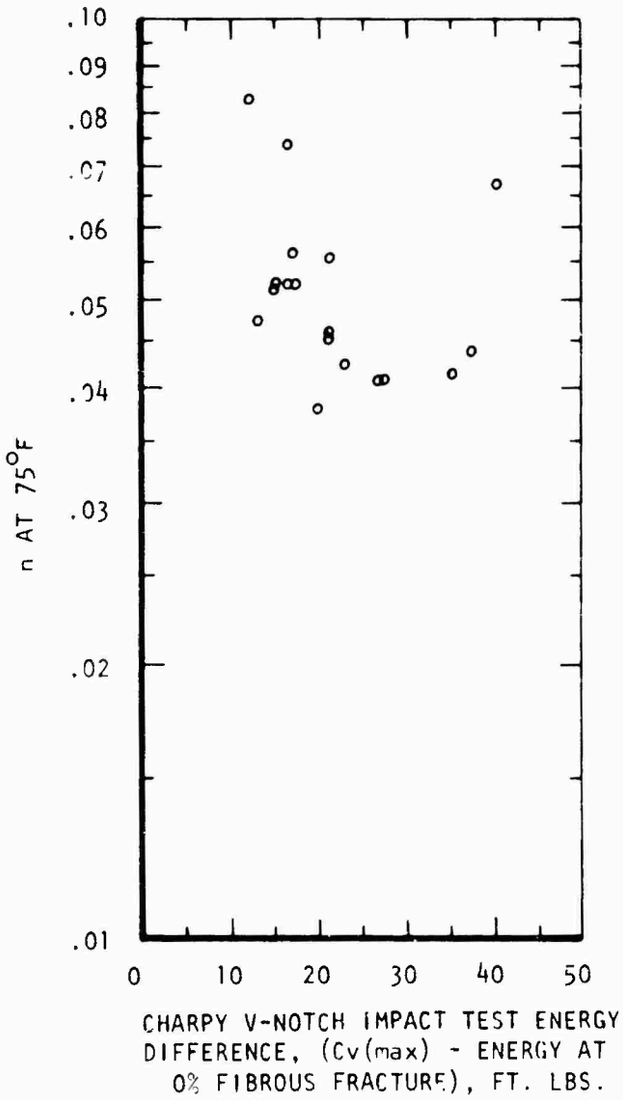

Figure 24. Effect of work hardening exponent on Charpy V-notch impact energy.

and the variations in strength level were slight. The fact that K_{max} at 75°F did not increase with n probably occurred because the fractures were still mixed mode and an upper shelf of purely slant fracture was not observed. Thus the expected effect of n in this region (14) would be to decrease toughness.

The ambiguous effect of n in affecting Charpy impact and notch bend toughness suggests that n, a measure of the tensile instability strain, may not be the governing fracture parameter. Instead, in this region a critical strain criterion based on fracture ductility rather than necking strain may be operating. Figures 25 and 26 show the effect of tensile ductility in notch bend tests, at 75°F and -321°F, and Charpy impact tests at the upper shelf energy and -321°F. The "upper shelf" toughness values exhibited good correlation with true fracture strain. At -321°F, where a critical stress relationship would probably apply, the toughness was fracture strain independent. Similar correlations of tensile ductility with C_v(max) have been observed for other steels (15) including the 4340 steel investigated by Larson and Nunes (10).

Quantitative Models:

A thorough understanding of how material parameters influence toughness requires a separation of their effects. This, however, is generally difficult to achieve experimentally. An alternate approach is offered by certain models which relate fracture toughness to mechanical and structural parameters. Krafft has proposed a tensile instability fracture model which regards crack propagation as occurring by the successive rupture of small tensile specimen-like regions of size d_T (16). The initiation of unstable rupture of these ligaments is considered to occur when the uniaxial tensile necking strain (equal to n) is reached. The equation $K_{Ic} = En\sqrt{2\pi d_T}$ where E is Young's modulus, has been correlated with structure for .45% C-Ni-Cr-Mo steels containing different sulfur levels (17).

Hahn and Rosenfield (18) have developed a ductile fracture model which avoids the difficulty of having to measure the process zone size d_T. Instead the equation $K_{Ic} = (2/3\ EY\bar{\varepsilon}^{*2}n^2)^{1/2}$, where E = Young's modulus, Y = yield strength, $\bar{\varepsilon}^*$ = true fracture strain and n = work hardening exponent, provides a direct relation between ordinary tensile parameters and K_{Ic}. K_{Ic} values calculated from tensile properties of a few steels, titanium and aluminum alloys indicated reasonably good agreement with experimentally measured values, considering that the tensile and K_{Ic} data employed in the comparison were obtained from different sources.

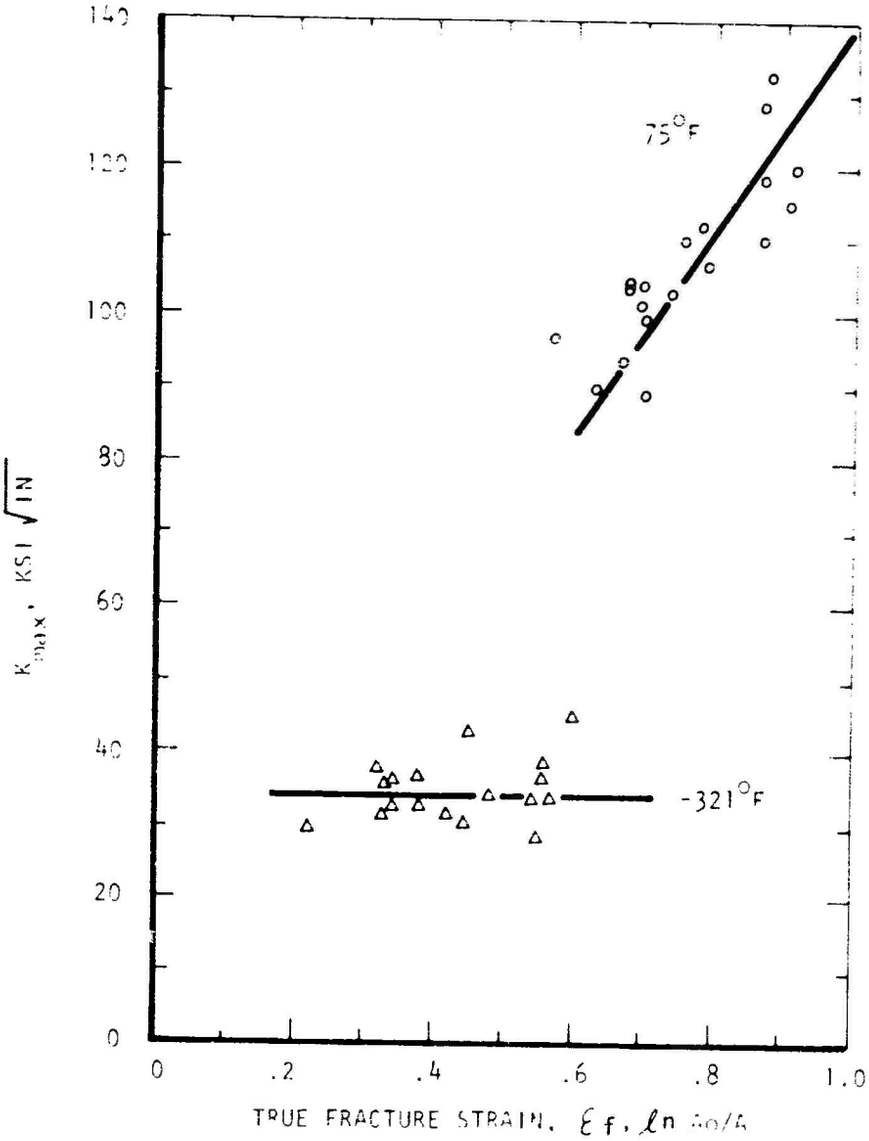

Figure 25. Effect of tensile ductility on notch bend fracture toughness of two test temperatures.

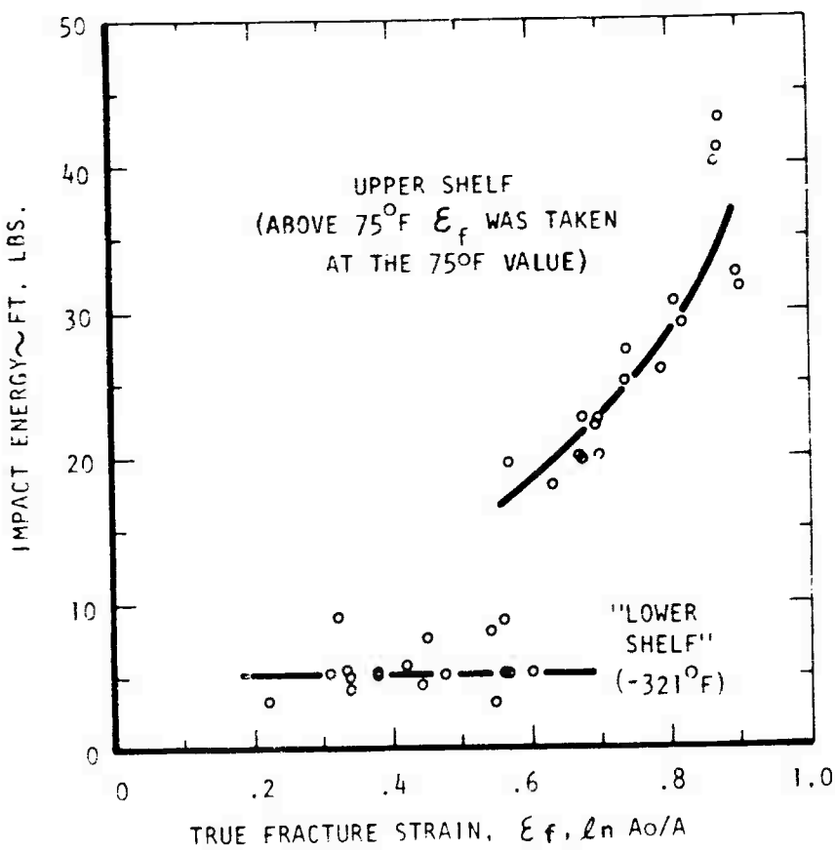

Figure 26. Effect of tensile ductility on the Charpy upper shelf energy and -321°F energy.

A further examination of this model can be performed using the K_{Ic} and tensile data generated on the steels used in the current study. K_{Ic} was computed from tensile test results obtained over the temperature range of -321 to 75°F. Young's modulus is essentially independent of composition for low alloy steels; based on data for 4340 steel (19) it was assumed to vary linearly from a 75°F value of 29×10^3 ksi to 31×10^3 ksi at -321°F.

A valid comparison of calculated and measured K_{Ic} was possible only at low temperatures. In general the variation of calculated K_{Ic} with composition within a particular alloying element series differed from the results of the actual notch bend tests. Furthermore, with decreasing test temperature the calculated K_{Ic} values changed slightly in comparison with the experimental data which exhibited a sharp drop. At -321°F the predicted values were approximately double the observed results. The curves in Figure 27 are typical of those obtained in attempting to apply the Hahn-Rosenfield model.

The large discrepancy at -321°F is believed to be the result of an increase in yield strength and change in microscopic fracture mode at low temperatures. In a fractographic study of 4340 steel Charpy specimens Bucher et al (20) observed an increasing amount of quasi-cleavage fracture with increasing strength level both at room temperature (by varying tempering temperature) and at a single tempering temperature (by decreasing the test temperature). Hahn and Rosenfield have compared the predicted and calculated room temperature K_{Ic} values for 4340 steel as a function of tensile strength (18). Figure 28 shows that the discrepancy tends to increase appreciably at strength levels above 200 ksi ultimate strength.

These observations add support to the earlier suggestion that a critical strain criterion may not apply to fracture in low alloy steels at low temperatures. Any use of the Hahn-Rosenfield model to predict K_{Ic} should involve an appreciation for the microscopic fracture mode. If a portion of the fracture involves quasicleavage or intergranular crack propagation then the observed toughness will be less than predicted from the model.

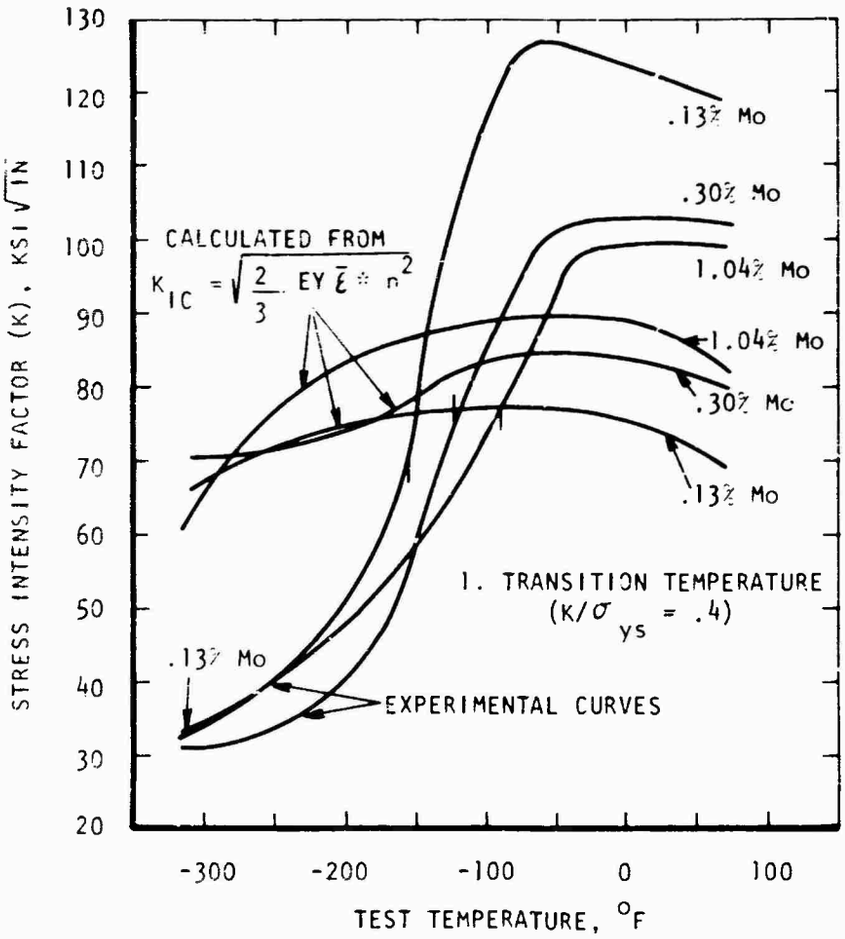

Figure 27. Comparison of measured and calculated K_{Ic} (typical results).
Note: Above the transition temperature experimental values are generally not valid K_{Ic}.

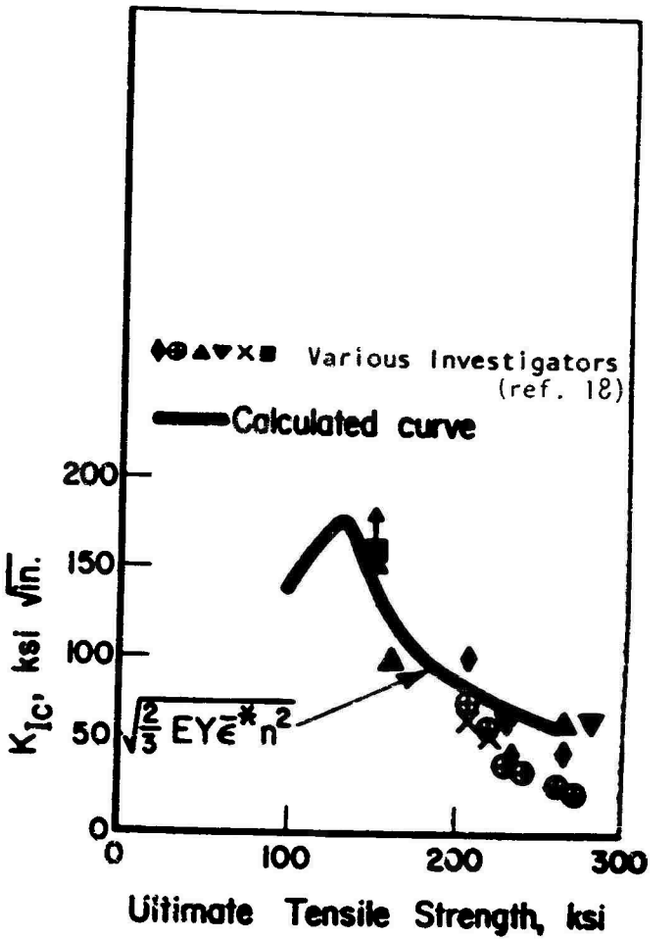

Figure 28. Calculated and measured K_{Ic} values for 4340 steel. (ref. 18)

IV SUMMARY AND CONCLUSIONS

This study has examined the effects of various elements on the notch bend fracture toughness and Charpy impact behavior of a .35%C, 3%Ni, Cr-Mo-V martensitic steel at a room temperature yield strength of approximately 160-180 ksi. A classical approach was used in the design of alloys which permitted an evaluation of single element effects rather than interactions.

An analysis of the toughness data was conducted in terms of the effects of alloying elements on yield strength, tensile ductility, and work hardening exponent. The elements C, Mn, Si, Cr, and Mo raised both the notch bend fracture mode transition temperature and the Charpy propagation transition temperature. These elements generally raised the work hardening exponent and reduced toughness. In amounts above that required for deoxidation and grain refinement, aluminum appeared to degrade the transition temperature and toughness slightly. Increasing the vanadium content from 0.1 to 0.28% produced a significant improvement in toughness and transition temperature.

Relative changes in transition temperature in the notch bend test corresponded with shifts in the Charpy impact test propagation transition temperature.

Over the range of compositions examined (1.26 - 6.23%) nickel decreased the transition temperature and improved toughness at the lower test temperatures. For most alloy series the notch bend transition temperature was lowered as n decreased, but nickel acted in an opposite manner.

Charpy shelf energy, C_v(max), and K_{max} at 75°F did not correlate well with n. Good agreement was obtained however when these parameters were plotted versus true fracture strain. At -321°F toughness was essentially fracture strain independent suggesting that a critical strain criterion based on fracture strain is valid only when fracture is principally fibrous.

A comparison of K_{Ic} calculated from tensile data using the Hahn-Rosenfield model with measured values suggested that the increased contribution of non-ductile fracture which accompanies increases in strength and/or decreases in test temperature in low alloy steels can lead to large errors in the predicted toughness.

V LIST OF REFERENCES

1. Military Specification, "Tubular Parts for Cannons over 30mm, Steel Forgings for," MIL-T-10458D(MR), (1 April 1966).

2. Military Specification, "Steel Forgings, Tubular Parts for Cannon, High Yield Strength (160-180 Ksi)," MIL-S-46119(MR), (23 March 1967).

3. J. F. Throop, D. P. Kendall, J. H. Underwood, and R. R. Fujczak, "Fatigue Crack Propagation in Single-Notch Tensile Specimens of Steel," Prepared for presentation to ASTM Committee E-9, Watervliet Arsenal, (March, 1967).

4. E. A. Steigerwald and C. Vishnevsky, "Literature Survey on the Influence of Alloy Elements on the Fracture Toughness of High Strength Steels," TRW Inc., Contract DAAG 46-67-C-0171, AMMRC CR-67-13(F), (February, 1968).

5. ASTM E-24, "Recommended Practice for Plane-Strain Fracture Toughness Testing of High Strength Metallic Materials Using a Crack-Notch Bend Specimen," (1967).

6. W. F. Brown and J. E. Srawley, Plane Strain Crack Toughness Testing of High Strength Metallic Materials, ASTM STP. No. 410, (December, 1966).

7. E. F. Walker and M. J. May, "Single Edge Notch Specimens of Two High Strength Martensitic Steels Tested in Tension and Bending," BISRA Report MG/EB/337/67, (1967).

8. E. F. Walker and M. J. May, "Note on the Effect of Fatigue Pre-Cracking Stress on the Plane Strain Fracture Toughness of Several Martensitic Steels," presented to ASTM E-24 Subcommittee 1, (March 13, 1968).

9. M. F. Amateau and E. A. Steigerwald, "Test Methods for Determining Fracture Toughness of Metallic Materials," Final Report, Contract AF 33(615)-3827, (May, 1967).

10. F. R. Larson and J. Nunes, "Relationships Between Energy, Fibrosity, and Temperature in Charpy Impact Tests on AISI 4340 Steel," Proc. ASTM, 62, 1192 (1962).

11. M. Gensamer, "Strength and Ductility - Campbell Memorial Lecture," Trans. ASM, 36, (1946).

12. W. W. Gerberich, "Fracture Toughness of SAE 4340 Steel Heat-Treated to 200,000 to 300,000 psi Yield Strengths," TR32-96, Jet Propulsion Laboratory, Pasadena, California, (1961).

13. W. W. Gerberich, "Plane Strains and Energy Density in Cracked Plates," Experimental Mechanics, 4, 335, (1964).

14. E. A. Steigerwald and G. L. Hanna, "Influence of Work Hardening Exponent on the Fracture Toughness of High-Strength Materials," Trans. AIME, 242, 320, (February, 1968).

15. A. S. Tetelman and A. J. McEvily, Jr., Fracture of Structural Materials, John Wiley, New York, (1967).

16. J. M. Krafft, "Correlation of Plane Strain Crack Toughness with Strain Hardening Characteristics of a Low, a Medium, and a High Strength Steel," Applied Materials Research, 88, (April, 1964).

17. A. J. Birkle, R. P. Wei and G. E. Pellissier, "Analysis of Plane-Strain Fracture in a Series of 0.45C - Ni-Cr-Mo steels with Different Sulfur Contents," ASM Trans. Quart., 59, 981, (1966).

18. G. T. Hahn and A. R. Rosenfield, "Source of Fracture Toughness: The Relation Between K_{Ic} and the Ordinary Tensile Properties of Metals," Applications Related Phenomena in Titanium and its Alloys, ASTM STP. No. 432, 5, (1968).

19. Mil. Handbook 5A, Metallic Materials and Elements for Aerospace Vehicle Structures, Table 2.3.1.1(a), Figure 2.3.1.2.4, (February 8, 1966).

20. J. H. Bucher, J. T. Cammett, J. C. Jasper, G. W. Powell and J. W. Spertnak, "The Relationship of Microstructure to Strength and Toughness in High-Strength Steel," AFML-TR-65-60, (March, 1965).

APPENDIX

TABLE A1 (a)

Summary of Smooth Tensile Properties

Specimen (Heat No. - Test No.)	Test Temp. °F	Tensile Strength (ksi)	.2% Yield Strength (ksi)	%Elong. 1"G.L.	% Red. in Area	Work Hard. Exponent (n)
5-1	75	199.9	177.9	14	49.7	-
5-2	"	200.9	176.4	14	45.2	.053
5-8	20	206.4	181.9	15	49.1	.056
5-7	-40	207.6	179.6	15	47.3	.059
5-5	-100	216.9	188.6	13	47.3	.058
5-6	-215	229.4	-	-	37.3	-
5-6D	"	226.2	201.7	12	36.6	.050
5-3	-321	256.3	230.1	-	-	.051
5-4	"	251.2	-	-	18.1	-
5-10	"	253.6	229.0	-	-	.056
5-11	"	254.5	-	-	33.6	-
5-12	"	254.0	-	-	34.3	-
6-1	75	197.8	182.5	14	50.7	-
6-2	"	198.0	176.4	15	56.3	.052
6-8	20	200.8	178.6	15	50.7	.049
6-7	-40	207.5	183.9	16	51.3	.051
6-5	-100	213.4	190.9	15	48.4	.047
6-9	-140	214.9	187.6	15	45.5	.057
6-6	-215	223.9	-	-	-	-
6-6D	"	222.2	201.5	-	-	.050
6-3	-321	256.3	230.1	-	-	.042
6-4	"	251.0	-	-	42.1	-
6-11	"	251.0	-	-	43.9	-
6-12	"	252.0	-	-	32.7	-
7-1	75	195.8	169.6	15	50.3	.055
7-2	"	191.6	165.8	17	48.7	.057
7-8	20	200.2	171.1	15	48.5	.063
7-7	-40	204.5	-	16	44.9	-
7-5	-100	210.4	180.2	14	46.7	.062
7-9	-150	215.5	182.9	16	45.5	.063
7-6	-215	220.5	196.7	-	-	.063
7-6D	"	223.9	195.3	14	41.3	.057
7-3	-321	248.1	210.5	14	26.4	.068
7-4	"	251.0	-	15	37.0	-

TABLE AI(a) (Continued)

Specimen (Heat No.-Test No.	Test Temp. °F	Tensile Strength(ksi)	.2% Yield Strength(ksi)	%Elong. 1"G.L.	% Red. in Area	Work Hard. Exponent(n)
8-1	75	200.2	182.2	15	54.6	.040
8-2	"	200.7	183.7	15	57.4	.041
8-8	20	205.4	187.4	15	53.7	.044
8-7	-40	207.6	189.5	14	53.6	.045
8-5	-100	214.9	199.1	12	57.2	.043
8-9	-150	218.0	200.8	15	54.1	.048
8-6	-215	230.6	213.8	-	43.6	.047
8-3	-321	253.4	240.6	15	35.9	.029
8-4	"	250.6	241.8	16	42.0	.035
8-10	"	249.3	235.0	15	31.2	.036
9-1	75	189.3	171.4	14	59.6	.044
9-2	"	187.2	168.5	16	58.6	.045
9-8	20	195.4	176.4	15	54.2	.046
9-7	-40	198.2	177.4	16	53.7	.050
9-5	-100	204.7	184.3	16	51.5	.046
9-9	-150	208.5	186.0	15	50.3	.053
9-6	-215	214.7	195.3	-	49.2	.045
9-3	-321	242.4	224.2	16	42.2	.040
9-4	"	241.8	222.4	18	40.9	.040
9-10	"	242.4	-	16	44.0	-
12-1	75	181.6	165.3	15	59.5	.040
12-2	"	182.6	165.3	16	56.9	.042
12-8	20	189.7	171.5	16	59.3	.046
12-7	-40	192.4	173.8	17	58.9	.046
12-5	-100	197.2	178.7	16	56.1	.043
12-9	-150	206.3	-	16	55.1	-
12-6	-215	211.0	192.8	-	53.1	.045
12-3	-321	234.7	221.8	-	-	.043
12-4	"	237.9	-	-	46.7	-
12-10	"	234.8	218.5	17	40.3	.039

TABLE A1(a) (Continued)

Specimen (Heat No.-Test No.)	Test Temp.°F	Tensile Strength(ksi)	.2% Yield Strength(ksi)	%Elong. 1"G.L.	% Red. in Area	Work Hard. Exponent(n)
13-1	75	209.5	183.0	15	49.9	.051
13-2	"	207.6	182.0	14	51.6	.054
13-8	20	214.2	185.3	15	49.8	.059
13-7	-40	217.6	190.9	14	48.8	.054
13-5	-100	222.7	193.6	14	47.7	.056
13-9	-150	225.7	199.6	16	49.8	.052
13-6	-215	234.3	206.2	-	45.2	.054
13-3	-321	259.1	234.9	15	28.8	.046
13-4	"	261.0	-	-	-	-
13-10	"	260.4	235.9	-	-	.047
14-1	75	193.7	175.8	17	59.9	.041
14-2	"	193.0	175.0	16	59.4	.041
14-8	20	197.1	179.9	16	59.8	.041
14-7	-40	202.4	185.4	17	57.8	.042
14-5	-100	205.6	187.3	18	57.7	.045
14-9	-150	211.7	192.0	15	54.1	.046
14-6	-215	219.2	194.0	-	-	.036
14-6D	"	217.2	189.5	-	-	.045
14-3	-321	244.2	228.5	18	46.2	.038
14-4	"	243.8	227.2	16	44.3	.039
16-1	75	188.5	171.5	20	59.2	.047*
16-2	"	187.1	168.7	20	57.8	.056*
16-8	20	194.3	176.6	18	54.9	.044*
16-7	-40	189.6	180.7	20	57.2	.048*
16-5	-100	204.7	185.3	19	50.9	.045*
16-5D	"	204.5	185.0	16	52.7	.050*
16-9	-150	210.4	190.8	20	54.4	.048*
16-6	-215	216.7	193.2	-	49.2	.050*
16-3	-321	242.2	217.5	-	-	.053*
16-4	"	243.5	-	19	42.4	-

* Values based on lease squares fit of $\log\sigma$ - $\log\varepsilon$ data, however, n was considered to be approximately .067 at all temperatures (see text for detailed explanation).

TABLE AI(a) (Continued)

Specimen (Heat No.-Test No.	Test Temp.°F	Tensile Strength(ksi)	.2% Yield Strength(ksi)	%Elong. 1"G.L.	% Red. in Area	Work Hard. Exponent (n)
17-1	75	204.7	170.0	14	44.3	.072
17-2	"	204.3	168.2	15	42.2	.077
17-8	20	210.7	175.0	15	45.1	.080
17-7	-40	214.9	174.7	15	44.3	.081
17-5	-100	219.6	177.1	14	42.6	.080
17-9	-150	226.8	175.6	13	39.4	.091
17-6	-215	227.8	186.4	-	40.7	.079
17-3	-321	257.7	216.8	-	-	.071
17-4	"	258.7	-	16	17.2	-
17-10	"	259.2	216.5	15	23.5	.071
18-1	75	199.6	1[illegible].0	16	56.6	.055
18-2	"	200.5	175.2	15	51.4	.055
18-8	20	205.2	178.1	15	52.3	.058
18-7	-40	211.1	181.4	15	49.5	.063
18-5	-100	214.0	183.6	14	48.3	.061
18-9	-150	217.9	188.5	14	48.3	.061
18-6	-215	228.6	197.6	-	-	.061
18-6D	"	229.0	200.2	14	45.4	.058
18-3	-321	253.4	221.5	14	29.0	.057
18-4	"	255.9	223.5	-	-	.065
19-1	75	200.8	177.4	14	51.3	.050
19-2	"	200.9	176.6	14	49.8	.053
19-8	20	203.8	179.8	14	47.3	.053
19-7	-40	211.6	184.9	15	46.7	.059
19-5	-100	216.7	188.9	13	45.4	.056
19-9	-150	221.7	190.7	14	43.7	.060
19-6	-215	228.4	199.5	-	43.1	.057
19-3	-321	25318	224.1	-	-	.058
19-4	"	256.9	-	15	31.7	-
19-10	"	255.3	225.6	14	31.7	.053
20-1	75	202.0	178.9	13	50.2	.051
20-2	"	203.6	180.5	13	48.5	.051
20-8	20	209.3	183.2	14	47.8	.057
20-7	-40	213.2	187.5	13	41.8	.056
20-5	-100	219.9	192.4	14	44.2	.056
20-9	-150	223.2	198.0	14	43.6	.051
20-6	-215	228.8	204.3	-	38.3	.050
20-3	-321	255.3	229.7	14	28.5	.042
20-4	"	256.1	228.4	-	-	.051
20-10	"	258.5	231.9	-	-	.050

TABLE AI (a) (Continued)

Specimen (Heat No.-Test No.)	Test Temp.°F	Tensile Strength(ksi)	.2% Yield Strength(ksi)	%Elong. 1"G.L.	% Red. in Area	Work Hard. Exponent(n)
21-1	75	193.7	173.1	15	55.2	.046
21-2	"	194.6	173.7	14	53.6	.046
21-8	20	196.3	174.1	13	52.4	.049
21-7	-40	202.3	180.2	15	50.2	.051
21-5	-100	207.2	184.4	15	50.2	.052
21-9	-150	211.6	188.6	14	46.7	.051
21-6	-215	220.7	199.6	-	-	.048
21-3	-321	245.9	225-5	16	36.6	.046
21-4	"	245.4	224.9	18	40.1	.046
21-10	"	247.7	226.2	16	38.2	.039
22-1	75	197.4	182.3	13	52.4	.036
22-2	"	198.6	182.6	15	53.0	.040
22-8	20	203.1	187.5	14	52.3	.042
22-7	-40	208.4	193.4	15	53.4	.038
22-5	-100	210.2	193.0	15	50.7	.045
22-9	-150	219.1	202.5	14	47.8	.040
22-6	-215	224.7	207.4	-	-	.040
22-6D	"	225.7	208.9	-	-	.043
22-3	-321	251.2	236.9	16	35.8	.036
22-4	"	252.4	237.0	18	35.5	.038
26-1	75	192.0	174.5	16	61.5	.041
26-2	"	191.5	172.8	15	58.0	.044
26-8	20	196.8	177.9	16	60.4	.045
26-7	-40	199.7	179.8	15	57.7	.047
26-5	-100	204.2	185.1	15	55.1	.044
26-9	-150	208.8	189.8	16	54.8	.043
26-6	-215	216.9	198.9	-	54.2	.042
26-3	-321	243.1	224.2	17	43.5	.042
26-4	"	246.0	228.9	16	45.3	.039
26-10	"	244.4	226.2	17	40.1	.040
27-1	75	186.4	169.2	15	54.0	.044
27-2	"	185.9	163.9	17	61.4	.045
27-8	20	189.9	169.5	17	59.5	.049
27-7	-40	196.2	174.5	17	59.5	.049
27-5	-100	199.5	180.3	15	56.2	.044
27-9	-150	208.1	-	18	55.1	-
27-6	-215	216.1	198.0	-	-	.047
27-6D	"	209.4	188.2	15	56.6	.040
27-3	-321	237.2	217.7	18	41.3	.041
27-4	"	236.6	215.5	16	45.0	.037

TABLE A1 (a) (Continued)

Specimen (Heat No. - Test No.)	Test Temp. °F	Tensile Strength (ksi)	.2% Yield Strength (ksi)	%Elong. 1"G.L.	% Red. in Area	Work Hard. Exponent (n)
28-1	75	208.7	187.0	12	48.0	.048
28-2	"	209.9	188.4	14	48.0	.047
28-8	20	211.5	186.9	15	42.0	.054
28-7	-40	217.6	188.6	16	44.4	.060
28-5	-100	222.5	196.5	13	44.3	.052
28-9	-150	226.6	198.4	14	43.2	.055
28-6	-215	231.1	204.9	-	44.4	.053
28-3	-321	259.6	235.4	14	24.4	.046
28-4	"	262.4	233.8	15	35.0	.050
28-10	"	261.4	231.7	-	-	.053
29-1	75	198.4	162.1	15	48.6	.076
29-2	"	197.3	161.3	15	49.2	.089
29-8	20	202.8	165.2	15	49.2	.079
29-7	-40	208.8	164.9	15	44.3	.089
29-5	-100	217.1	171.0	14	45.1	.088
29-9	-150	220.9	171.3	13	42.1	.092
29-6	-215	225.1	182.9	-	47.3	.078
29-3	-321	251.8	206.3	16	32.0	.069
29-4	"	251.4	205.2	-	-	.077
29-10	"	252.0	209.8	14	23.7	.074

TABLE AI (b)

EFFECT OF ORIENTATION ON ROOM TEMPERATURE

TENSILE TEST RESULTS FOR A BASE COMPOSITION HEAT

Heat	Specimen	Tempering Temp., °F	Tensile Strength Ksi	Yield Strength 2% Offset, Ksi	Reduction of Area, %	Elongation in 1", %
5	A - Long.*	1000	185.1	165.4	58.0	18
5	B - Long.*	1000	182.3	163.5	56.4	18
5	C - Trans.**	1000	183.2	164.4	45.5	
5	D - Trans.**	1000	180.8	162.0	50.3	

* Longitudinal; 250" diameter, 1-1/4" straight section, 1" gage length.

** Transverse; 250" diameter, 3/4" straight section.

TABLE AII

Fracture Toughness Data, Three Point Loading, Major Span 3.68"

Specimen	Test Temp. °F	Thick. B, (in)	Width W, (in)	Crack Length a, (in)	Curve Type	% (4) Shear	Load (lbs) P_{max}	Load (lbs) P_Q	Fracture Toughness Ksi $\sqrt{in}$ K_{max} (1)	Fracture Toughness Ksi $\sqrt{in}$ K_Q (2)	Ratio $(K_Q/\sigma_{ys})^2$	$\frac{B}{R}$	$\frac{a}{R}$	K_{IC} (3)
5-1	75	.480	.921	.445	I	31	4640	3770	101.5	82.5	.217	2.2	2.0	-
5-6	-10	.480	.920	.429	I	29	4893	4375	101.8	91.0	.251	1.9	1.7	-
5-4	-40	.481	.920	.435	I	23	4747	3952	100.6	83.7	.208	2.3	2.2	-
5-7	-70	.481	.921	.456	II	15	3717	3717	84.3	84.3	.207	2.3	2.2	-
5-3	-100	.480	.920	.431	III	13	3431	3431	71.8	71.8	.146	3.3	3.0	71.8
5-8	-130	.480	.921	.445	III	9	3210	3210	70.2	70.2	.135	3.6	3.3	70.2
5-5	-155	.480	.920	.442	II	5	2400	2265	52.2	49.2	.064	7.5	6.9	49.2
5-9	-155	.480	.920	.469	II	9	2665	2665	63.6	63.6	.107	4.5	4.4	63.6
5-10	-155	.480	.920	.433	III	7	3055	3055	64.4	64.4	.110	4.4	3.9	64.4
5-2	-321	.480	.921	.432	III	0	1502	1502	31.4	31.4	.018	26.0	23.4	31.4
6-1	75	.479	.920	.448	I	33	4670	3640	103.8	80.9	.209	2.3	2.1	-
6-6	-10	.480	.919	.433	I	29	4915	4020	104.0	85.0	.219	2.2	2.0	-
6-4	-40	.481	.920	.422	I	27	5140	4480	104.3	90.9	.245	2.0	1.8	-
6-7	-70	.480	.919	.436	I	31	4775	3945	102.0	84.3	.207	2.3	2.1	-
6-3	-100	.480	.920	.425	II	10	4420	4420	90.8	90.9	.234	2.1	1.8	-
6-10	-120	.479	.919	.429	II	13	4035	4035	84.4	84.4	.197	2.4	2.2	-
6-8	-130	.480	.921	.444	II	11	3215	2985	70.1	65.1	.135	3.6	3.3	65.1
6-9	-140	.481	.921	.425	III	11	3430	3430	70.1	70.1	.133	3.6	3.2	70.1
6-5	-155	.480	.920	.442	III	5	2895	2895	58.2	58.2	.090	5.3	4.9	58.2
6-2	-321	.480	.921	.423	III	0	1560	1560	31.7	31.7	.019	25.3	22.3	31.7

(1) fracture toughness computed using maximum load P_{max}

(2) tentative K_{IC} computed using load P_Q

(3) valid plain strain fracture toughness value, Ksi $\sqrt{in}$

(4) proportion of oblique fracture midway between crack tip and unnotched specimen edge.

TABLE AII (Continued)

Specimen	Test Temp. °F	Thick. B, (in)	Width W, (in)	Crack Length a, (in)	Curve Type	% (4) Shear	Load (lbs) P_{max}	Load (lbs) P_Q	Fracture Toughness Ksi $\sqrt{in}$ K_{max} (1)	Fracture Toughness Ksi $\sqrt{in}$ K_Q (2)	Ratio $(K_Q/\sigma_{ys})^2$ (R)	$\frac{B}{R}$	$\frac{a}{R}$	K_{IC} (3)
7-1	75	.480	.920	.432	I	31	4917	4112	103.3	86.4	.266	1.8	1.6	-
7-6	-10	.480	.921	.451	I	29	4625	3600	103.6	80.7	.216	2.2	2.1	-
7-4	-40	.480	.921	.435	I	27	4690	3850	99.2	81.5	.214	2.2	2.0	-
7-7	-70	.479	.921	.431	I	23	4800	4060	100.4	85.0	.227	2.1	1.9	-
7-3	-100	.479	.919	.426	II	19	4606	4606	94.9	94.9	.273	1.8	1.6	-
7-10	-120	.480	.920	.438	II	17	4015	4015	86.1	86.1	.219	2.2	2.0	-
7-8	-130	.480	.921	.419	II	15	3603	3603	72.3	72.3	.153	3.1	2.7	72.3
7-9	-140	.479	.920	.431	II	15	3415	3415	71.7	71.7	.149	3.2	2.9	71.7
7-5	-155	.479	.921	.430	III	7	3132	3132	65.3	65.3	.121	4.0	3.6	65.3
7-2	-321	.480	.921	.438	III	0	1713	1713	36.6	36.6	.030	16.0	14.6	36.6
8-1	75	.480	.920	.429	I	33	5377	4600	111.9	95.7	.273	1.8	1.6	-
8-6	-10	.480	.921	.426	I	27	5476	4421	112.5	90.8	.240	2.0	1.8	-
8-4	-40	.479	.920	.428	I	17	4645	4345	96.5	90.3	.224	2.1	1.9	-
8-7	-70	.480	.919	.429	II	13	3580	3580	74.7	74.7	.149	3.2	2.9	74.7
8-3	-100	.481	.920	.441	III	8	3204	3204	69.4	69.4	.124	3.9	3.6	69.4
8-10	-100	.480	.920	.416	III	9	2965	2965	59.1	59.1	.090	5.3	4.6	59.1
8-8	-130	.481	.919	.436	III	7	2542	2542	54.2	54.2	.073	6.6	6.0	54.2
8-9	-130	.480	.920	.421	III	7	3160	3160	64.1	64.1	.102	4.7	4.1	64.1
8-5	-155	.480	.919	.428	III	3	2416	2416	50.3	50.3	.061	7.9	7.0	50.3
8-2	-321	.480	.920	.432	III	0	1430	1430	30.0	30.0	.016	30.0	27.0	30.0

(1) fracture toughness computed using maximum load P_{max}
(2) tentative K_{IC} computed using load P_Q
(3) valid plain strain fracture toughness value, Ksi $\sqrt{in}$
(4) proportion of oblique fracture midway between crack tip and unnotched specimen edge

TABLE AII (Continued)

Specimen	Test Temp. °F	Thick. B, (in)	Width W, (in)	Crack Length a, (in)	Curve Type	% (4) Shear	Load (lbs) P_{max}	Load (lbs) P_Q	Fracture Toughness Ksi √in K_{max} (1)	Fracture Toughness Ksi √in K_Q (2)	Ratio (R) $(K_Q/\sigma_{ys})^2$	$\frac{B}{R}$	$\frac{a}{R}$	K_{IC} (3)
9-1	75	.480	.921	.428	I	36	5322	4612	110.3	95.4	.315	1.5	1.3	-
9-6	-10	.480	.921	.464	I	38	5032	4050	117.6	94.6	.289	1.7	1.6	-
9-4	-40	.479	.921	.440	I	36	5365	4215	115.7	90.9	.259	1.8	1.7	-
9-7	-70	.481	.919	.434	I	32	5329	4169	112.9	88.3	.239	2.0	1.8	-
9-3	-100	.480	.921	.438	I	17	5410	4560	116.1	97.9	.286	1.7	1.5	-
9-10	-100	.481	.920	.454	I	19	5135	4305	116.0	97.3	.283	1.7	1.6	-
9-8	-130	.480	.921	.436	I	17	4672	4672	99.2	99.2	.287	1.7	1.5	-
9-9	-130	.480	.920	.438	I	17	5160	4525	110.6	97.0	.275	1.7	1.6	-
9-5	-155	.481	.919	.430	II	12	4067	4067	85.0	85.0	.206	2.3	2.1	-
9-2	-321	.480	.919	.437	III	0	1552	1552	33.3	33.3	.022	21.6	19.7	33.3
12-1	75	.480	.920	.466	I	44	5025	3960	118.6	93.5	.319	1.5	1.5	-
12-6	-10	.481	.919	.442	I	42	5710	3900	124.2	84.9	.244	2.0	1.8	-
12-4	-40	.480	.920	.436	I	33	5868	4823	125.0	102.7	.344	1.4	1.3	-
12-7	-70	.480	.920	.450	I	23	5675	4050	126.7	90.4	.259	1.9	1.7	-
12-3	-100	.480	.918	.428	I	17	5377	4650	111.5	96.4	.285	1.7	1.5	-
12-10	-130	.480	.921	.434	I	13	4600	4600	97.0	97.0	.279	1.7	1.6	-
12-9	-140	.479	.920	.436	I	13	4945	4435	105.5	94.7	.263	1.8	1.7	-
12-5	-155	.480	.920	.438	III	10	3436	3436	73.7	73.7	.157	3.1	2.8	73.7
12-2	-321	.480	.920	.425	III	0	1632	1632	33.5	33.5	.023	20.8	18.4	33.5

(1) fracture toughness computed using maximum load P_{max}
(2) tentative K_{IC} computed using load P_Q
(3) valid plain strain fracture toughness value, Ksi √in
(4) proportion of oblique fracture midway between crack tip and unnotched specimen edge

TABLE A11 (Continued)

Specimen	Test Temp. °F	Thick. B, (in)	Width W, (in)	Crack Length a, (in)	Curve Type	% (4) Shear	Load (lbs) P_{max}	Load (lbs) P_Q	Fracture Toughness Ksi $\sqrt{in}$ K_{max} (1)	Fracture Toughness Ksi $\sqrt{in}$ K_Q (2)	Ratio (R) $(K_Q/\sigma_{ys})^2$	$\frac{B}{R}$	$\frac{a}{R}$	K_{IC} (3)
13-1	75	.481	.919	.429	I	29	4760	3900	99.2	81.2	.195	2.4	2.2	-
13-6	-10	.481	.919	.443	I	29	4478	4125	97.8	90.1	.231	2.1	1.9	-
13-4	-40	.480	.920	.429	I	25	4720	4050	98.2	84.3	.198	2.4	2.2	-
13-8	-70	.479	.920	.432	II	17	3970	3970	83.6	83.6	.190	2.5	2.3	83.6
13-9	-70	.479	.920	.434	II	17	4025	4025	85.3	85.3	.197	2.4	2.2	-
13-3	-100	.480	.919	.430	III	13	3540	3540	73.9	73.9	.145	3.3	3.0	73.9
13-10	-130	.480	.919	.438	III	11	3168	3168	68.1	68.1	.120	4.0	3.7	68.1
13-5	-155	.480	.919	.436	III	7	2690	2690	57.5	57.5	.083	5.8	5.3	57.5
13-2	-321	.480	.919	.439	III	0	1514	1514	32.6	32.6	.019	25.0	22.9	32.6
14-1	75	.481	.921	.444	I	38	5283	4540	115.0	98.8	.315	1.5	1.4	-
14-6	-10	.481	.919	.436	I	40	5626	4761	120.0	101.5	.313	1.5	1.4	-
14-4	-40	.481	.921	.440	I	37	5530	4425	118.7	95.0	.268	1.8	1.6	-
14-7	-70	.479	.921	.439	I	38	5683	4200	122.0	90.3	.237	2.0	1.9	-
14-3	-100	.480	.921	.448	I	23	5340	4245	118.2	94.0	.251	1.9	1.8	-
14-10	-120	.481	.920	.446	I	19	5475	4500	120.4	98.9	.274	1.8	1.6	-
14-8	-130	.481	.921	.441	I	17	5500	5120	118.5	110.3	.337	1.4	1.3	-
14-9	-130	.480	.921	.439	I	17	5500	4460	119.0	95.6	.253	1.9	1.7	-
14-5	-155	.481	.919	.455	II	10	3984	3984	90.6	90.6	.223	2.2	2.0	-
14-2	-321	.480	.919	.443	III	0	2050	2050	44.8	44.8	.039	12.5	11.5	44.8

(1) fracture toughness computed using maximum load P_{max}
(2) tentative K_{IC} computed using load P_Q
(3) valid plain strain fracture toughness value, Ksi $\sqrt{in}$
(4) proportion of oblique fracture midway between crack tip and unnotched specimen edge

TABLE AII (Continued)

pecimen	Test Temp. °F	Thick. B, (in)	Width W, (in)	Crack Length a, (in)	Curve Type	% (4) Shear	Load (lbs) P_{max}	Load (lbs) P_Q	Fracture Toughness Ksi √in K_{max} (1)	Fracture Toughness Ksi √in K_Q (2)	Ratio (R) $(K_Q/\sigma_{ys})^2$	$\frac{B}{R}$	$\frac{a}{R}$	K_{IC} (3)
16-1	75	.480	.919	.438	I	44	6160	4770	132.5	102.6	.360	1.3	1.2	-
16-6	-10	.480	.920	.408	I	25	6660	4800	129.5	93.3	.276	1.7	1.5	-
16-4	-40	.480	.921	.447	III	17	3362	3362	74.1	74.1	.168	2.8	2.7	74.1
16-9	-40	.481	.919	.441	II	17	3500	3500	75.9	75.9	.177	2.7	2.5	75.9
16-7	-70	.480	.920	.441	II	11	3010	3010	65.2	65.2	.127	3.8	3.5	65.2
16-10	-70	.480	.919	.450	III	11	3140	3140	70.4	70.4	.148	3.2	3.0	70.4
16-3	-100	.480	.921	.444	III	4	2450	2450	53.7	53.7	.084	5.7	5.3	53.7
16-E2	-100	.480	.921	.458	III	7	2475	2475	56.6	56.6	.093	5.2	9.9	56.6
16-8	-130	.479	.919	.444	III	7	2148	2148	47.3	47.3	.063	7.6	7.1	47.3
16-5	-155	.481	.920	.452	III	0	1892	1892	42.5	42.5	.050	9.7	9.1	42.5
16-2	-321	.479	.921	.451	III	0	1245	1245	27.9	27.9	.017	29.0	27.3	27.9
17-1	75	.481	.921	.439	I	22	4525	4180	96.8	89.5	.279	1.7	1.6	-
17-6	-10	.481	.921	.433	I	17	4055	4055	85.1	85.1	.243	2.0	1.8	-
17-4	-40	.480	.919	.449	III	12	3555	3555	79.4	79.4	.208	2.3	2.2	-
17-7	-70	.479	.920	.448	II	11	2932	2832	65.2	63.2	.130	3.7	3.5	63.2
17-10	-80	.481	.921	.447	II	11	2885	2770	63.4	60.9	.120	4.0	3.7	60.9
17-3	-100	.481	.420	.455	II	7	2601	2601	59.1	59.1	.111	4.3	4.1	59.1
17-9	-100	.481	.919	.445	II	7	2795	2795	61.4	61.4	.120	4.0	3.7	61.4
17-8	-130	.481	.420	.455	II	7	2364	2240	53.6	50.8	.081	6.0	5.6	50.8
17-5	-155	.480	.921	.455	II	3	2125	2125	48.1	48.1	.071	6.8	6.4	48.1
17-2	-321	.480	.919	.451	III	0	1315	1315	29.5	29.5	.019	25.9	24.3	29.5

(1) fracture toughness computed using maximum load P_{max}
(2) tentative K_{IC} computed using load P_Q
(3) valid plain strain fracture toughness value, Ksi √in
(4) proportion of oblique fracture midway between crack tip and unnotched specimen edge

TABLE AII (Continued)

Specimen	Test Temp. °F	Thick. B, (in)	Width W, (in)	Crack Length a, (in)	Curve Type	% (4) Shear	Load (lbs) P_{max}	Load (lbs) P_Q	Fracture Toughness Ksi √in K_{max} (1)	Fracture Toughness Ksi √in K_Q (2)	Ratio (R) $(K_Q/\sigma_{ys})^2$	$\frac{B}{R}$	$\frac{a}{R}$	K_{IC} (3)
18-1	75	.481	.920	.452	I	31	4590	4050	103.0	90.9	.268	1.8	1.7	-
18-7	-10	.481	.917	.435	I	23	4720	3630	101.0	77.8	.188	2.6	2.3	77.8
18-4	-40	.481	.921	.452	I	17	4331	4056	96.9	90.7	.251	1.9	1.8	-
18-8	-70	.481	.921	.447	II	15	3123	3123	68.7	68.7	.141	3.4	3.2	68.7
18-9	-70	.481	.921	.447	II	11	3010	3010	66.4	66.4	.132	3.7	3.4	66.4
18-3	-100	.480	.920	.449	III	8	2685	2685	59.7	59.7	.104	4.6	4.3	59.7
18-10	-130	.480	.921	.452	III	9	2510	2510	56.3	56.3	.091	5.3	5.0	56.3
18-5	-155	.480	.919	.443	III	5	2655	2655	50.1	50.1	.070	6.9	6.3	50.1
18-2	-321	.481	.921	.441	III	0	1675	1675	36.0	36.0	.026	18.4	16.8	36.0
19-1	75	.480	.919	.434	I	25	4200	3830	89.1	81.3	.211	2.3	2.1	-
19-6	-10	.480	.920	.438	I	27	4455	4150	95.5	89.0	.238	2.0	1.8	-
19-4	-40	.480	.919	.444	II	19	3840	3840	84.3	84.3	.209	2.3	2.1	-
19-7	-70	.480	.921	.433	II	17	4209	4209	88.5	88.5	.225	2.1	1.9	-
19-3	-100	.480	.919	.437	III	12	3399	3399	72.6	72.6	.148	3.2	2.9	72.6
19-9	-100	.480	.921	.439	III	15	3125	3125	67.0	67.0	.126	3.8	3.5	67.0
19-8	-130	.480	.919	.434	III	9	2968	2968	63.0	63.0	.109	4.4	4.0	63.0
19-10	-130	.480	.920	.432	II	9	3450	3450	72.5	72.5	.145	3.3	3.0	72.5
19-5	-155	.480	.920	.418	III	6	2520	2520	50.6	50.6	.069	6.4	6.0	50.6
19-2	-321	.480	.918	.424	III	0	1575	1575	32.5	32.5	.021	23.0	20.3	32.5

(1) fracture toughness computed using maximum load P_{max}
(2) tentative K_{IC} computed using load P_Q
(3) valid plain strain fracture toughness value, Ksi √in
(4) proportion of oblique fracture midway between crack tip and unnotched specimen edge

TABLE AII (Continued)

Specimen	Test Temp. °F	Thick. B, (in)	Width W, (in)	Crack Length a, (in)	Curve Type	% (4) Shear	Load (lbs) P_{max}	Load (lbs) P_Q	Fracture Toughness Ksi $\sqrt{in}$ K_{max} (1)	Fracture Toughness Ksi $\sqrt{in}$ K_Q (2)	Ratio (R) $(K_Q/\sigma_{ys})^2$	$\frac{B}{R}$	$\frac{a}{R}$	K_{IC} (3)
20-1	75	.480	.921	.437	I	27	4395	4038	93.6	86.0	.230	2.1	1.9	-
20-6	-10	.480	.921	.436	I	23	4560	3990	96.8	84.7	.208	2.3	2.1	-
20-4	-40	.479	.919	.449	II	20	3925	3895	87.8	87.1	.215	2.2	2.1	-
20-7	-70	.481	.921	.449	II	13	3838	3838	85.0	85.0	.199	2.4	2.3	-
20-3	-100	.480	.919	.427	III	13	3589	3589	74.1	74.1	.147	3.3	2.9	74.1
20-9	-100	.480	.919	.418	III	11	3610	3610	72.7	72.7	.141	3.4	3.0	72.7
20-8	-130	.480	.921	.433	III	11	2971	2971	62.5	62.5	.102	4.7	4.3	62.5
20-10	-155	.479	.920	.455	III	9	2486	2486	56.6	56.6	.081	5.9	5.6	56.6
20-2	-321	.481	.919	.410	III	0	1820	1820	35.7	35.7	.024	19.9	16.9	35.7
21-1	75	.481	.919	.454	I	36	4702	4162	106.6	94.3	.297	1.6	1.5	-
21-6	-10	.480	.920	.432	I	32	5245	4275	110.2	89.8	.257	1.9	1.7	-
21-4	-40	.480	.921	.443	I	33	4995	4045	108.6	87.9	.241	2.0	1.8	-
21-7	-70	.480	.920	.449	I	25	4940	4215	109.9	93.8	.266	1.8	1.7	-
21-3	-100	.479	.920	.440	II	18	3675	3675	79.4	79.4	.185	2.6	2.4	79.4
21-9	-100	.480	.921	.446	I	17	4300	4180	94.4	91.8	.248	1.9	1.8	-
21-8	-130	.480	.921	.435	III	13	3629	3629	76.8	76.8	.167	2.9	2.6	76.8
21-10	-130	.480	.920	.434	I	11	4670	4380	98.8	92.7	.243	2.0	1.8	-
21-5	-155	.480	.921	.443	II	10	3020	3020	65.6	65.6	.118	4.1	3.8	65.6
21-2	-321	.481	.919	.440	III	0	1582	1582	34.2	34.2	.023	20.9	19.1	34.2

(1) fracture toughness computed using maximum load P_{max}
(2) tentative K_{IC} computed using load P_Q
(3) valid plain strain fracture toughness value, Ksi $\sqrt{in}$
(4) proportion of oblique fracture midway between crack tip and unnotched specimen edge

TABLE AII (Continued)

Specimen	Test Temp. °F	Thick. B, (in)	Width W, (in)	Crack Length a, (in)	Curve Type	% (4) Shear	Load (lbs) P_{max}	Load (lbs) P_Q	Fracture Toughness Ksi √in K_{max} (1)	Fracture Toughness Ksi √in K_Q (2)	Ratio (R) $(K_Q/\sigma_{ys})^2$	$\frac{B}{R}$	$\frac{a}{R}$	K_{IC} (3)
22-1	75	.480	.919	.439	I	40	5325	4475	114.9	96.6	.279	1.7	1.6	-
22-6	-10	.480	.920	.390	I	38	6610	5250	121.5	96.5	.258	1.9	1.5	-
22-4	-40	.480	.919	.430	I	35	5608	4663	117.5	97.7	.256	1.9	1.7	-
22-7	-70	.480	.921	.450	I	36	5584	4750	124.3	105.7	.294	1.6	1.5	-
22-3	-100	.479	.921	.448	I	23	5162	4337	114.5	96.2	.236	2.0	1.9	-
22-8	-130	.480	.921	.442	I	15	4896	4834	106.0	104.7	.273	1.8	1.6	-
22-9	-130	.480	.919	.442	I	19	5040	4200	109.9	91.6	.209	2.3	2.1	-
22-5	-155	.480	.921	.436	II	10	4365	4365	92.7	92.7	.209	2.3	2.1	-
22-10	-155	.479	.921	.432	II	15	4260	4260	89.4	89.4	.194	2.5	2.2	89.4
22-2	-321	.481	.919	.444	III	0	1940	1940	42.5	42.5	.032	15.0	13.8	42.5
26-1	75	.481	.919	.447	I	40	5417	4620	119.9	102.2	.349	1.4	1.3	-
26-4	-40	.479	.919	.444	I	36	5165	3935	113.6	86.6	.231	2.1	1.9	-
26-8	-70	.481	.919	.459	I	29	5277	4187	121.7	96.6	.280	1.7	1.6	-
26-3	-100	.481	.920	.441	I	19	5352	4520	115.7	97.7	.279	1.7	1.6	-
26-6	-130	.480	.919	.427	I	17	5230	4670	108.5	96.8	.265	1.8	1.6	-
26-7	-130	.480	.919	.452	I	15	4575	4500	103.2	101.5	.291	1.6	1.6	-
26-5	-155	.480	.919	.446	II	10	3265	3265	72.2	72.2	.144	3.3	3.1	72.2
26-2	-321	.480	.919	.454	III	0	1695	1695	38.5	38.5	.029	16.7	15.8	38.5

(1) fracture toughness computed using maximum load P_{max}
(2) tentative K_{IC} computed using load P_Q
(3) valid plain strain fracture toughness value, Ksi √in
(4) proportion of oblique fracture midway between crack tip and unnotched specimen edge

TABLE AII (Continued)

Specimen	Test Temp. °F	Thick. B, (in)	Width W, (in)	Crack Length a, (in)	Curve Type	% (4) Shear	Load (lbs) P_{max}	P_Q	Fracture Toughness Ksi $\sqrt{in}$ K_{max} (1)	K_Q (2)	Ratio $(\bar{R})^2$ $(K_Q/\sigma_{ys})^2$	$\frac{B}{\bar{R}}$	$\frac{a}{\bar{R}}$	K_{IC} (3)
27-1	75	.481	.919	.447	I	44	5809	4560	128.5	100.9	.365	1.3	1.2	-
27-6	-10	.480	.919	.433	I	40	5705	4330	120.7	91.6	.282	1.7	1.5	-
27-4	-40	.480	.921	.438	I	25	5725	4200	122.4	89.8	.265	1.8	1.7	-
27-7	-70	.481	.919	.445	II	17	4610	4610	101.3	101.3	.328	1.5	1.4	-
27-3	-100	.481	.920	.465	III	13	3501	3501	82.3	82.3	.209	2.3	.2	-
27-8	-130	.479	.919	.441	III	9	3737	3737	81.4	81.4	.197	2.4	2.2	-
27-9	-130	.481	.919	.451	III	9	3444	3444	77.3	77.3	.177	2.7	2.5	77.3
27-5	-155	.479	.919	.448	II	5	2976	2976	66.4	66.4	.127	3.8	3.5	66.4
27-2	-321	.481	.919	.443	III	0	1665	1665	36.4	36.4	.028	17.1	15.7	36.4
28-1	75	.479	.919	.431	I	25	4260	3960	89.7	83.4	.199	2.4	2.2	-
28-6	-10	.480	.914	.433	I	23	4545	4200	96.1	88.9	.222	2.2	1.9	-
28-4	-40	.479	.919	.428	II	21	4127	3962	86.1	82.6	.189	2.5	2.3	82.6
28-9	-40	.481	.919	.437	I	21	4090	3830	87.5	81.9	.186	2.6	2.4	81.9
28-7	-70	.479	.919	.445	II	17	3600	3600	79.5	79.5	.171	2.8	2.6	79.5
28-10	-70	.480	.919	.448	II	19	3770	3770	83.9	83.9	.191	2.5	2.3	83.9
28-3	-100	.480	.919	.434	III	13	3516	3516	74.5	74.5	.147	3.3	3.0	74.5
28-8	-130	.481	.918	.463	III	9	3032	3032	71.1	71.1	.130	3.7	3.6	71.1
28-5	-155	.479	.919	.450	III	8	2455	2455	55.1	55.1	.077	6.2	5.9	55.1
28-2	-321	.479	.919	.432	III	0	1568	1568	33.1	33.1	.020	24.0	21.7	33.1

(1) fracture toughness computed using maximum load P_{max}
(2) tentative K_{IC} computed using load P_Q
(3) valid plain strain fracture toughness value, Ksi $\sqrt{in}$
(4) proportion of oblique fracture midway between crack tip and unnotched specimen edge

TABLE AII (Continued)

Specimen	Test Temp. °F	Thick. B, (in)	Width W, (in)	Crack Length a, (in)	Curve Type	% (4) Shear	Load (lbs) P_{max}	Load (lbs) P_Q	Fracture Toughness Ksi $\sqrt{in}$ K_{max} (1)	Fracture Toughness Ksi $\sqrt{in}$ K_Q (2)	Ratio (R) $(K_Q/\sigma_{ys})^2$	$\frac{B}{R}$	$\frac{a}{R}$	K_{IC} (3)
29-1	75	.481	.919	.449	I	29	4690	3200	104.5	71.3	.195	2.47	2.3	-
29-6	-10	.480	.919	.425	I	27	5070	4630	104.5	95.4	.334	1.4	1.3	-
29-7	-10	.480	.920	.447	I	25	4712	3972	104.1	87.7	.283	1.7	1.6	-
29-4	-40	.479	.919	.458	I	21	4190	3490	96.7	80.5	.235	2.0	1.9	-
29-3	-100	.481	.918	.430	II	17	4250	4250	88.8	88.8	.274	1.8	1.6	-
29-8	-130	.481	.919	.453	III	11	3710	3710	83.8	83.8	.237	2.0	1.9	-
29-5	-155	.480	.919	.434	II	10	3270	3270	69.4	69.4	.159	3.0	2.7	69.4
29-2	-321	.480	.918	.445	III	0	1690	1690	37.3	37.3	.032	14.8	13.7	37.3

(1) fracture toughness computed using maximum load P_{max}
(2) tentative K_{IC} computed using load P_Q
(3) valid plain strain fracture toughness value, Ksi $\sqrt{in}$
(4) proportion of oblique fracture midway between crack tip and unnotched specimen edge

TABLE AIII

Summary of Charpy V-Notch Impact Properties

Specimen Heat No.-Test No.	Test Temp.°F	Impact Energy(ft.lbs.)	Fibrous Fracture (%)
5-8	170	23 1/4	100
5-6	140	23 1/4	100
5-7	110	21	95
5-9	92	21	80
5-1	75	20	50
5-10	50	17 1/2	40
5-5	20	16 1/4	30
5-2	-40	14	10
5-3	-100	11 3/4	15
5-4	-321	5 1/2	0
6-6	140	25	100
6-7	110	24 1/4	100
6-10	92	23 1/4	100
6-1	75	22 1/4	95
6-9	63	21 3/4	80
6-8	50	21 1/2	65
6-11	35	21	45
6-5	20	18 1/2	35
6-2	-40	14 1/2	15
6-3	-100	15	5
6-4	-321	6	0
7-6	140	22	100 sc*
7-7	110	23	100 sc*
7-1	75	22 1/2	95
7-9	63	21	75
7-8	50	19 1/2	60
7-10	35	19 1/4	45
7-5	20	17 1/2	35
7-2	-40	13 1/2	25
7-3	-100	12	15
7-4	-321	5 1/4	0
8-7	170	30	100
8-10	155	29 1/2	100
8-6	140	30 3/4	90
8-9	125	31	80
8-8	110	26	65
8-1	75	26 1/2	50
8-5	20	16 1/2	30
8-2	-40	15 1/2	10
8-3	-100	13 1/2	5
8-4	-321	4 1/4	0

* scattered crystalline

TABLE AIII (Continued)

Specimen Heat No.-Test No.	Test Temp. °F	Impact Energy (ft.lbs.)	Fibrous Fracture (%)
9-6	140	32	100
9-1	75	30 3/4	100
9-9	63	30 1/2	100
9-7	50	28	95
9-10	35	26 1/4	90
9-5	20	25 3/4	80
9-11	5	25	65
9-8	-10	23 1/2	50
9-2	-40	19 1/4	35
9-3	-100	15 3/4	15
9-4	-321	8	0
12-6	140	40 1/2	100
12-11	110	42	100
12-1	75	40 1/4	100
12-8	63	39 3/4	95
12-7	50	37	85
12-10	35	33	75
12-5	20	31 3/4	70
12-12	5	29 1/4	55
12-9	-10	26 1/4	45
12-2	-40	21	30
12-3	-100	16 1/4	5
12-4	-321	5	0
13-7	170	23	100
13-6	140	22 1/2	100
13-10	125	21 1/2	95
13-12	110	21 1/2	80
13-8	110	21 1/2	80
13-9	92	21 1/4	65
13-1	75	21 1/2	55
13-11	50	18	35
13-5	20	16 3/4	25
13-2	-40	17	10
13-3	-100	12	5
13-4	-321	4 3/4	0
14-6	140	35 1/2	100
14-1	75	38 1/4	100
14-7	50	33 1/2	100
14-10	35	31 1/4	100
14-5	20	31 3/4	95
14-9	5	30 1/2	90
14-8	-10	28 1/4	75
14-11	-25	26 1/2	65
14-2	-40	25	55
14-3	-100	18	15
14-4	-321	5 1/4	2

TABLE AIII (Continued)

Specimen Heat No.-Test No.	Test Temp.°F	Impact Energy (ft.lbs.)	Fibrous Fracture (%)
16-7	170	42 3/4	100
16-6	140	43 1/4	95
16-9	125	39 1/4	85
16-8	110	36 1/4	70
16-1	75	31 3/4	50
16-10	50	26	35
16-5	20	20 1/2	20
16-2	-40	16	5
16-3	-100	10 3/4	2
16-4	-321	3	0
17-9	250	21 1/4	100
17-8	212	18 1/2	90
17-7	170	18 3/4	60
17-1	140	18 1/4	45
17-6	140	18	45
17-10	75	13 3/4	20
17-11	50	14 1/2	20
17-5	20	13	15
17-2	-40	12	5
17-3	-100	10	2
17-4	-321	3 1/4	0
18-7	170	25 1/2	100
18-6	140	25 1/4	100
18-9	125	24 1/4	95
18-8	110	24 1/4	70
18-1	75	23	50
18-10	50	18 3/4	30
18-5	20	15 3/4	20
18-2	-40	15	10
18-3	-100	13 1/2	5
18-4	-321	4	0
19-7	170	21 1/4	100
19-6	140	22 3/4	100
19-8	110	19 1/2	90
19-9	92	19	80
19-1	75	19	55
19-10	50	18 1/4	45
19-5	20	14 1/4	20
19-2	-40	12 1/4	10
19-3	-100	11 1/2	5
19-4	-321	5	2

TABLE AIII (Continued)

Specimen Heat No.-Test No.	Test Temp. °F	Impact Energy (ft.lbs.)	Fibrous Fracture (%)
20-7	170	21	100
20-6	140	19 1/2	100
20-8	110	20	90
20-9	92	18 1/2	60
20-1	75	18 1/2	50
20-10	20	15 1/4	35
20-5	20	14 1/2	35
20-2	-40	13	10
20-3	-100	12	5
20-4	-321	5 1/4	0
21-7	170	27	100
21-8	110	27	100
21-10	92	26 1/2	100
21-6	75	26 1/4	95
21-1	75	25 1/4	95
21-9	50	23 1/2	75
21-5	20	20 1/2	50
21-11	-10	17 1/2	40
21-2	-40	17	25
21-3	-100	14	10
21-4	-321	5	0
22-6	140	30 1/4	100
22-1	75	29 1/2	100
22-9	63	27 1/2	100
22-7	50	28	100
22-11	35	25 1/2	95
22-10	20	29	80
22-12	5	22 1/2	70
22-8	-10	24 1/4	55
22-2	-40	21 3/4	50
22-3	-100	16 1/4	15
22-4	-321	7 1/2	2
26-6	140	34 1/2	100
26-7	110	34 1/4	100
26-1	75	32 1/2	100
26-9	63	32 1/2	100
26-8	50	30 1/4	95
26-10	35	30 1/4	90
26-5	20	26 3/4	80
26-2	-40	21	40
26-3	-100	16 3/4	10
26-4	-321	8 3/4	2

TABLE AIII (Continued)

Specimen Heat No.-Test No.	Test Temp.°F	Impact Energy (ft.lbs.)	Fibrous Fracture (%)
27-10	170	44 3/4	100
27-6	140	42	100
27-9	110	41 1/2	100
27-1	75	39 1/2	85
27-7	50	34	60
27-11	20	26 3/4	35
27-8	-10	24 3/4	25
27-2	-40	19	20
27-3	-100	16 1/2	10
27-4	-321	4	0
28-7	170	18	100
28-6	140	17 1/2	90
28-8	110	18	70
28-10	92	16 1/2	50
28-1	75	16 1/4	40
28-11	50	14	30
28-9	20	12	20
28-2	-40	11 1/2	10
28-3	-100	10 3/4	5
28-4	-321	5	0
29-7	110	20 3/4	100
29-1	75	20 1/4	100
29-9	63	18 1/4	90
29-8	50	18 1/2	60
29-11	35	19 1/2	45
29-12	35	19 1/2	45
29-5	20	16 1/2	35
29-10	-10	15 3/4	30
29-2	-40	14	20
29-3	-100	12 1/2	10
29-4	-321	9	2

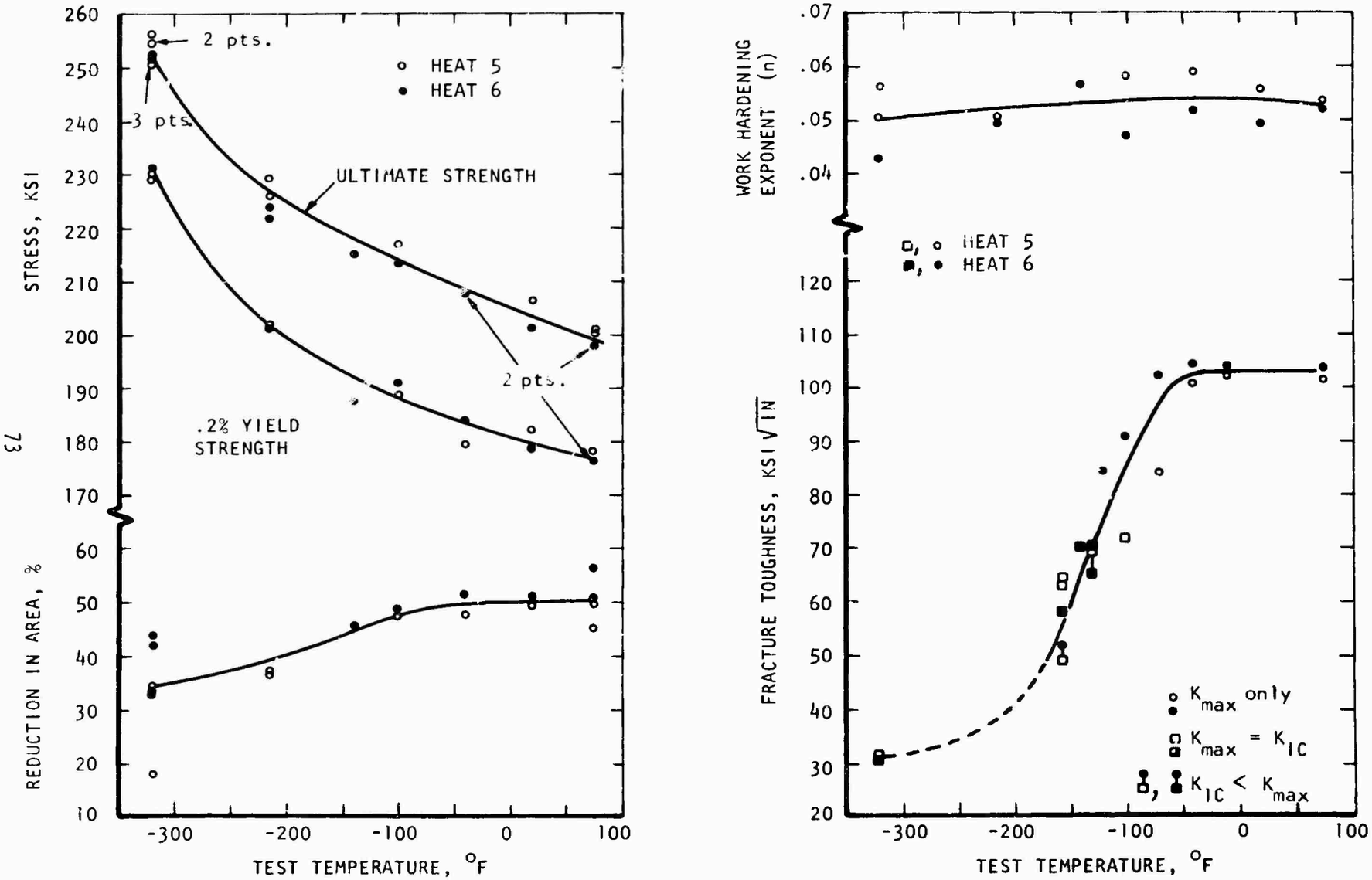

Figure A1: Tensile and notch bend test data for heats 5,6 (base composition).

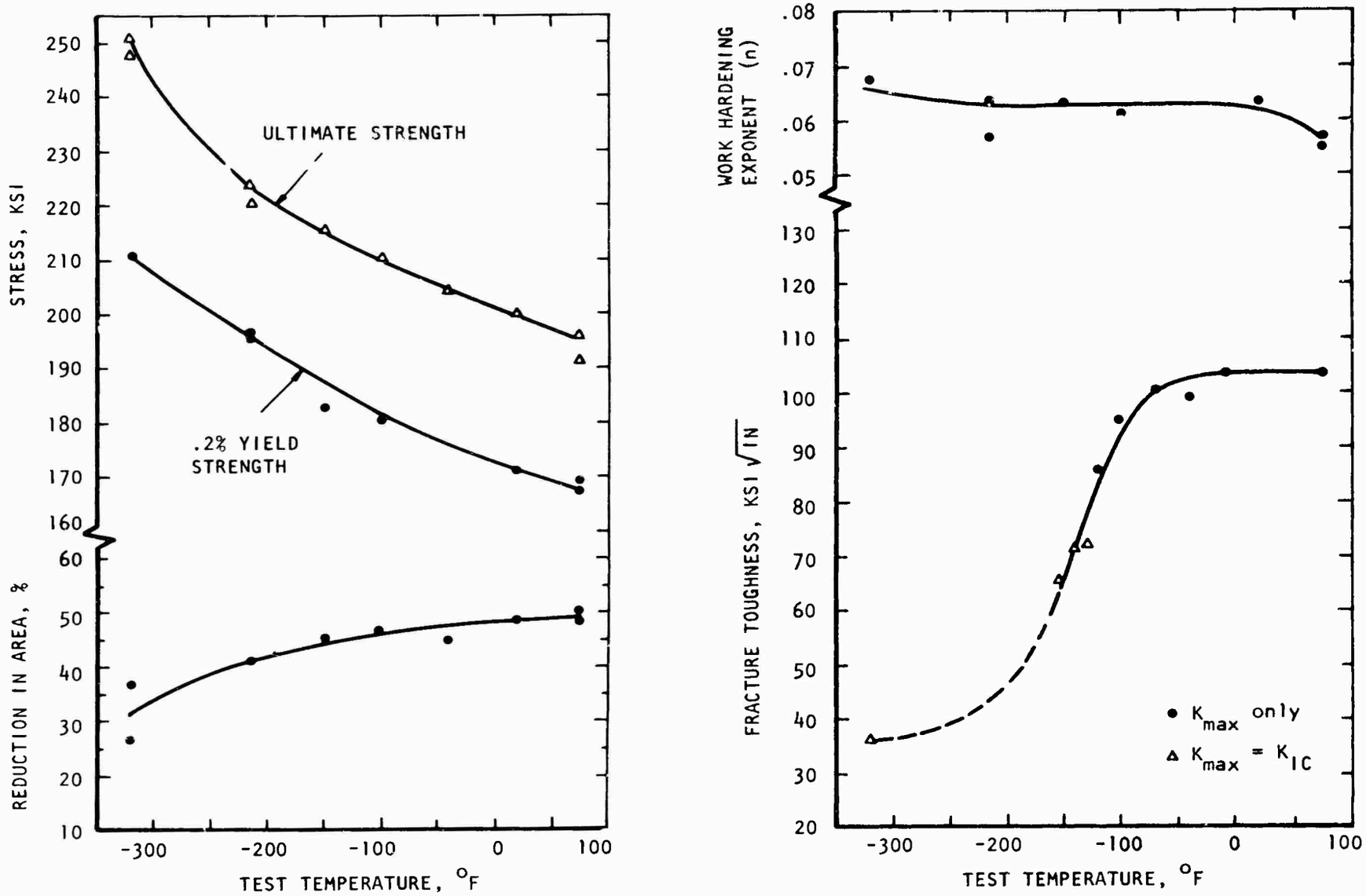

Figure A2. Tensile and notch bend test data for heat 7 (4.45%Ni).

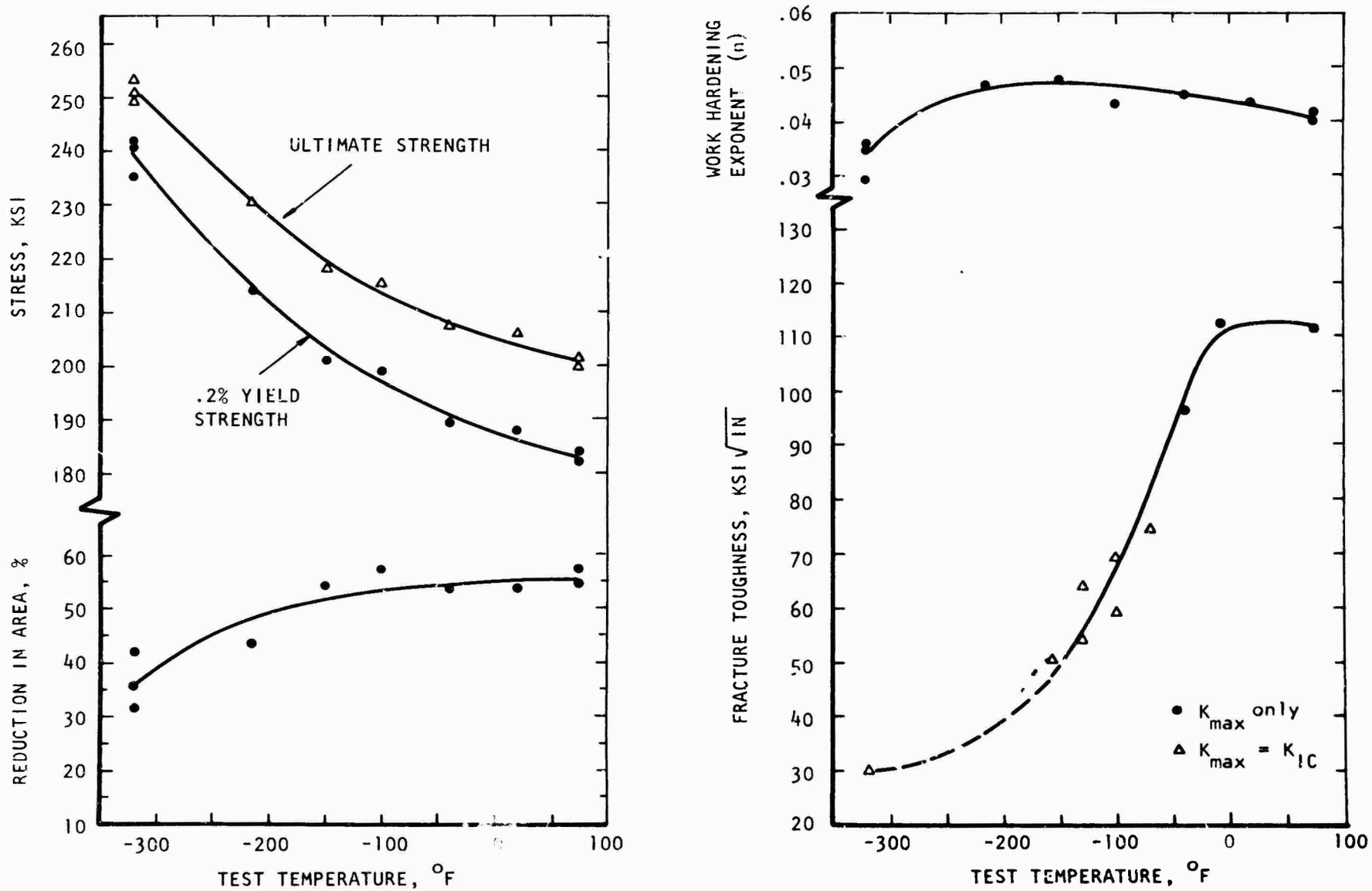

Figure A3.Tensile and notch bend test data for heat 8 (1.26%Ni)

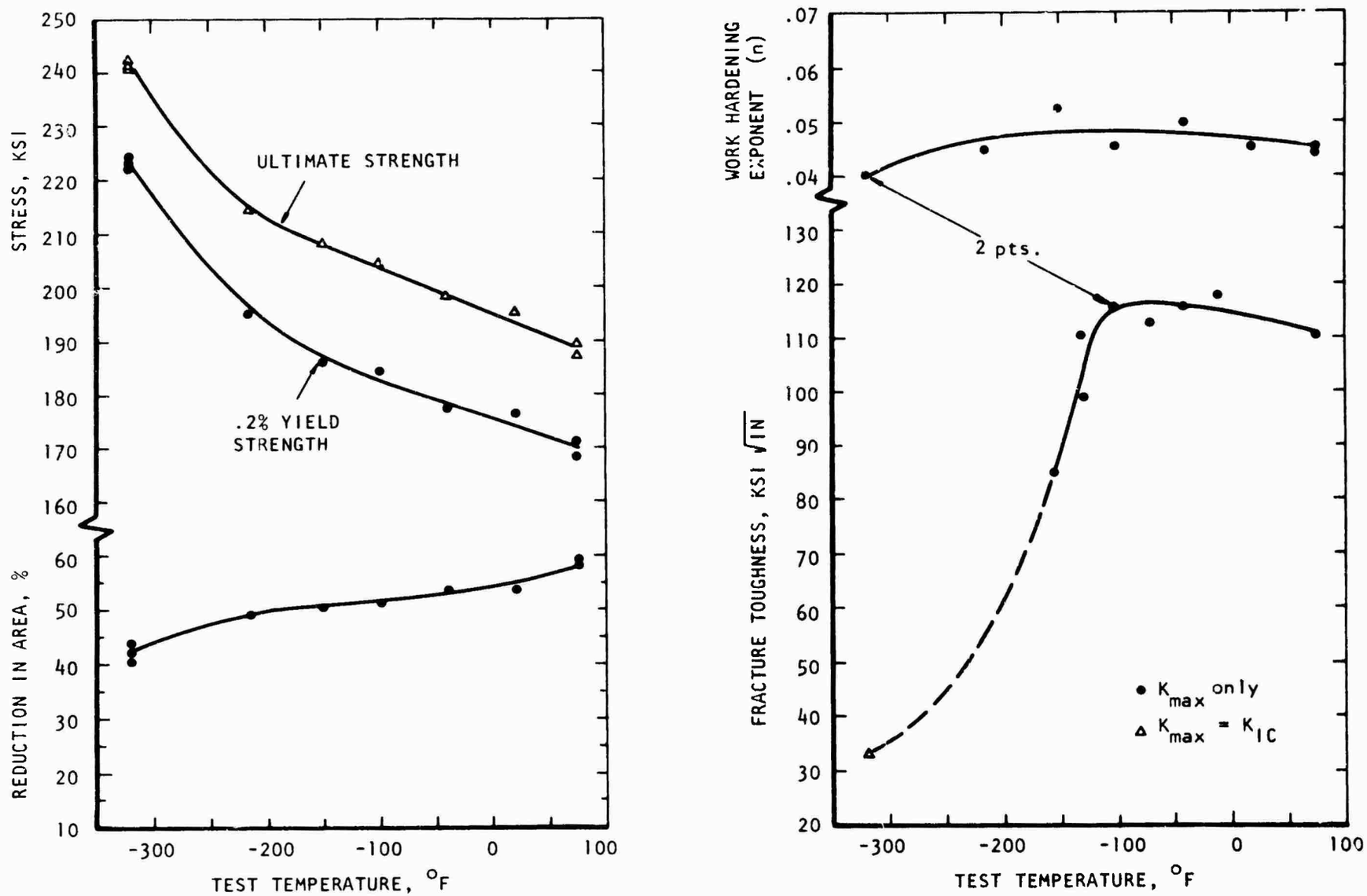

Figure A4. Tensile and notch bend test data for heat 9 (.51%Cr).

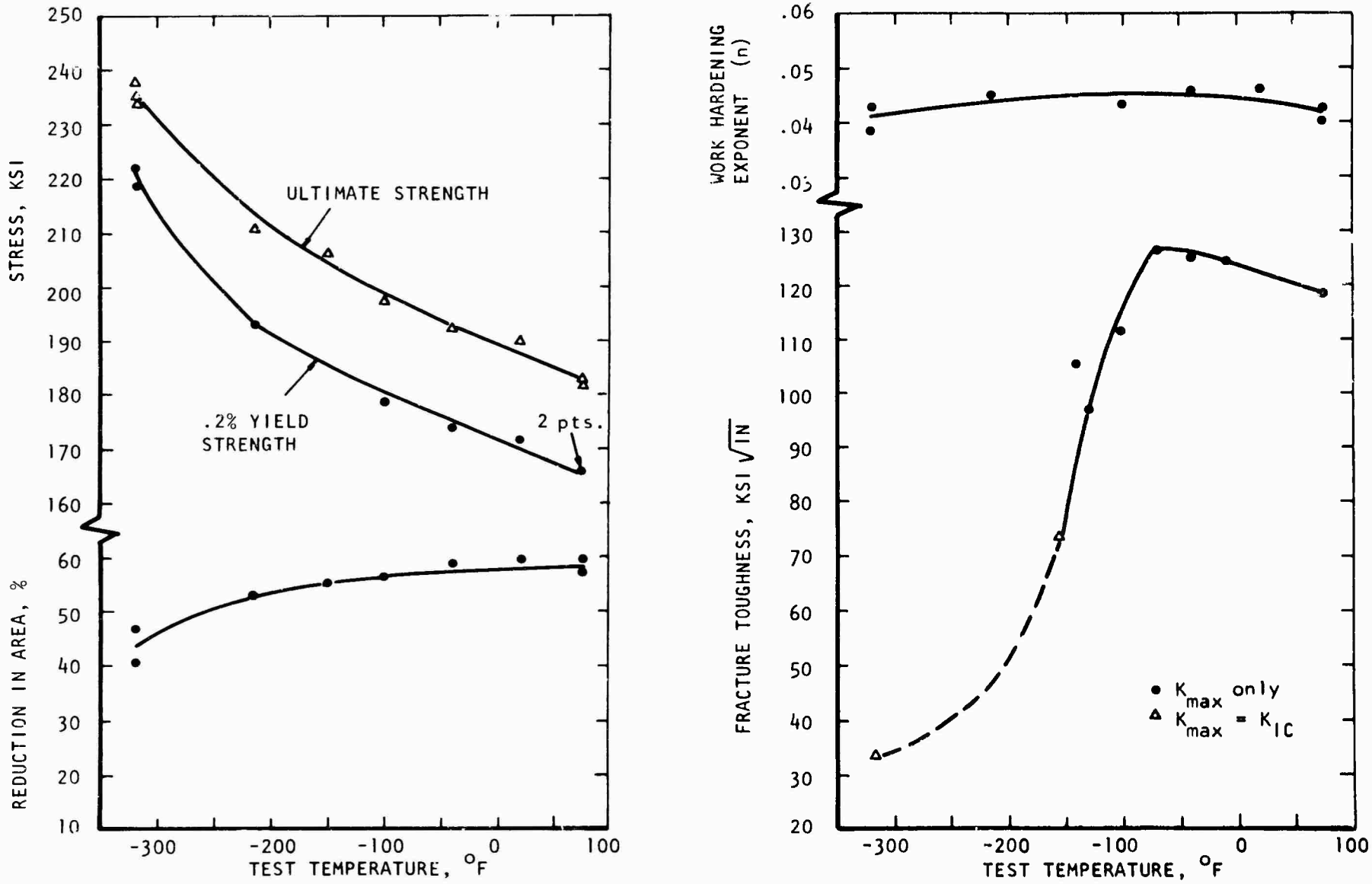

Figure A5. Tensile and notch bend test data for heat 12 (.13%Mo).

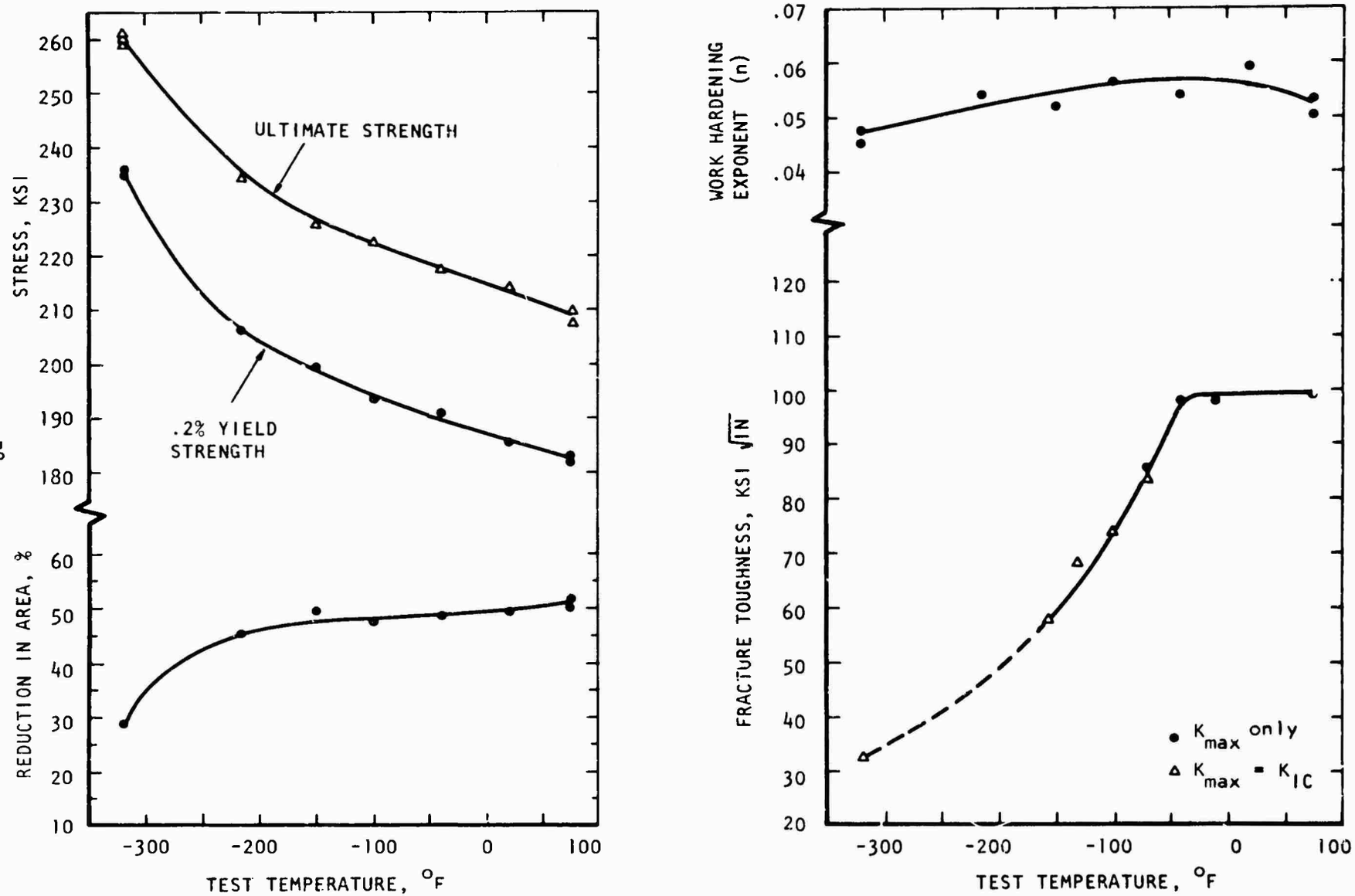

Figure A6. Tensile and notch bend test data for heat 13 (1.04% Mo).

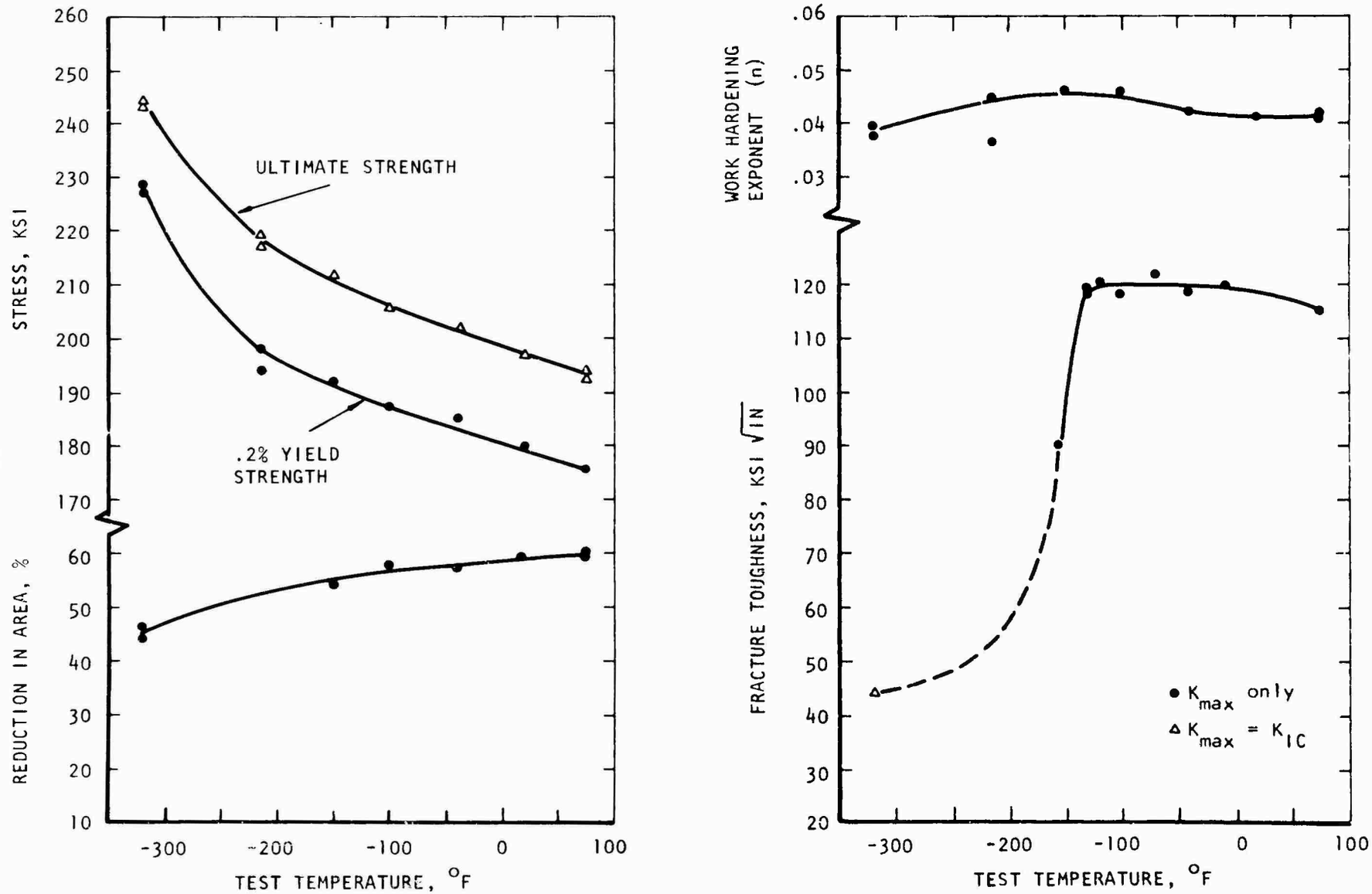

Figure A7. Tensile and notch bend test data for heat 14 (.06%Si).

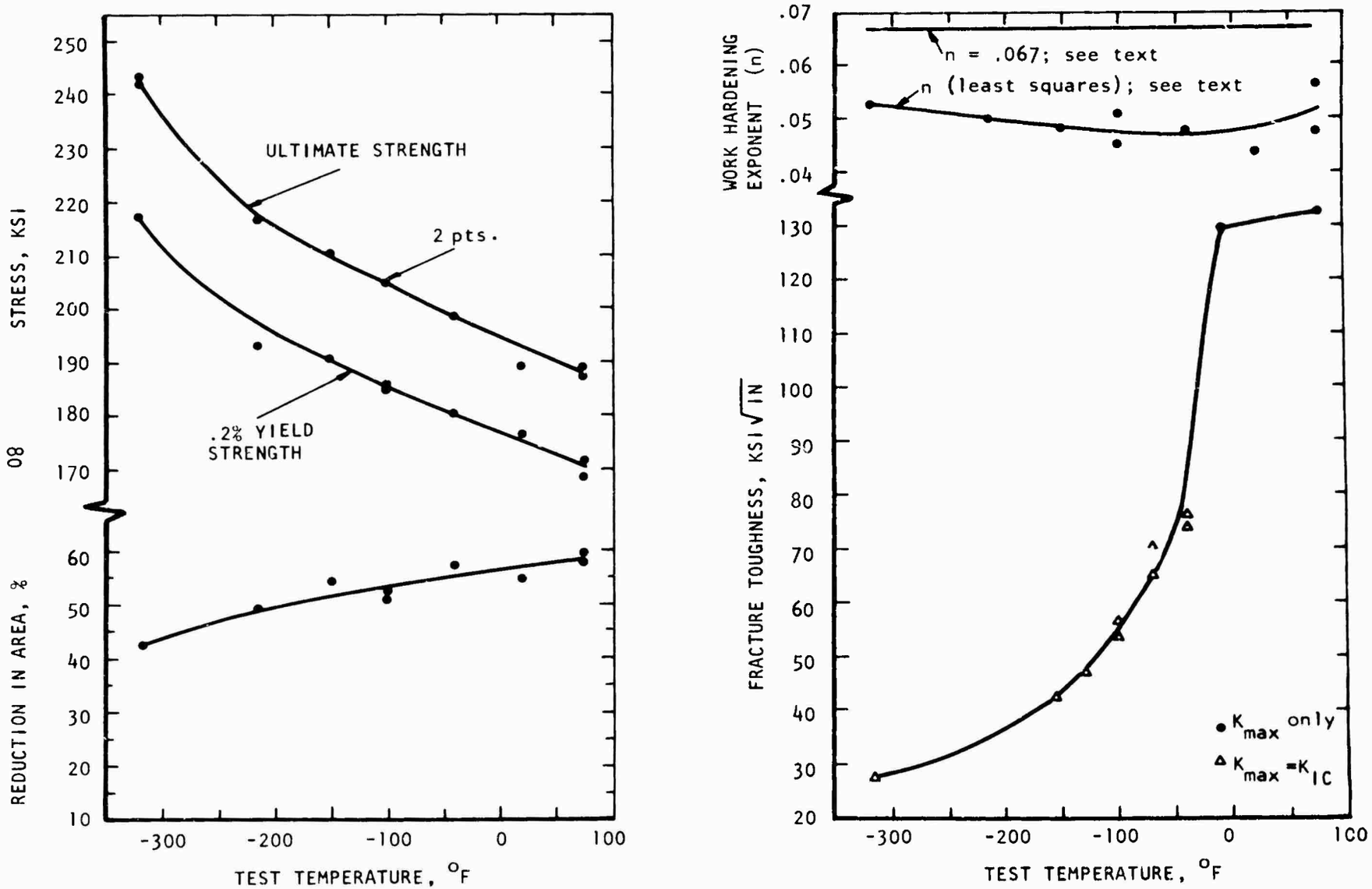

Figure A8. Tensile and notch bend test data for heat 16 (1.38%Si).

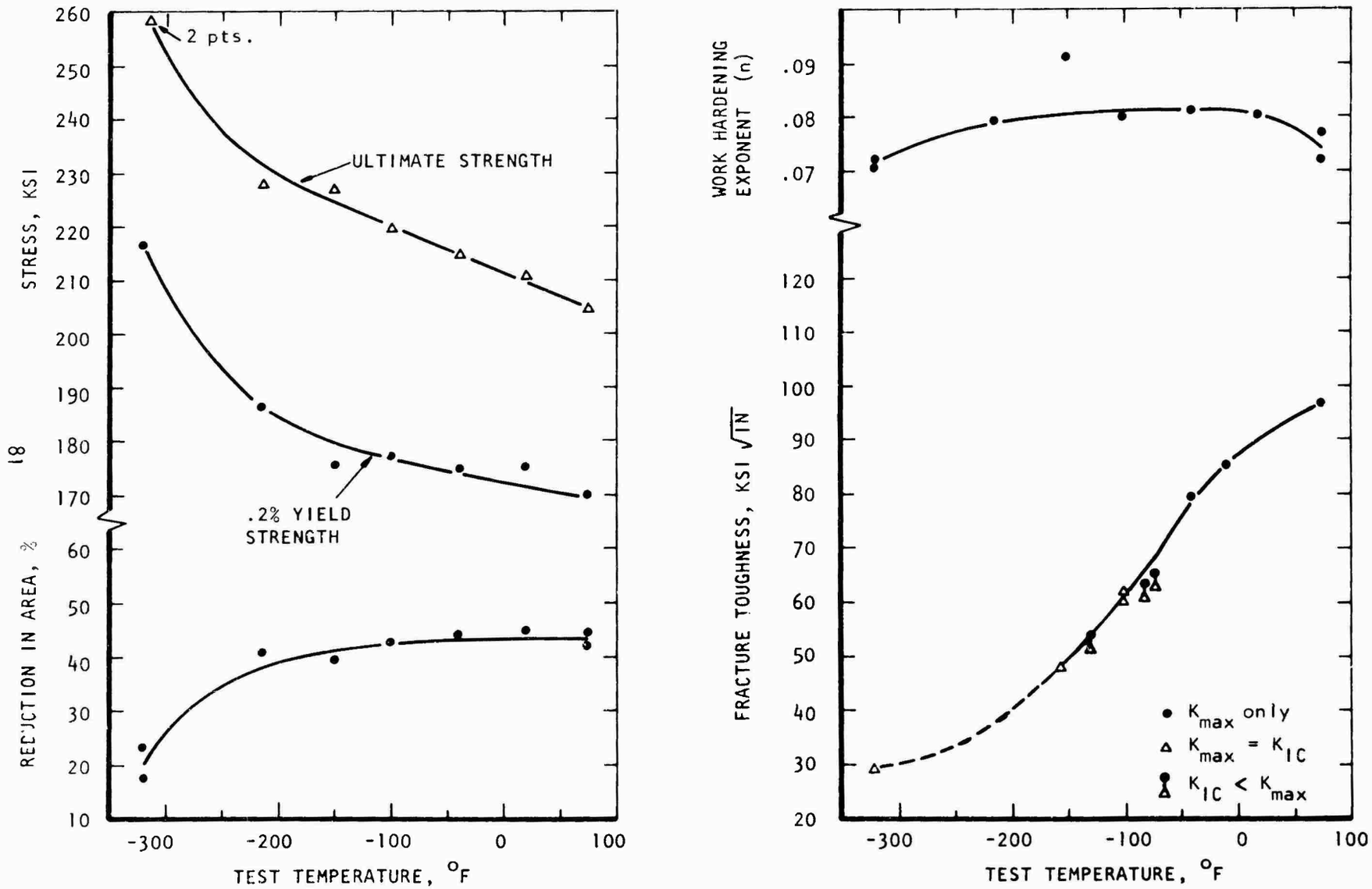

Figure A9. Tensile and notch bend test data for heat 17(1.51%Mn).

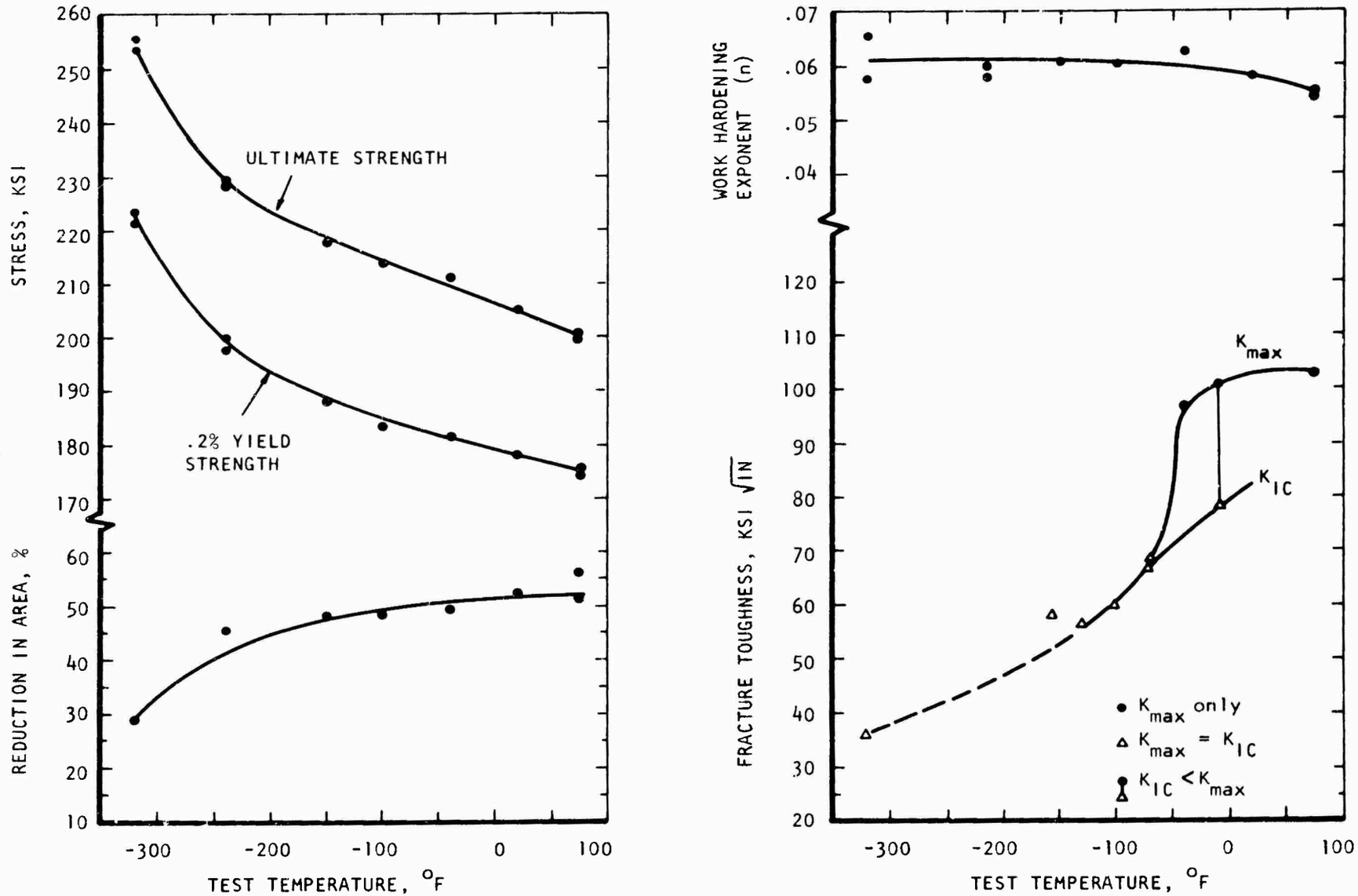

Figure A10. Tensile and notch bend test data for heat 18 (1.61%Cr).

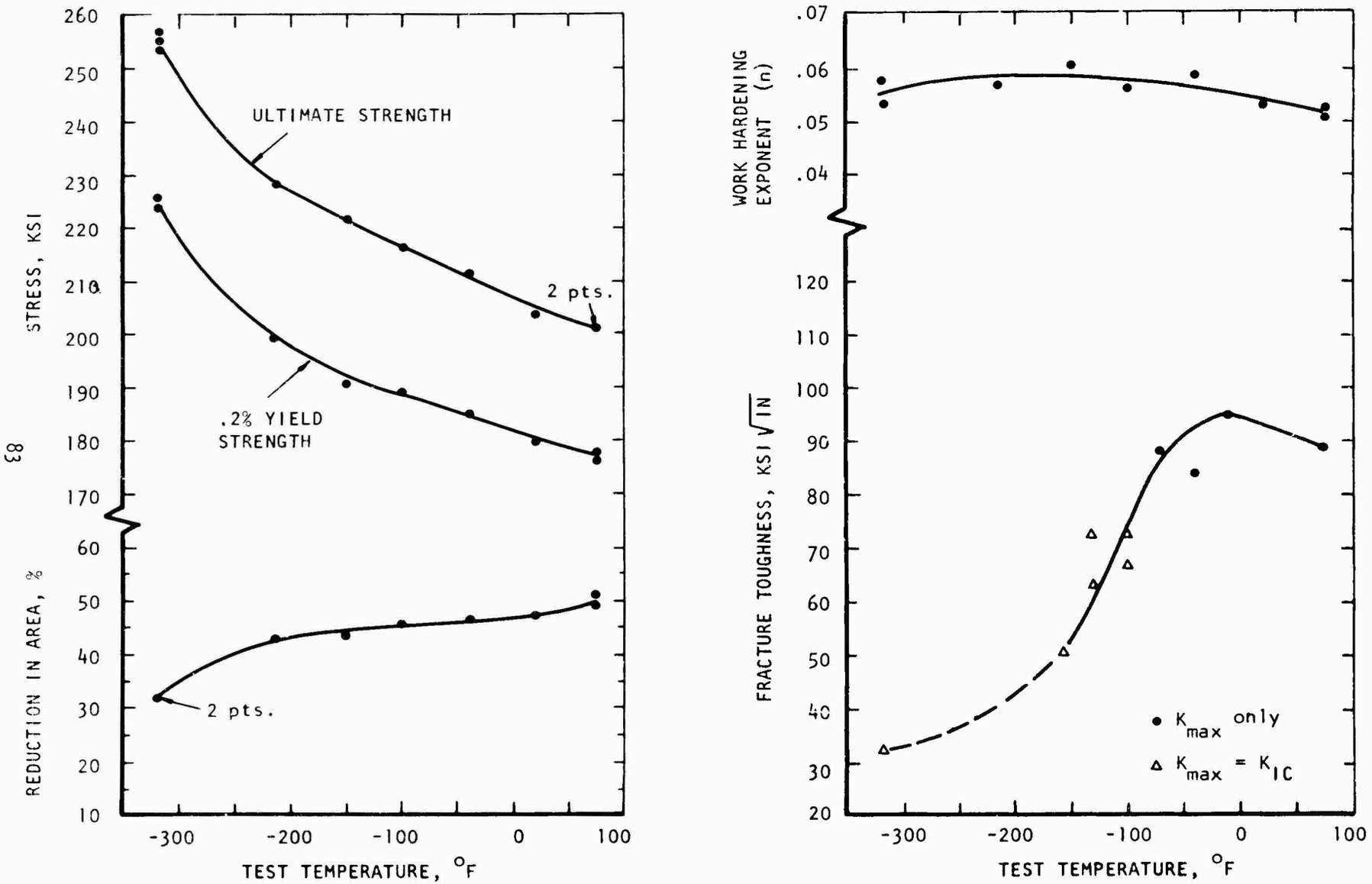

Figure A11. Tensile and notch bend test data for heat 19 (.34%Al).

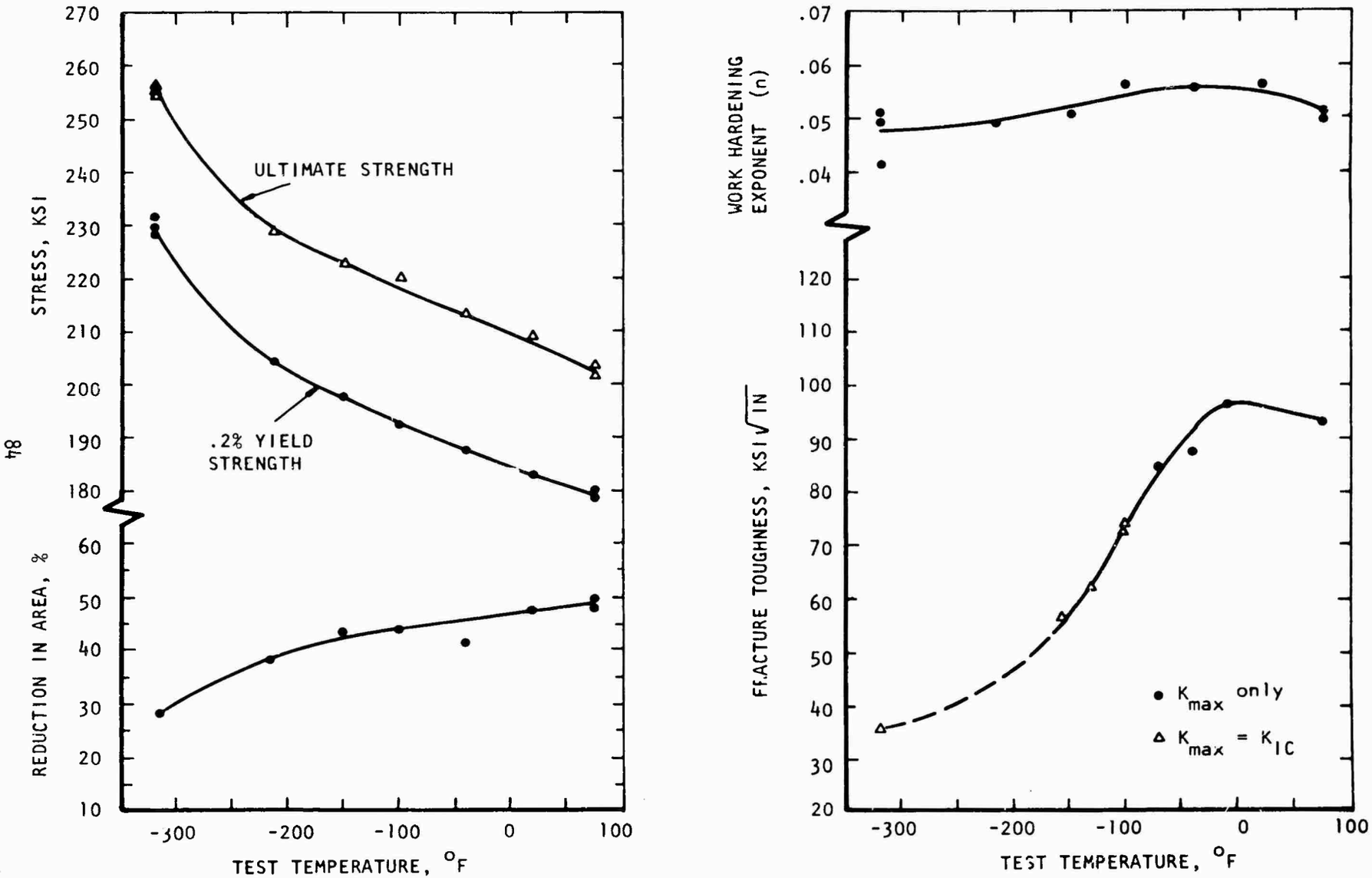

Figure A12. Tensile and notch bend test data for heat 20 (.13%Al).

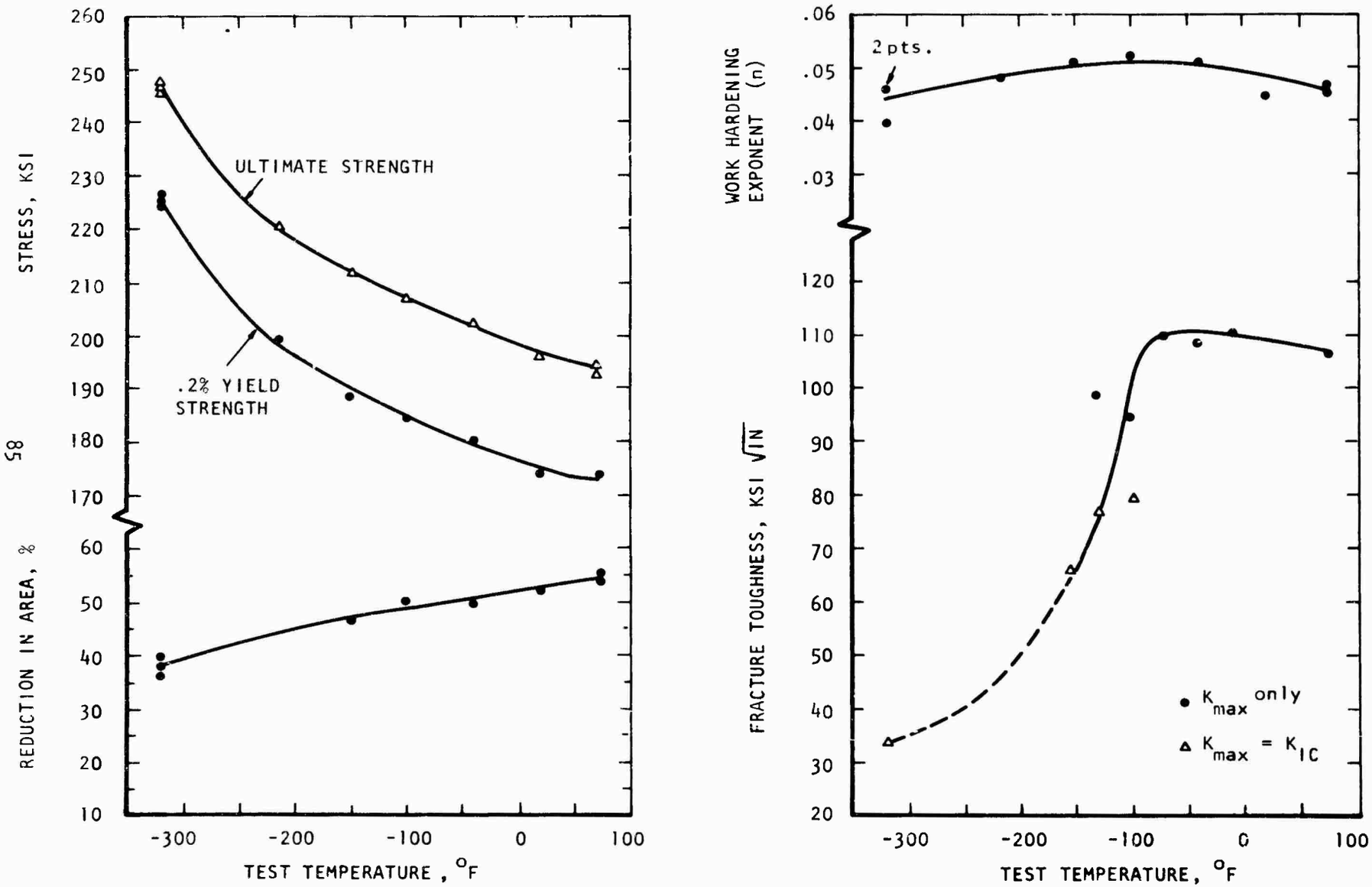

Figure A13. Tensile and notch bend test data for heat 21 (<.01%V).

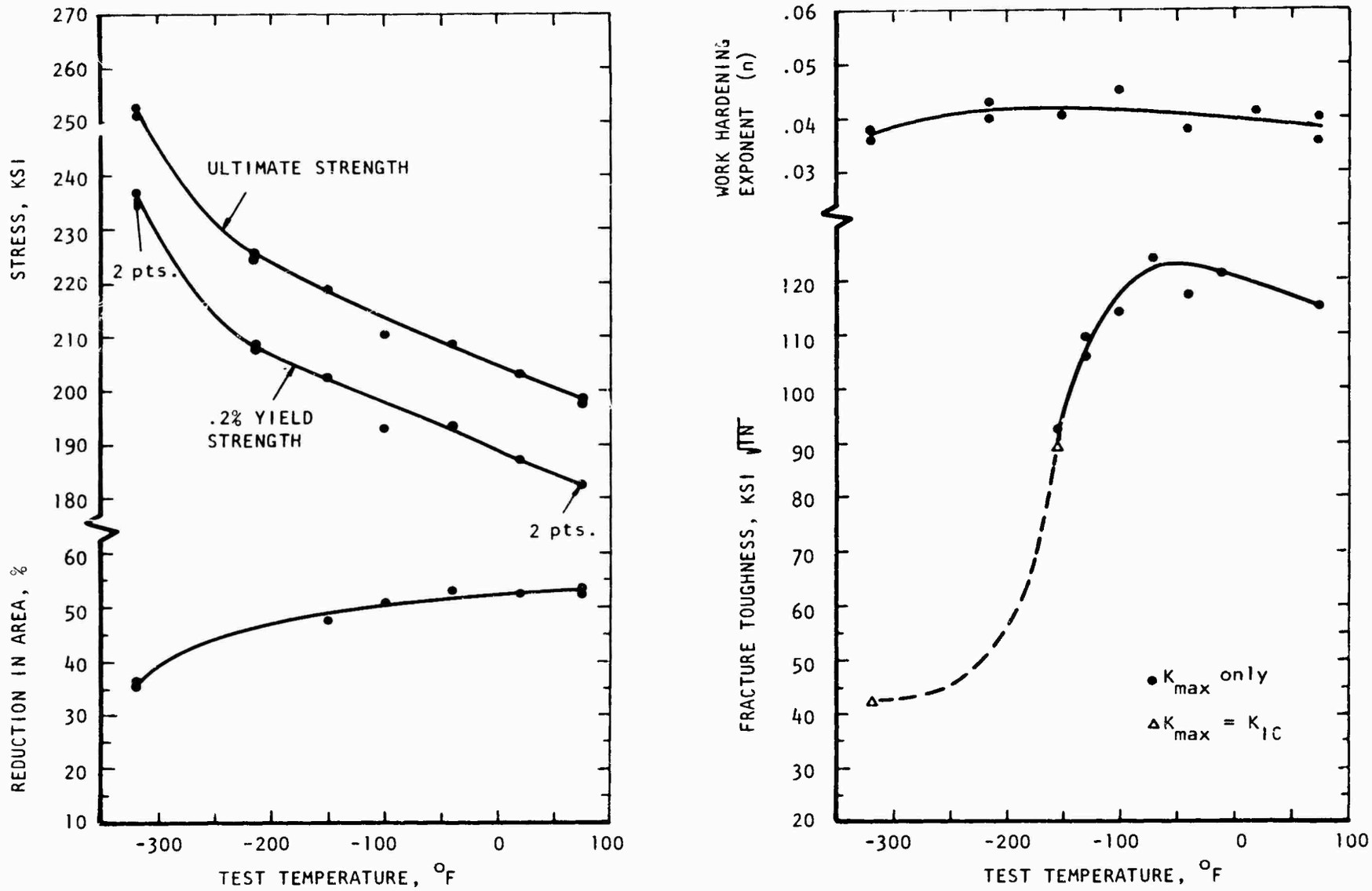

Figure A14. Tensile and notch bend test data for heat 22 (.28%V).

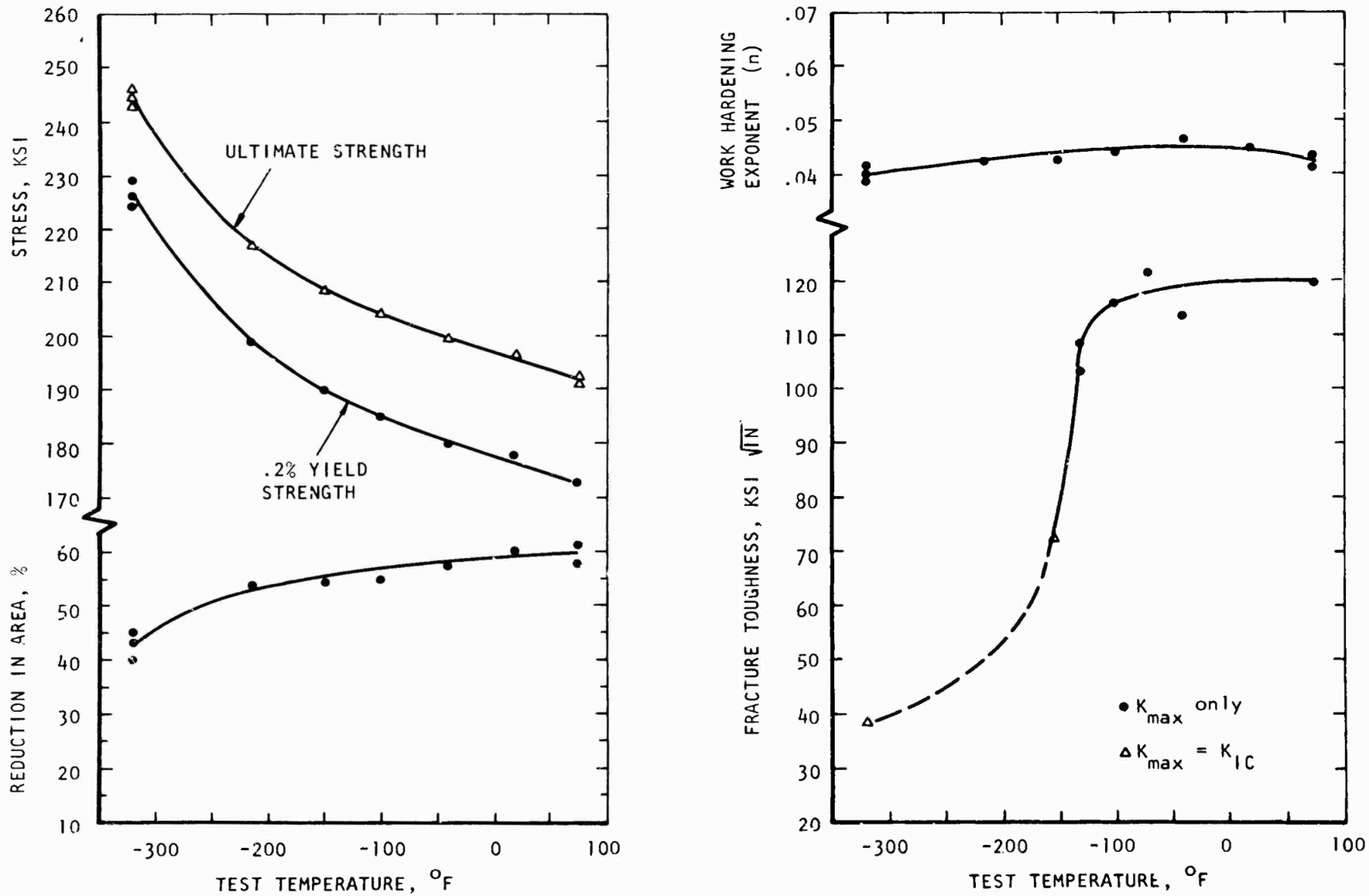

Figure A15. Tensile and notch bend test data for heat 26 (.21%Mn).

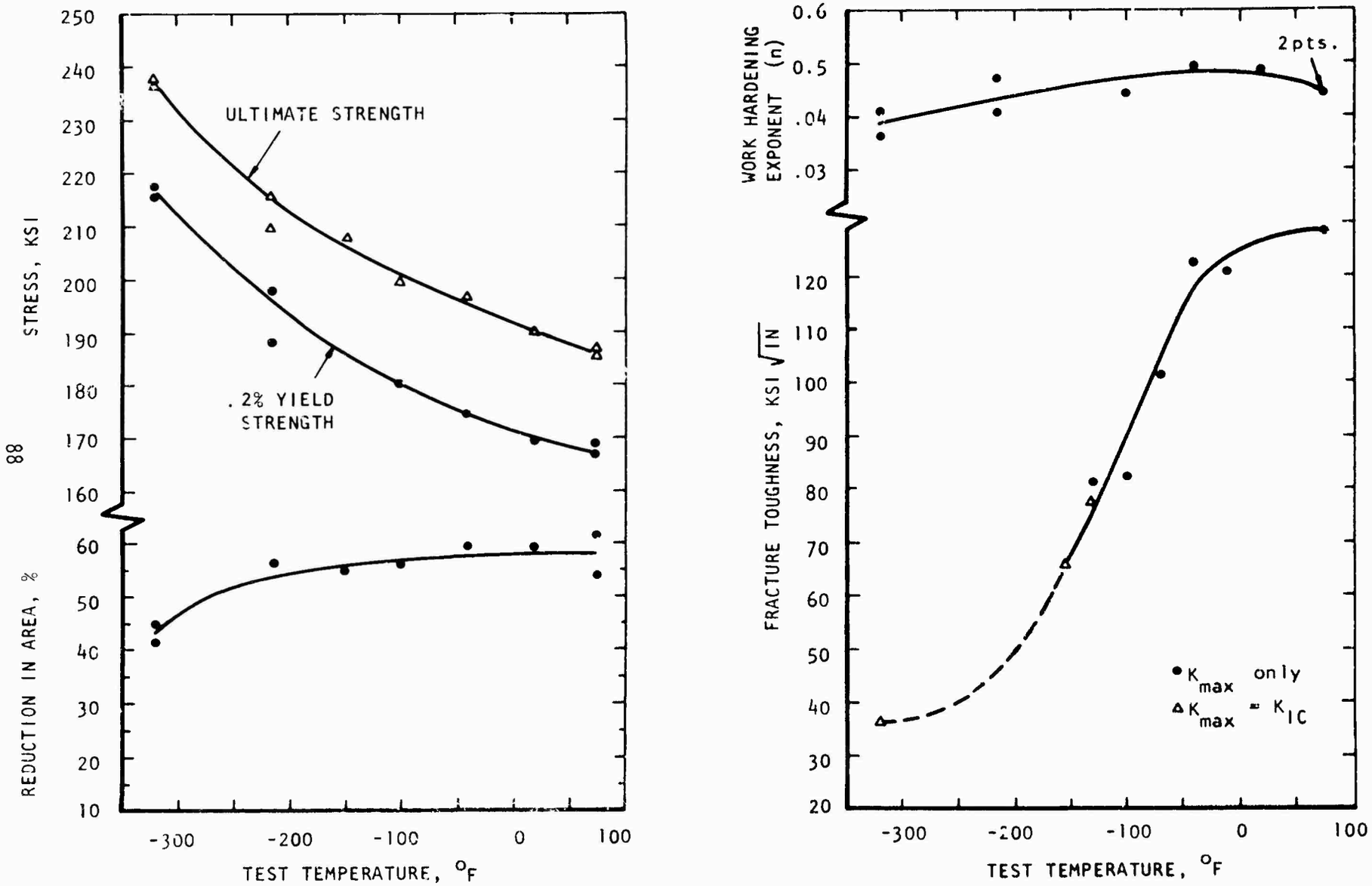

Figure A16. Tensile and notch bend test data for heat 27 (.28%C).

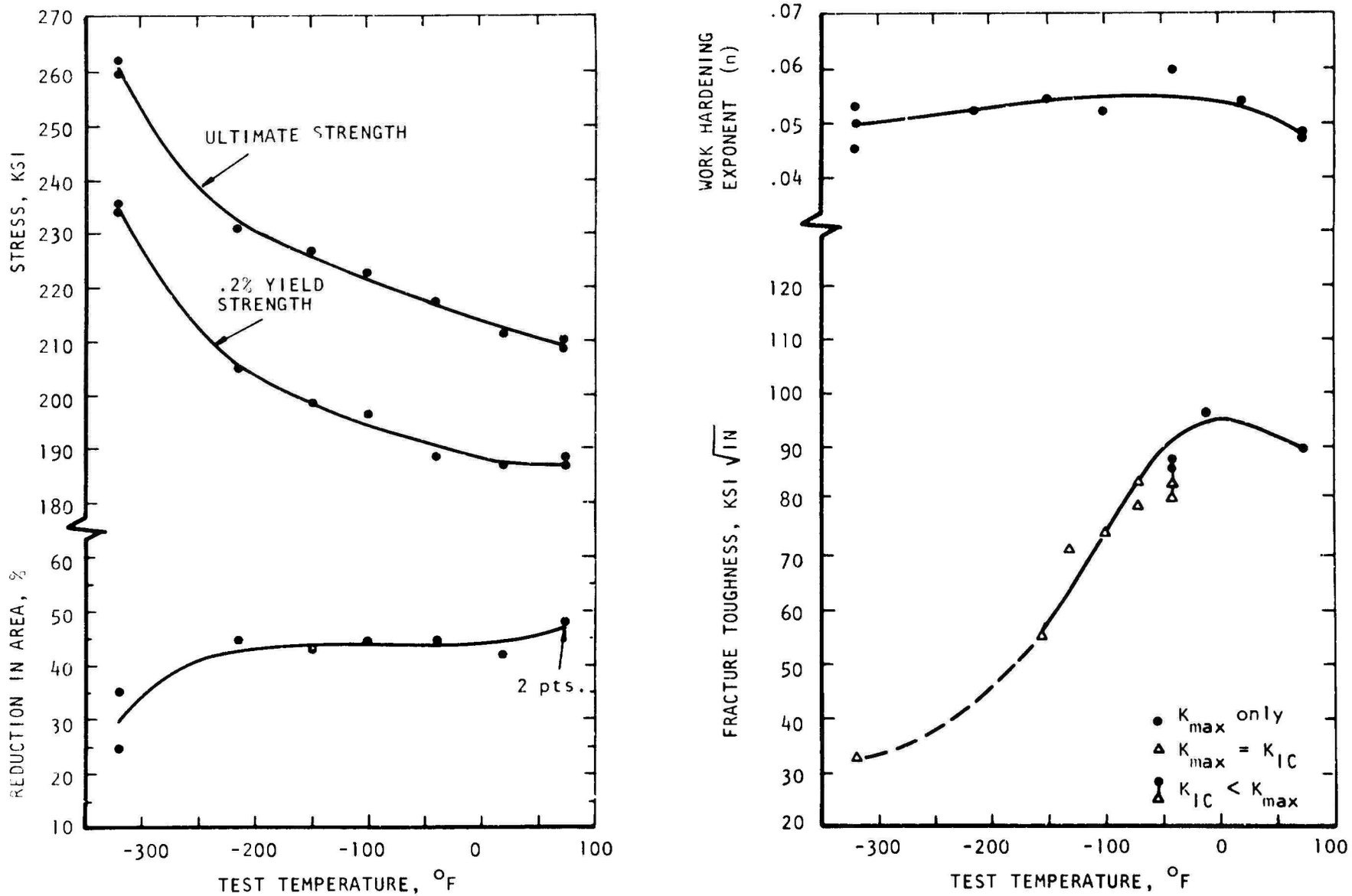

Figure A17. Tensile and notch bend test data for heat 28 (.41%C).

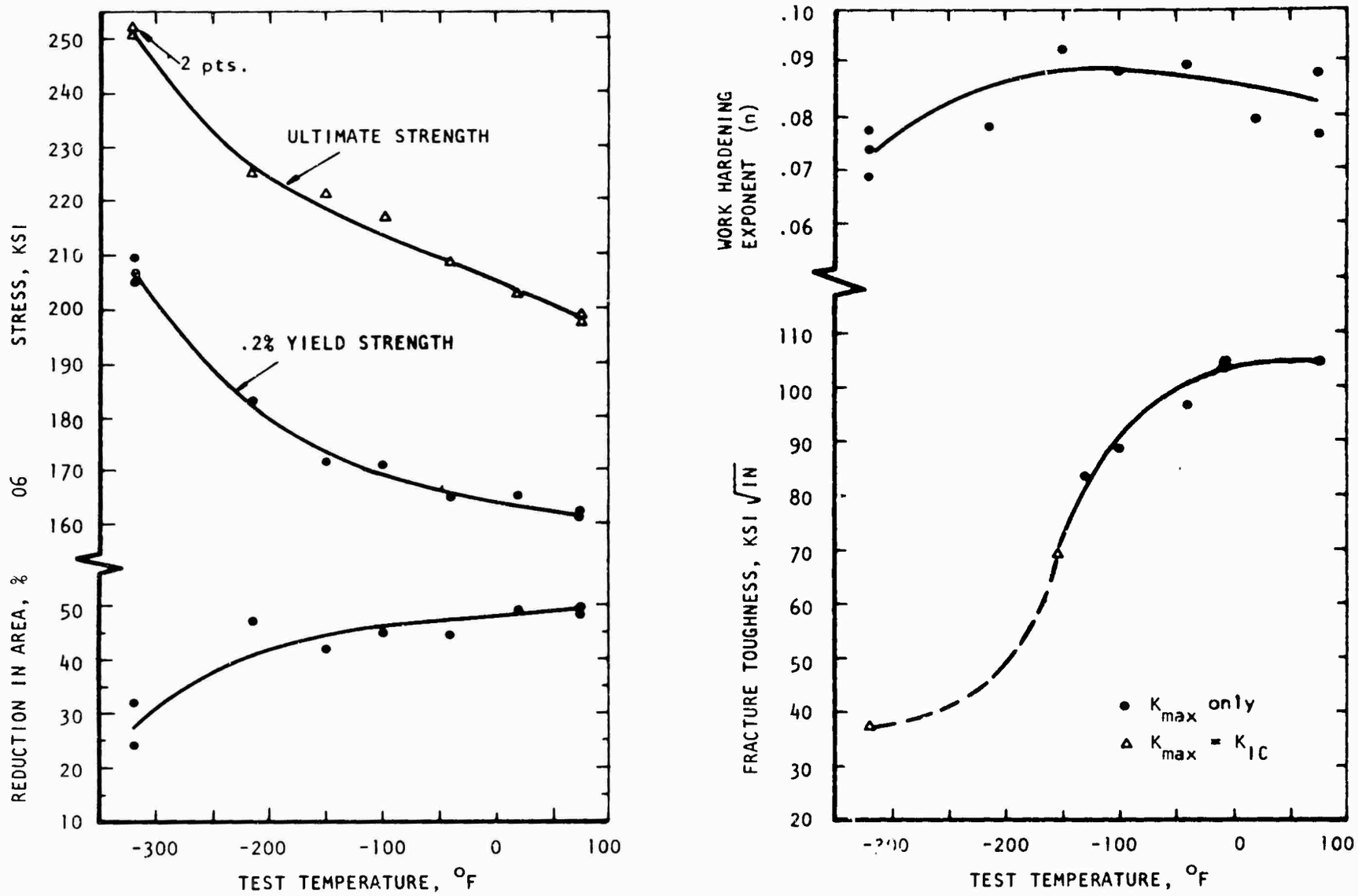

Figure A18. Tensile and notch bend test data for heat 29 (6.23%Ni).

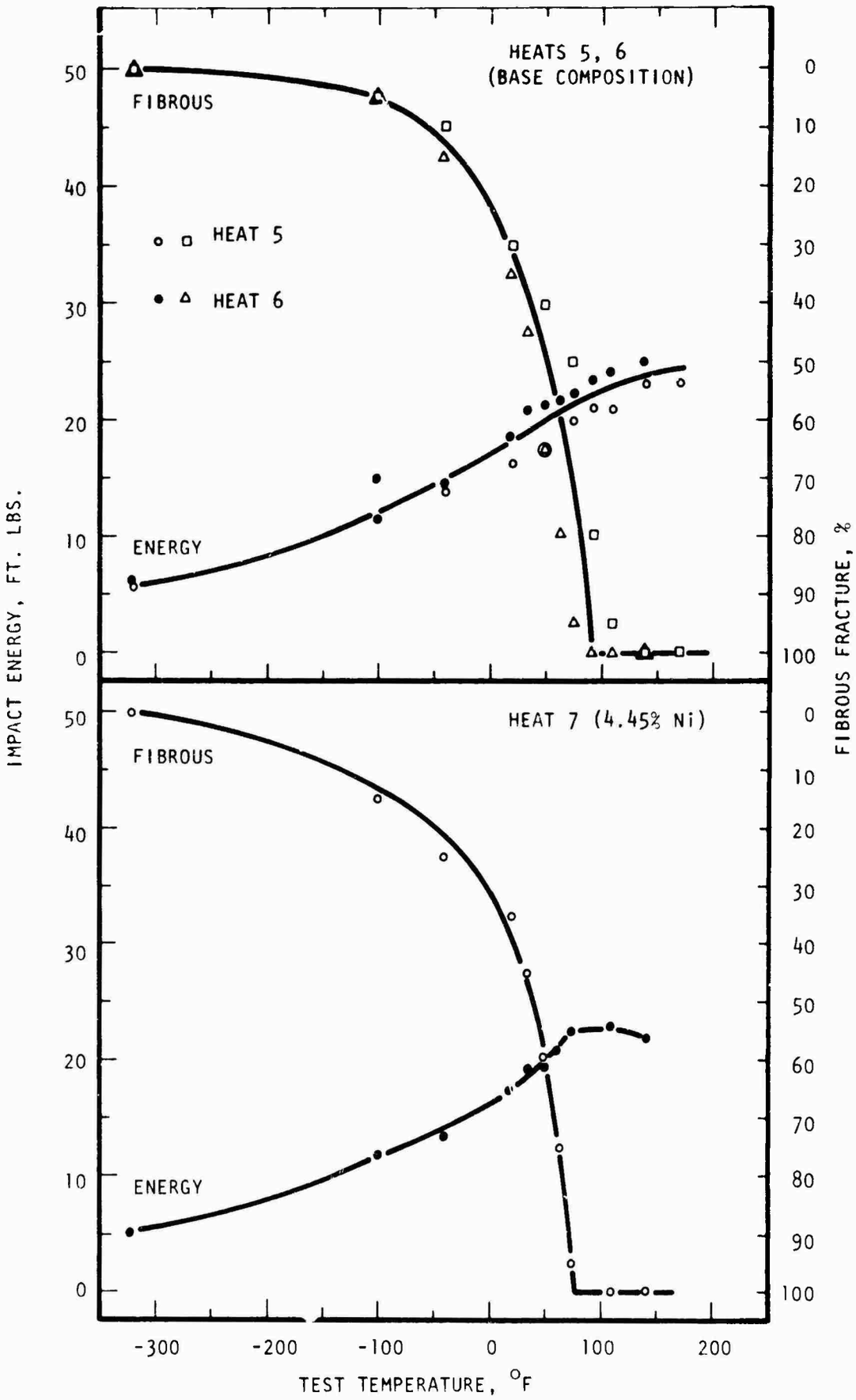

Figure A19. Charpy impact test data for heats 5, 6, and 7.

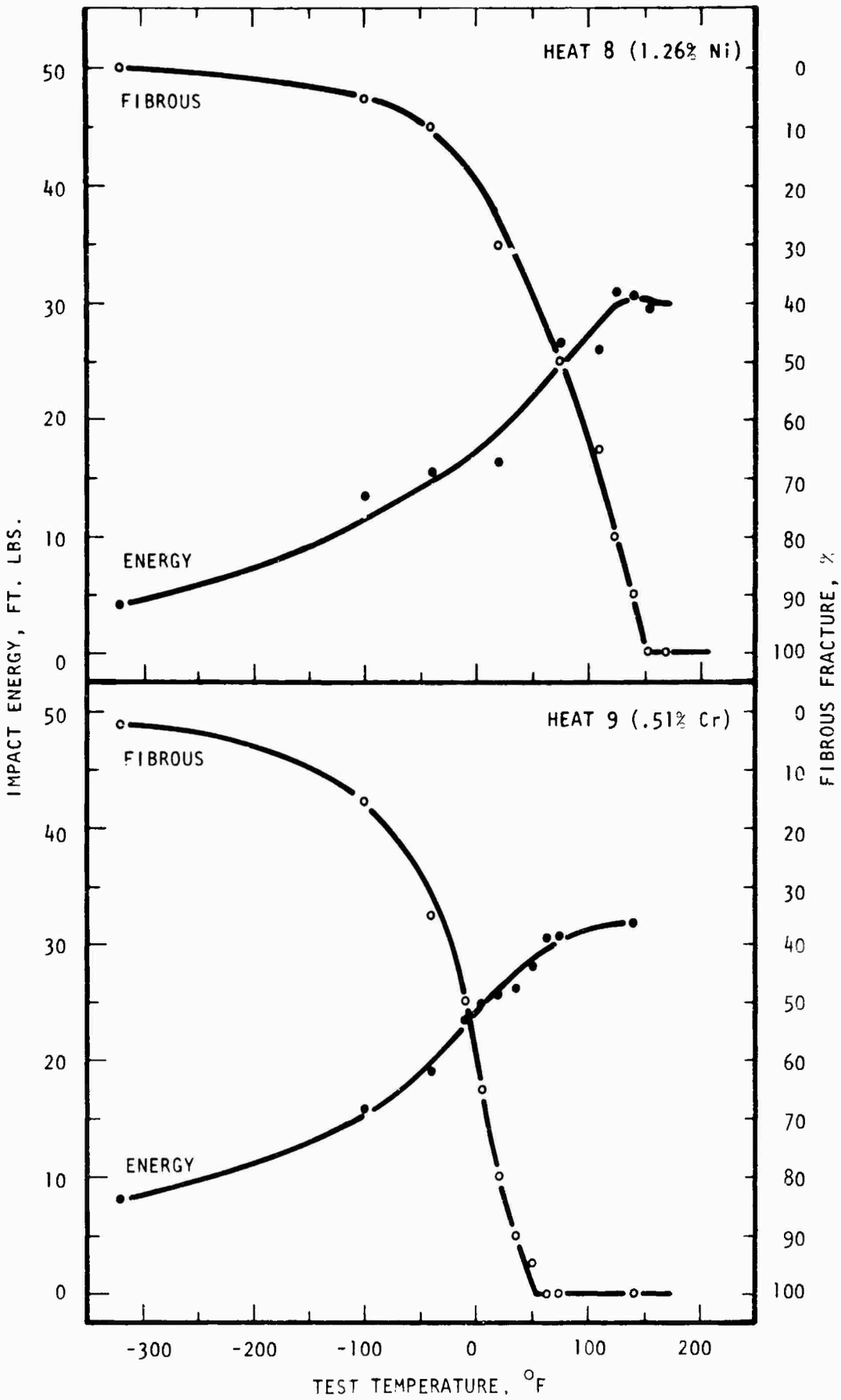

Figure A20. Charpy impact test data for heats 8 and 9.

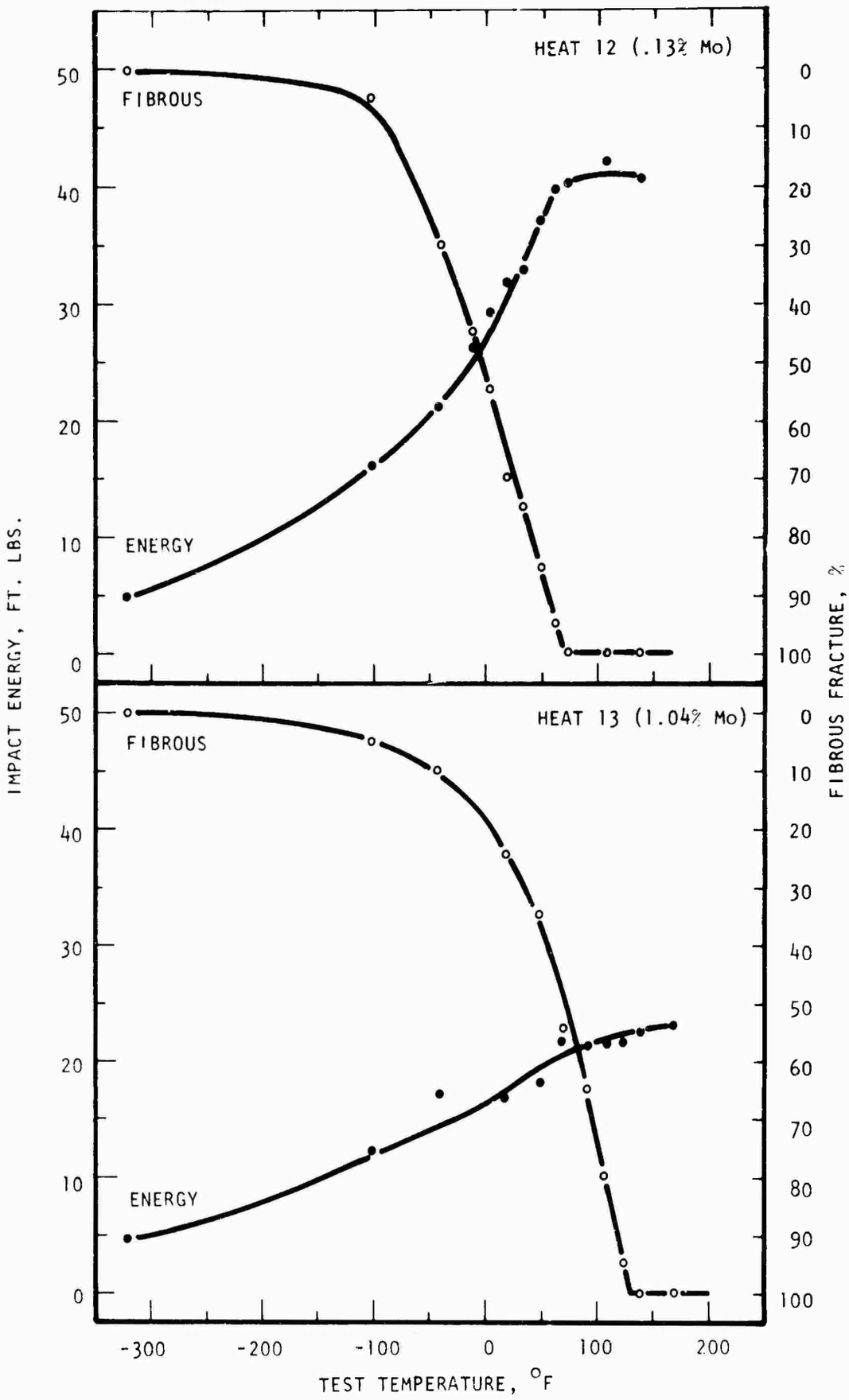

Figure A21. Charpy impact test data for heats 12 and 13.

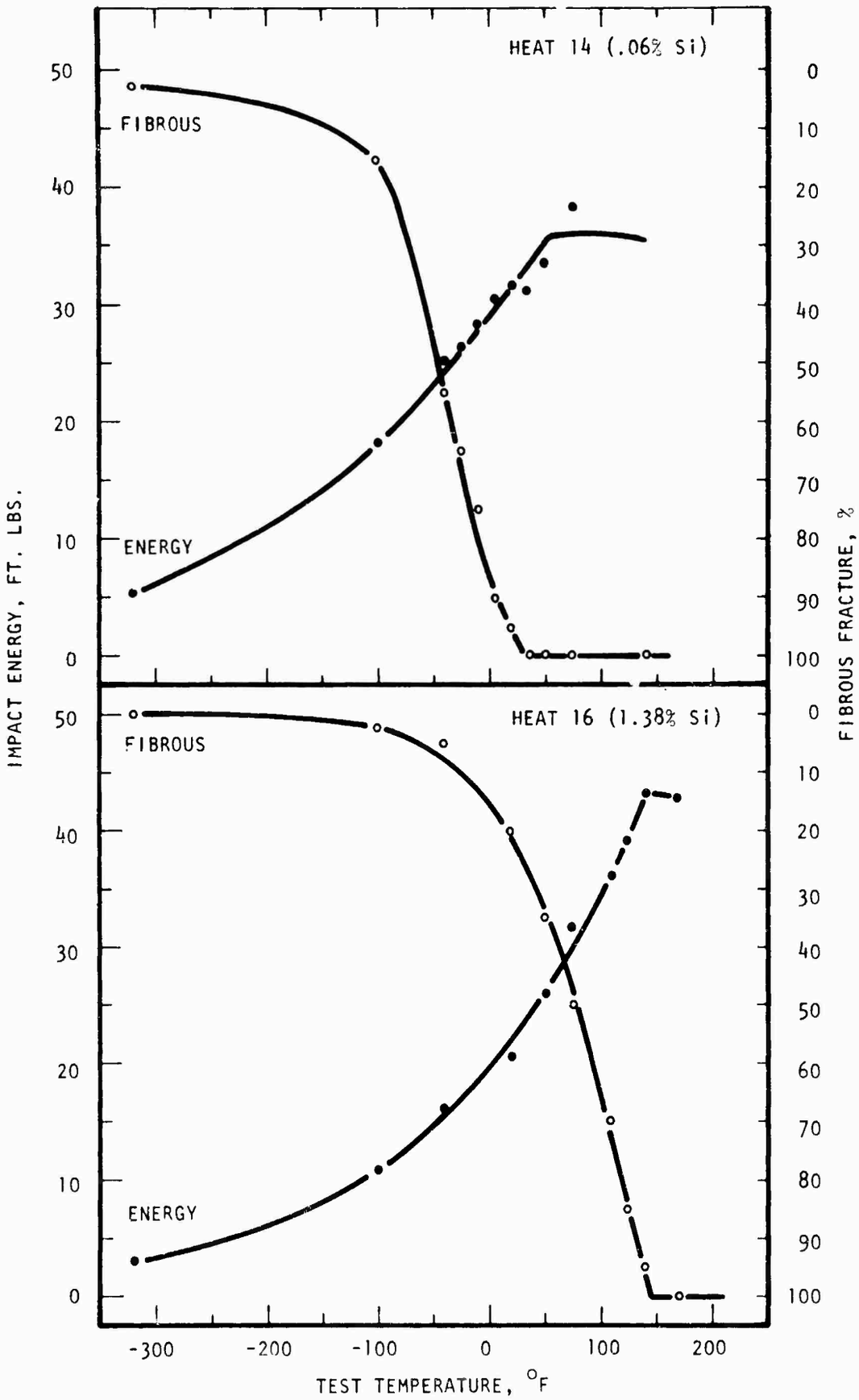

Figure A22. Charpy impact test data for heats 14 and 16.

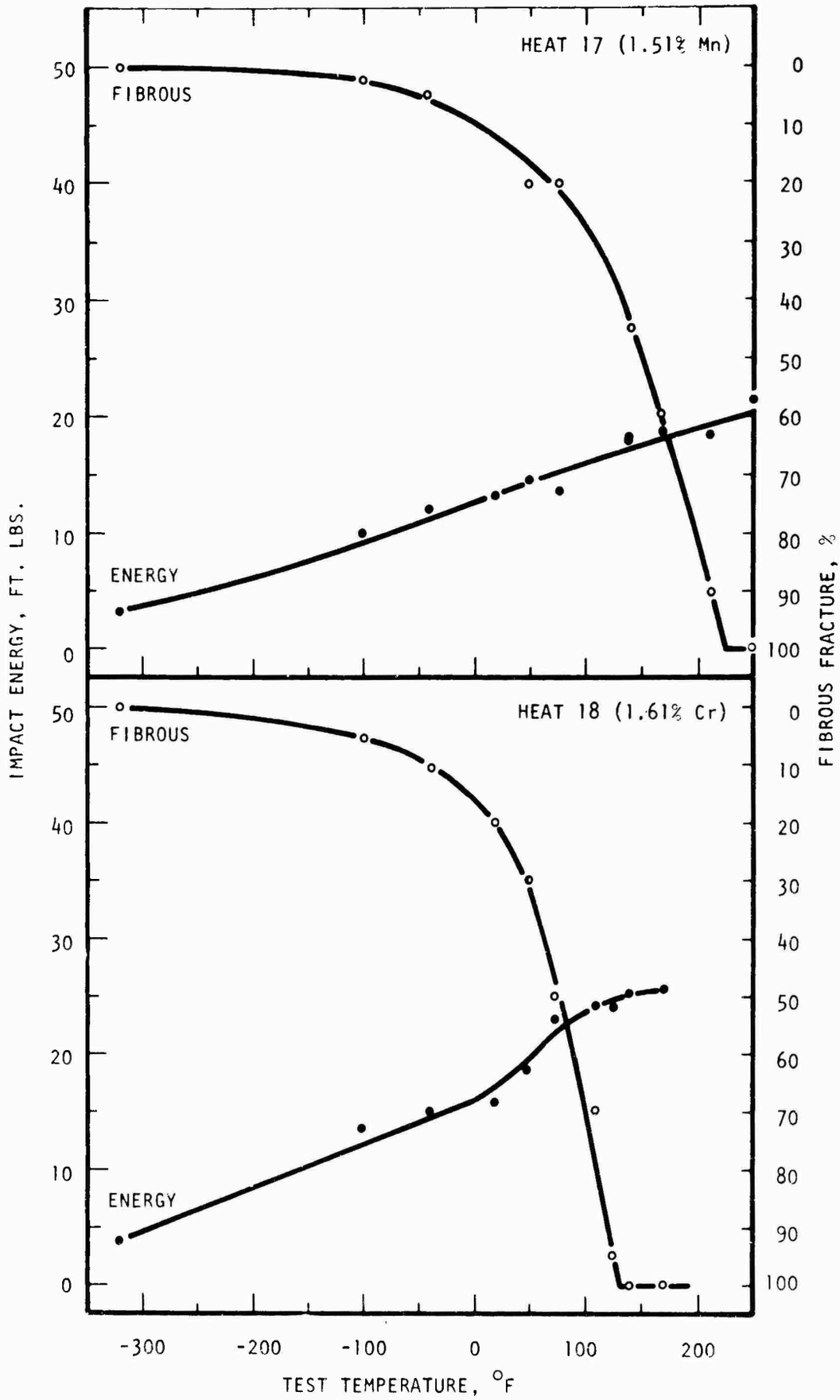

Figure A23. Charpy impact test data for heats 17 and 18.

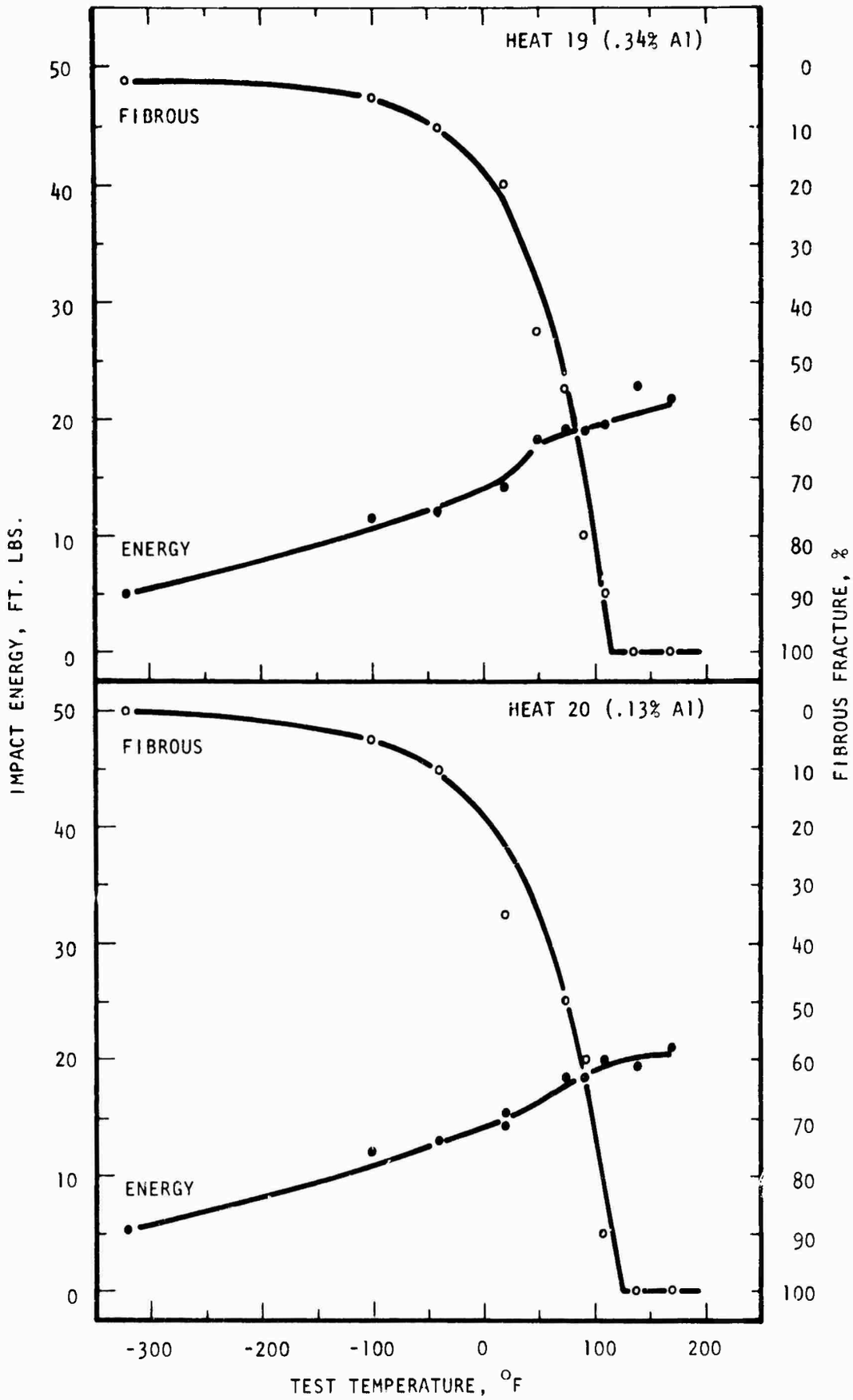

Figure A24. Charpy impact test data for heats 19 and 20

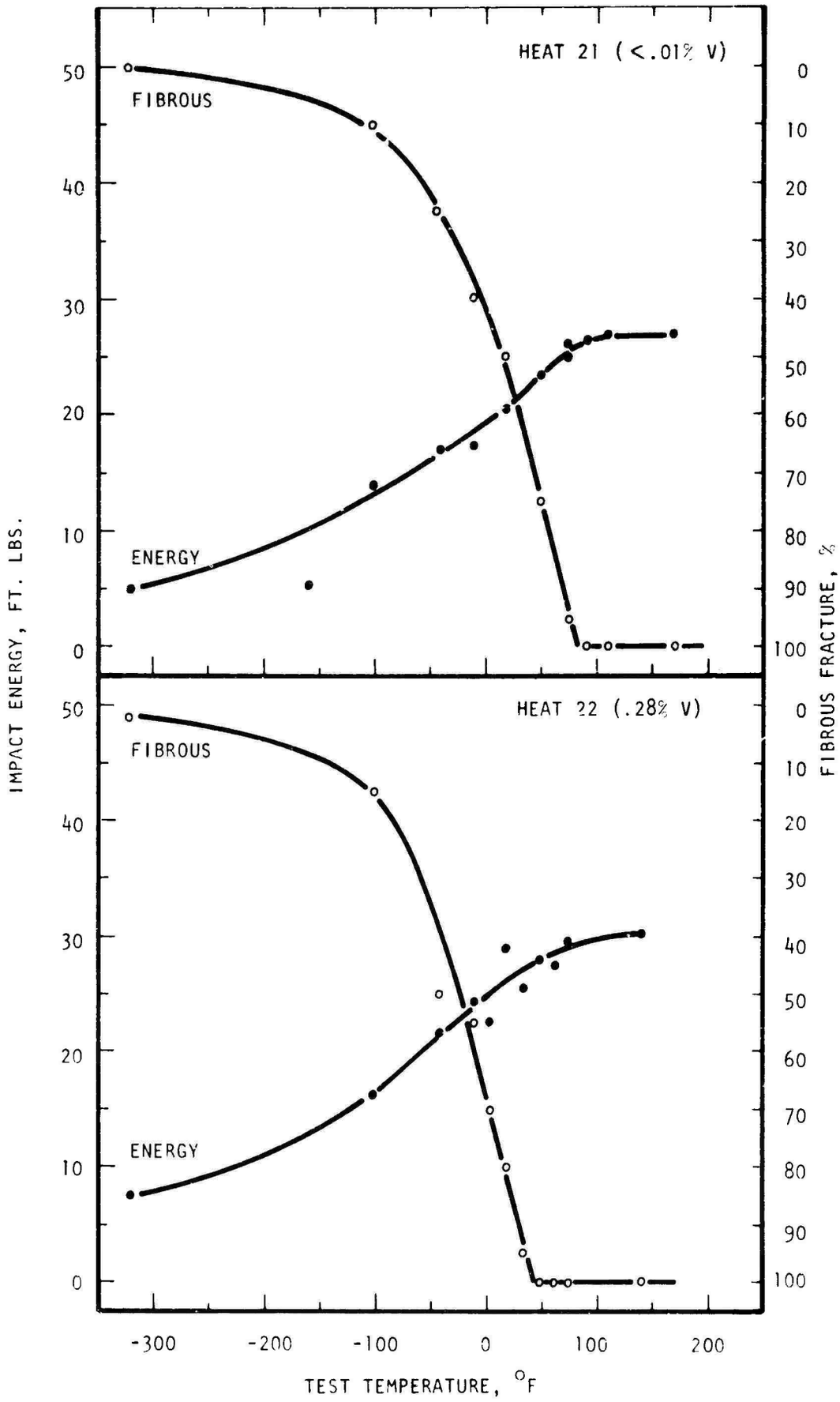

Figure A25. Charpy impact test data for heats 21 and 22.

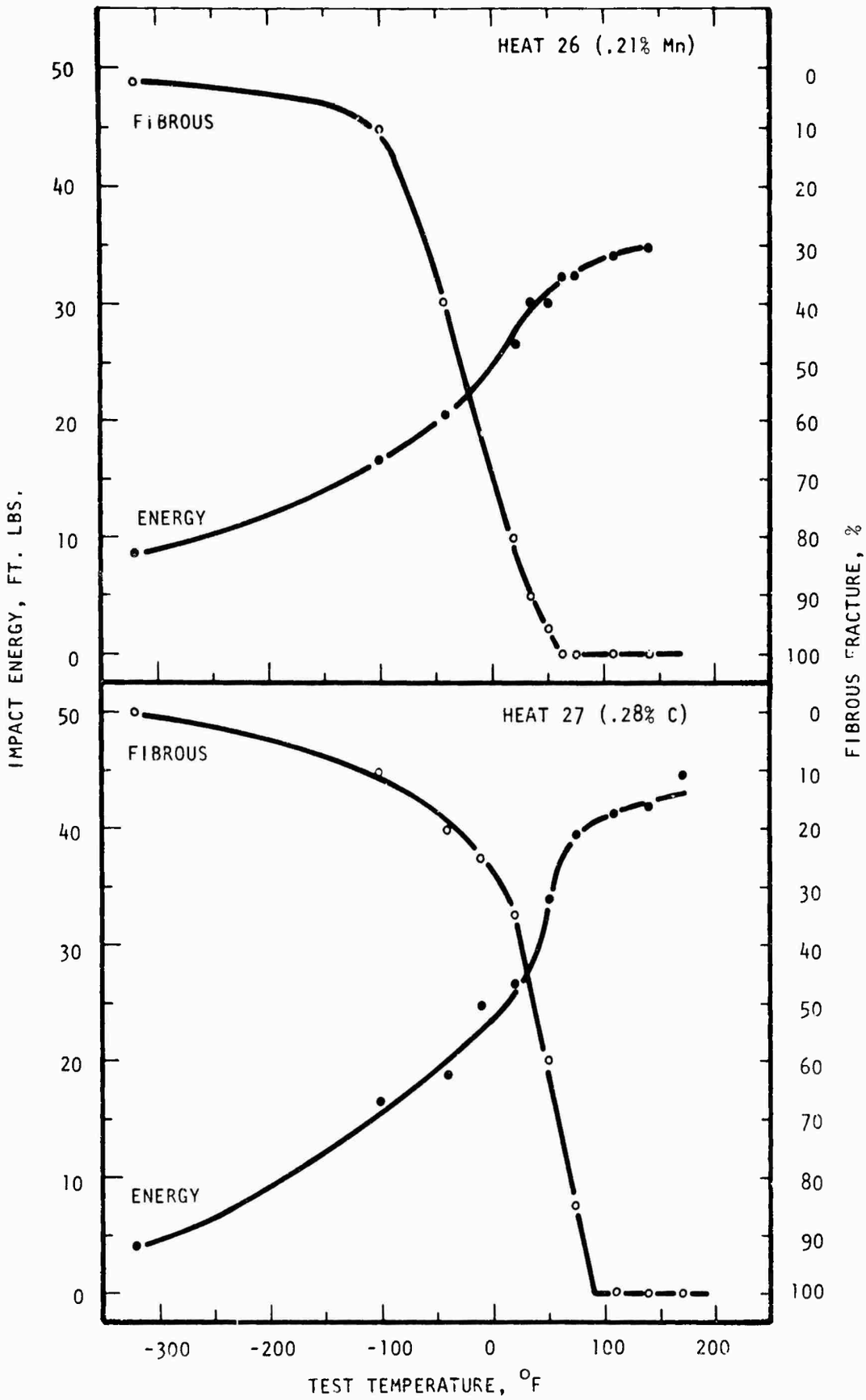

Figure A26. Charpy impact test data for heats 26 and 27.

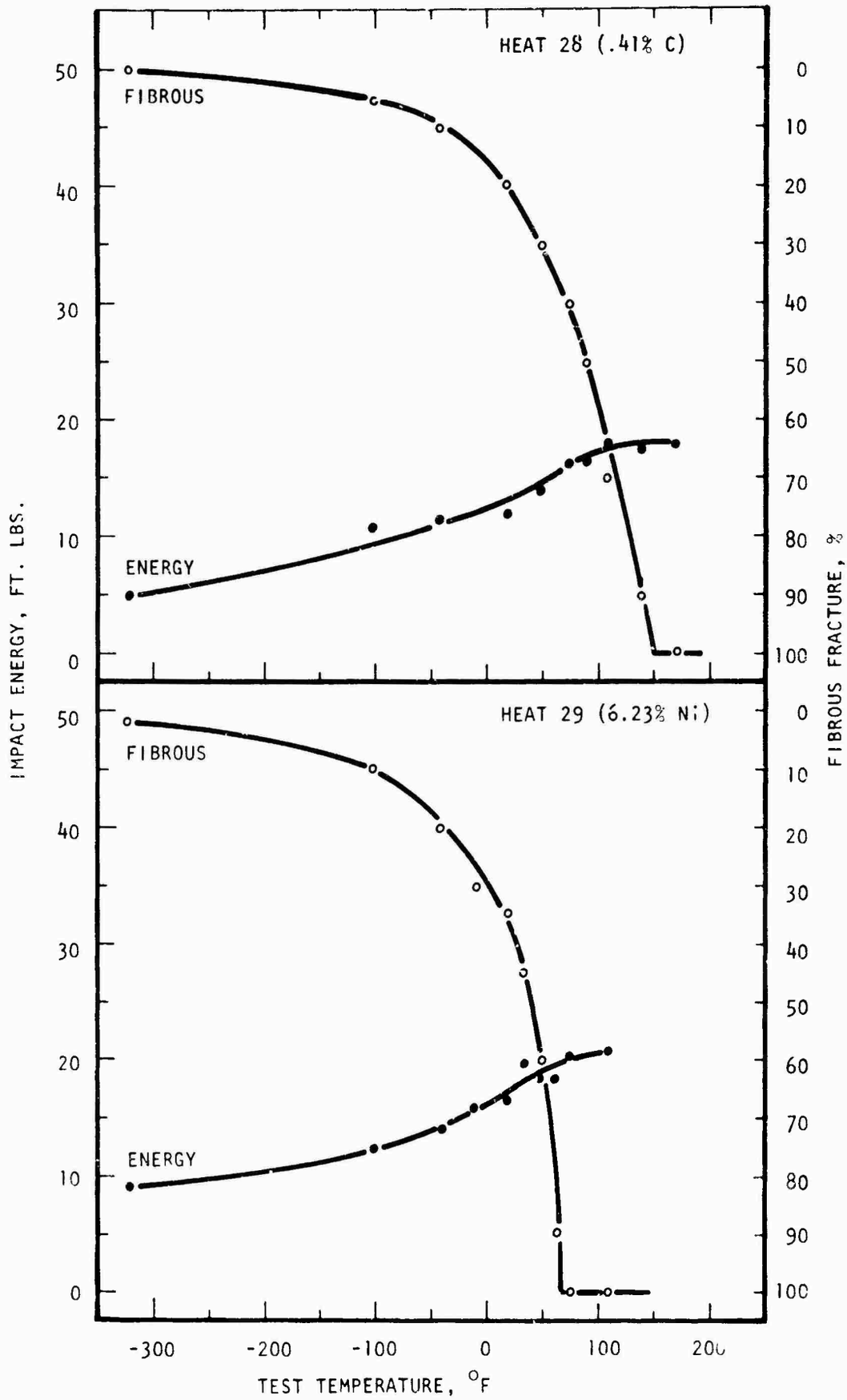

Figure A27. Charpy impact test data for heats 28 and 29.

Unclassified
Security Classification

DOCUMENT CONTROL DATA - R&D

(Security classification of title, body of abstract and indexing annotation must be entered when the overall report is classified)

1. ORIGINATING ACTIVITY (Corporate author)
TRW Inc.
Cleveland, Ohio

2a. REPORT SECURITY CLASSIFICATION
Unclassified

2b. GROUP

3. REPORT TITLE
Influence of Alloying Elements on the Toughness of Low Alloy Martensitic High Strength Steels

4. DESCRIPTIVE NOTES (Type of report and inclusive dates)
Final Technical Report July 1967 - September 1968

5. AUTHOR(S) (Last name, first name, initial)
Vishnevsky, C. and E. A. Steigerwald

6. REPORT DATE
November 1968

7a. TOTAL NO. OF PAGES
99

7b. NO. OF REFS
20

8a. CONTRACT OR GRANT NO.
DAAG 46-67-C-0171

b. PROJECT NO.
D/A 1C024401A349

c.
AMCMS Code 5025.13.842

d.

9a. ORIGINATOR'S REPORT NUMBER(S)
AMMRC CR 68-09(F)

9b. OTHER REPORT NO(S) (Any other numbers that may be assigned this report)

10. AVAILABILITY/LIMITATION NOTICES
This document has been approved for publication and sale; its distribution is unlimited.

11. SUPPLEMENTARY NOTES

12. SPONSORING MILITARY ACTIVITY
Army Materials and Mechanics Research Center, Watertown, Mass. 02172

13. ABSTRACT

This study has examined the effects of various elements on the notch bend fracture toughness and Charpy impact behavior of a 0.35 C, 3-Ni, Cr-Mo-V martensitic steel having a room temperature yield strength of approximately 160-180 ksi. A classical approach was used in the design of alloys which permitted a direct evaluation of single element effects rather than interactions.

The elements C, Mn, Si, Cr, and Mo raised both the notch bend fracture mode transition temperature and the Charpy V-notch transition temperature (100% fibrosity criterion). In amounts above that required for deoxidation and grain refinement aluminum degraded the transition temperature and toughness slightly. A minimum toughness occurred at a vanadium content of 0.1%. Over the entire range of compositions examined (1.26 - 6.23%) nickel decreased the transition temperature and improved toughness at the lower test temperatures.

Charpy shelf energy, C_v (max), and fracture toughness K_{max} (at 75°F), did not correlate well with work hardening exponent (n). Good agreement was obtained however when these parameters were plotted versus true fracture strain. At -321°F, toughness was essentially fracture strain independent suggesting that a critical strain criterion based on fracture strain is valid only when fracture is fibrous.

A comparison was made of measured K_{Ic} calculated from tensile data using the Hahn-Rosenfield model $K_{Ic} = (2/3EY\tau^{*}n^{2})^{1/2}$, where E = Young's modulus, Y = yield strength, τ^{*} = true fracture strain, n = work hardening exponent. The results indicated that the increased contribution on non-ductile fracture which accompanies increases in strength and/or decreases in test temperature in low alloy steels can lead to large errors in the predicted toughness.

DD FORM 1 JAN 64 1473

Unclassified
Security Classification

Unclassified
Security Classification

14. KEY WORDS	LINK A ROLE	WT	LINK B ROLE	WT	LINK C ROLE	WT
Toughness						
Fracture						
Impact Tests						
Transition Temperature						
Alloying						
Crack Propagation						
Plane Strain						
Plane Stress						
Elements						
Nickel Steel						
Gun Steels						

INSTRUCTIONS

1. ORIGINATING ACTIVITY: Enter the name and address of the contractor, subcontractor, grantee, Department of Defense activity or other organization *(corporate author)* issuing the report.

2a. REPORT SECURITY CLASSIFICATION: Enter the overall security classification of the report. Indicate whether "Restricted Data" is included. Marking is to be in accordance with appropriate security regulations.

2b. GROUP: Automatic downgrading is specified in DoD Directive 5200.10 and Armed Forces Industrial Manual. Enter the group number. Also, when applicable, show that optional markings have been used for Group 3 and Group 4 as authorized.

3. REPORT TITLE: Enter the complete report title in all capital letters. Titles in all cases should be unclassified. If a meaningful title cannot be selected without classification, show title classification in all capitals in parenthesis immediately following the title.

4. DESCRIPTIVE NOTES: If appropriate, enter the type of report, e.g., interim, progress, summary, annual, or final. Give the inclusive dates when a specific reporting period is covered.

5. AUTHOR(S): Enter the name(s) of author(s) as shown on or in the report. Enter last name, first name, middle initial. If military, show rank and branch of service. The name of the principal author is an absolute minimum requirement.

6. REPORT DATE: Enter the date of the report as day, month, year; or month, year. If more than one date appears on the report, use date of publication.

7a. TOTAL NUMBER OF PAGES: The total page count should follow normal pagination procedures, i.e., enter the number of pages containing information.

7b. NUMBER OF REFERENCES: Enter the total number of references cited in the report.

8a. CONTRACT OR GRANT NUMBER: If appropriate, enter the applicable number of the contract or grant under which the report was written.

8b, 8c, & 8d. PROJECT NUMBER: Enter the appropriate military department identification, such as project number, subproject number, system numbers, task number, etc.

9a. ORIGINATOR'S REPORT NUMBER(S): Enter the official report number by which the document will be identified and controlled by the originating activity. This number must be unique to this report.

9b. OTHER REPORT NUMBER(S): If the report has been assigned any other report numbers *(either by the originator or by the sponsor)*, also enter this number(s).

10. AVAILABILITY LIMITATION NOTICES: Enter any limitations on further dissemination of the report, other than those imposed by security classification, using standard statements such as:

(1) "Qualified requesters may obtain copies of this report from DDC."

(2) "Foreign announcement and dissemination of this report by DDC is not authorized."

(3) "U. S. Government agencies may obtain copies of this report directly from DDC. Other qualified DDC users shall request through _____."

(4) "U. S. military agencies may obtain copies of this report directly from DDC. Other qualified users shall request through _____."

(5) "All distribution of this report is controlled. Qualified DDC users shall request through _____."

If the report has been furnished to the Office of Technical Services, Department of Commerce, for sale to the public, indicate this fact and enter the price, if known.

11. SUPPLEMENTARY NOTES: Use for additional explanatory notes.

12. SPONSORING MILITARY ACTIVITY: Enter the name of the departmental project office or laboratory sponsoring *(paying for)* the research and development. Include address.

13. ABSTRACT: Enter an abstract giving a brief and factual summary of the document indicative of the report, even though it may also appear elsewhere in the body of the technical report. If additional space is required, a continuation sheet shall be attached.

It is highly desirable that the abstract of classified reports be unclassified. Each paragraph of the abstract shall end with an indication of the military security classification of the information in the paragraph, represented as *(TS)*, *(S)*, *(C)*, or *(U)*.

There is no limitation on the length of the abstract. However, the suggested length is from 150 to 225 words.

14. KEY WORDS: Key words are technically meaningful terms or short phrases that characterize a report and may be used as index entries for cataloging the report. Key words must be selected so that no security classification is required. Identifiers, such as equipment model designation, trade name, military project code name, geographic location, may be used as key words but will be followed by an indication of technical context. The assignment of links, rules, and weights is optional.

Unclassified
Security Classification